# Translational profiling of stress-induced small proteins uncovers an unexpected connection among distinct signaling systems

Sangeevan Vellappan[1,2,3], Junhong Sun[1], John Favate [2,3], Pranavi Jagadeesan[1], Debbie Cerda[1,2], Premal Shah [2,3], Srujana S. Yadavalli[1,2]*
[1]Waksman Institute of Microbiology, Rutgers University, Piscataway, NJ USA
[2]Department of Genetics, School of Arts and Sciences, Rutgers University, Piscataway, NJ USA
[3]Human Genetics Institute of New Jersey, Rutgers University, Piscataway, New Jersey, USA

*Corresponding author
Waksman Institute of Microbiology
Rutgers University
190 Frelinghuysen Rd
Piscataway NJ 08854
Phone: 848-445-0251
Email: sam.yadavalli@rutgers.edu

## Highlights

- Ribo-RET identifies 17 small proteins induced under low $Mg^{2+}$ stress in *E. coli*
- Many of these proteins are transcriptionally activated by PhoQP signaling system
- Half of the stress-induced small proteins localize to the membrane
- Deletion or overexpression of specific small proteins affects growth under stress
- Small protein YoaI connects PhoR-PhoB and EnvZ-OmpR signaling networks

## Summary

Signaling networks in bacteria enable sensing and adaptation to challenging environments by activating specific genes that help counteract stressors. Small proteins (≤ 50 amino acids long) are a rising class of bacterial stress response regulators. *Escherichia coli* encodes over 150 small proteins, most of which lack known phenotypes and their biological roles remain elusive. Using magnesium limitation as a stressor, we investigate small proteins induced in response to stress using ribosome profiling, RNA sequencing, and transcriptional reporter assays. We uncover 17 small proteins with increased translation initiation, a majority of which are transcriptionally upregulated by the PhoQ-PhoP two-component signaling system, crucial for magnesium homeostasis. Next, we describe small protein-specific deletion and overexpression phenotypes, which underscore the physiological significance of their expression in low magnesium stress. Most remarkably, our study reveals that a small membrane protein YoaI is an unusual connector of the major signaling networks – PhoR-PhoB and EnvZ-OmpR in *E. coli*, advancing our understanding of small protein regulators of cellular signaling.

## Graphical abstract

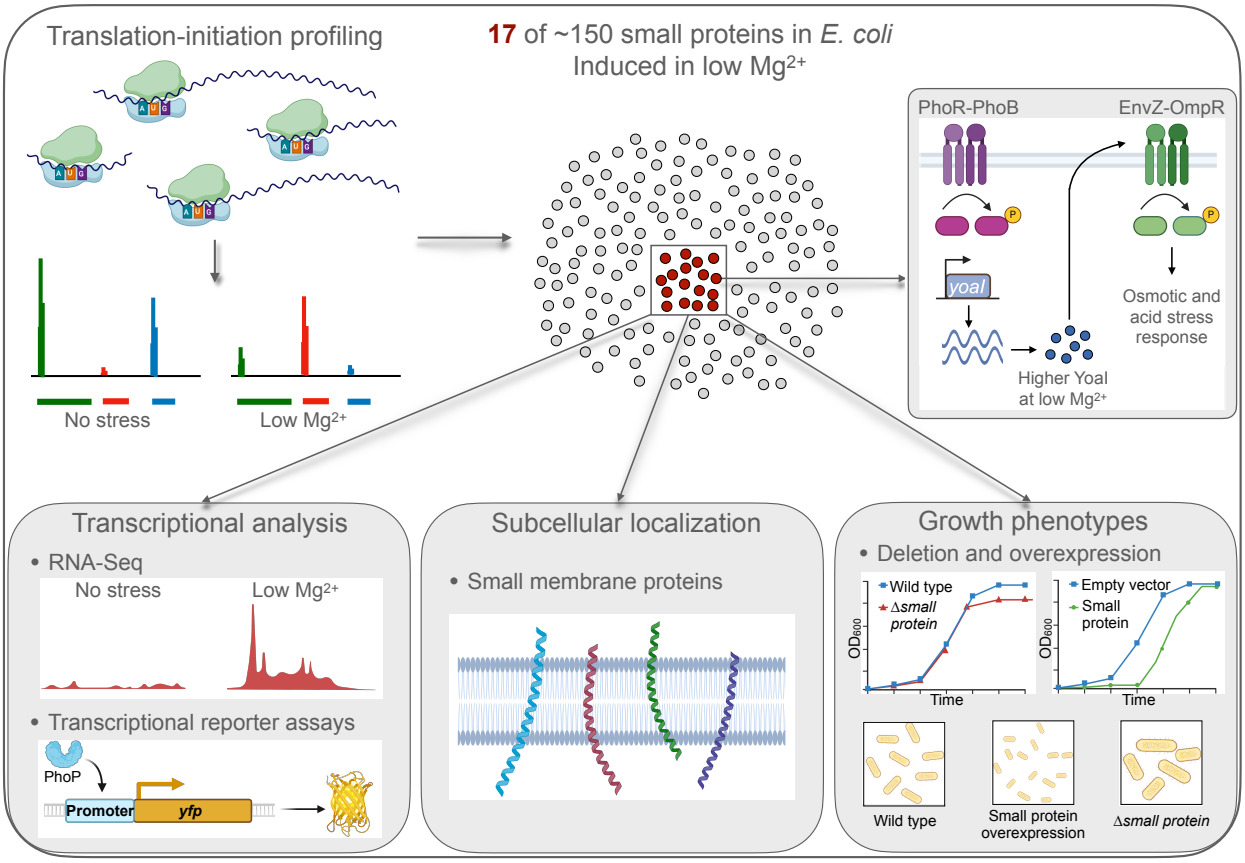



## Keywords

Bacterial stress response, translation-profiling, small proteins, magnesium starvation, two-component signaling, PhoQ-PhoP, fluorescent reporters


## Introduction

Living organisms sense and respond to environmental stressors through a wide variety of gene regulatory mechanisms [1]. In bacteria, signal transduction is primarily carried out by two-component signaling systems [2–4]. Gene expression regulation can occur at various stages including transcription, post-transcription, translation, and post-translation [5–8]. While some of these mechanisms involving regulators such as transcription factors and small RNAs have been extensively studied [9–11], other regulatory pathways essential for stress adaptation remain less well understood. Small proteins (≤50 amino acids in prokaryotes and ≤100 amino acids in eukaryotes), encoded by authentic small open reading frames, are emerging as key regulators of stress response [12–14], highlighting a need for further investigation into their roles and mechanisms of action.

Advances in bioinformatics, gene expression studies, and ribosome profiling have identified hundreds of previously unannotated small proteins in all kingdoms of life including humans [13,15–20]. In *Escherichia coli,* more than 150 small proteins have been documented [13,15]. While there has been significant progress in identifying small proteins, a major gap in our knowledge is the lack of understanding of the functions of most of these proteins [12,15]. Small proteins are typically non-essential, at least under standard growth conditions used in the labs, and their requirement is likely conditional when the activity of a larger target needs fine-tuning. In support of this idea, it was previously observed that some small proteins accumulate at higher levels in a specific growth phase, medium, or stress condition [21,22]. Magnesium ($Mg^{2+}$) is an important cofactor affecting the catalysis and stability of numerous proteins and RNAs involved in vital cellular processes, including translation [23]. Given the central role of $Mg^{2+}$, its deprivation poses a major stress to the cells. The signal transduction and physiological response to low $Mg^{2+}$ is fairly well understood, which involves the activation of the master regulator, PhoQP two-component signaling system in gammaproteobacteria [23–25].

So far, three small proteins are known to mediate stress response to magnesium limitation in bacteria. Firstly, MgrB, a 48-aa transmembrane protein negatively regulates the sensor kinase PhoQ of the PhoQP signaling system [26,27]. During magnesium starvation, the absence of MgrB leads to hyperactivation of the PhoQP pathway, resulting in cell division inhibition and filamentation in *E. coli* [28]. In addition to its role in $Mg^{2+}$ stress, loss of MgrB in *E. coli* increases tolerance to trimethoprim, an antibiotic commonly used to treat bacterial infections [29]. In clinical isolates of *Klebsiella pneumoniae*, disruption of MgrB-mediated inhibition of PhoQ also leads to acquired colistin resistance [30]. A second small membrane protein, MgtS is also induced under low $Mg^{2+}$ stress and is important for magnesium homeostasis [31,32]. MgtS protects the magnesium transporter, MgtA, from degradation when $Mg^{2+}$ is limited [31]. PmrR is the third small membrane protein shown to be expressed under low $Mg^{2+}$ stress in *Salmonella enterica* [33,34]. PmrR is activated by the PmrAB two-component system [33,35,36] in a PhoP-dependent manner and inhibits the lipopolysaccharide modification enzyme, LpxT.

Here we ask, what subset of the ~150 small proteins in *E. coli* are induced under magnesium limitation? We hypothesized that, like MgrB, MgtS, and PmrR, many other small proteins with potential regulatory roles are yet to be identified as part of this stress response. We leveraged the translation-initiation profiling method, Ribo-RET [37,38] to identify small proteins induced by low magnesium stress, revealing a set of 17 proteins representing a substantial proportion (~11%) of the documented small proteins in *E. coli*. To investigate the transcriptional regulation of the stress-induced small proteins, we utilized RNA-Seq and transcriptional reporter assays, we investigated the transcriptional regulation of these stress-induced small proteins, shedding light on the genomic regions responsible for their expression and discerning any regulatory influence from the PhoQP system. Additionally, using epitope tagging, microscopy, and biochemical analysis, we meticulously examined the localization, overexpression, and loss-of-function phenotypes of these small proteins. Through these experiments, we unexpectedly uncovered how the small membrane protein YoaI, transcriptionally controlled by the PhoRB signaling pathway [39], displays increased protein levels under magnesium stress and activates another well-studied two-component system EnvZ-OmpR [40] in *E. coli*.

110 # Results

111 **Identification of low magnesium stress-induced small proteins in *E. coli* using**
112 **translation-initiation profiling.**

113 To identify small proteins that accumulate under low magnesium stress, we adapted the
114 translation initiation profiling method called Ribo-RET (Figure 1A) – a modified ribosome
115 profiling approach utilizing translation initiation inhibitors for the identification of small proteins in
116 bacteria [41]. Retapamulin (RET) is an antimicrobial compound that can stall ribosomes at the
117 translation start sites to help identify previously unannotated open reading frames [37,38]. In this
118 study, we prepared Ribo-RET libraries of wild-type *E. coli* cells grown in media with or without
119 magnesium to examine small proteins expressed in response to magnesium starvation.
120
121 In our Ribo-RET data, we observe an increase in reads mapping to a specific distance of the
122 ribosomal P-site codon from the 3' end of the reads in our libraries, ~6-10 nucleotides (nt)
123 downstream of the expected start codon (Figure S1), similar to the pattern observed in previous
124 translation initiation profiling studies [38]. We calculated ribosome density at annotated translation
125 initiation sites using reads mapped from 4 to 20 nt downstream of the first nucleotide in the start
126 codon, using a broad window of 16 nt to capture all relevant footprint sizes. In our analysis, the
127 ribosome footprint sizes range from 16-24 nt, as illustrated in Figure S1, as anticipated for the
128 bacterial systems [42].
129
130 The PhoQP signaling system is upregulated under $Mg^{2+}$ limitation [43] (Figures S2A-B). As
131 expected, the read counts at the translation start site for PhoP and PhoQ were more than 4-fold
132 and 10-fold higher, respectively, under stress conditions compared to no stress. Three small
133 proteins known to be induced under low $Mg^{2+}$ stress – MgrB, MgtS, and PmrR, show a 9-fold, 5-
134 fold, and 5-fold increase in the reads mapping to the translation start sites, respectively, under
135 stress vs. no stress (Figures 1B-C, S2C). Overall, in our Ribo-RET data, we see a moderate
136 correlation between the reads mapping to the start sites of all proteins expressed under these
137 two conditions (Figure 1C), which is indicative of the anticipated changes in the translation
138 initiation of proteins during stress response.
139
140 We detected 379 proteins with ≥3-fold increase in read counts under stress, several among
141 these are small proteins <50 aa in length (Table S4). We narrowed down a set of 17 small
142 proteins namely MgtS, MgrB, PmrR, MgtT, YmiC, YmiA, YoaI, YobF, YddY, YriB, YadX, YkgS,
143 YriA, YdgU, YqhI, YadW and DinQ for further analysis (Table 1). Ribosome footprints at the
144 start site of an open reading frame are a good proxy for the expression of the corresponding
145 protein. However, it is critical to establish whether a given small open reading frame (sORF)
146 results in a protein product of that specific size. All but one protein YoaI were previously
147 validated for expression via genomic epitope-tagging (Table S5). In the case of YoaI, the protein
148 could not be detected in rich media or specific growth conditions, including envelope stress, acid
149 stress, and heat shock [21,22]. Given the strong signal for expression of YoaI in our Ribo-RET data
150 (~12-fold increase in RPM for stress vs. no stress) (Figure S4A), we wondered if YoaI is
151 conditionally expressed during magnesium limitation. To examine the expression of YoaI, we
152 utilized a strain carrying chromosomally-encoded fusion protein YoaI-SPA [21,22]. We grew cells in

153 media containing different levels of $Mg^{2+}$, prepared membrane and cytoplasmic fractions, and
154 performed western blot analysis. Consistent with our hypothesis, we detected expression of
155 YoaI in a magnesium-dependent manner, where the protein level is highest at the lowest
156 concentration of magnesium (Figure S4B). In addition, this result also confirms that YoaI is
157 predominantly associated with the membranes, consistent with the bioinformatic prediction that
158 it is a membrane protein (Table S6).
159
160 14 of the 17 shortlisted small proteins were not previously associated with expression under low
161 magnesium stress. Small proteins YobF [22,44] and DinQ [45] have been linked to other stress
162 responses in *E. coli*, here we find the expression of these two proteins in low magnesium stress
163 as well. Many of these small proteins have not been characterized biochemically and have no
164 documented function yet. In the following sections, we systematically study these low-$Mg^{2+}$-
165 induced small proteins by investigating their transcriptional regulation and cellular localization
166 and characterizing their overexpression and deletion phenotypes.
167
168 **Transcriptional regulation of low magnesium stress-induced small proteins.**
169 To determine changes in the levels of transcripts encoding stress-induced small proteins, we
170 performed RNA-Seq using cells grown to early exponential phase in high and low $Mg^{2+}$
171 conditions. It is well-established that in cells depleted for $Mg^{2+}$, the PhoQP signaling system is
172 stimulated, leading to PhoP-mediated transcriptional activation of hundreds of genes necessary
173 for the stress response [24]. Not surprisingly, we see an increase in the mRNA abundances for
174 *phoQ* and *phoP* (Figure S3). Differential expression analysis of our RNA-seq data revealed
175 significant upregulation (fold change threshold of >2 and a p-value threshold of <0.05) in
176 transcription under low $Mg^{2+}$ stress for at least 10 of the 17 small proteins shortlisted, including
177 MgtS, MgtT, and MgrB (Figure 2). It is worth noting that YadX also showed a small increase
178 (1.7-fold) although it falls below the >2-fold threshold we applied in our data analysis.
179 Intriguingly, YriA, whose open reading frame overlaps with YriB by ~60% did not show an
180 increase in the transcript levels. In addition, we did not see a significant change in the mRNA
181 levels corresponding to YoaI, YobF, YkgS, and DinQ. In these cases, it is possible that the
182 change in transcript abundances is generally low and therefore fell below the significance
183 threshold. Alternatively, gene expression might be regulated at a post-transcriptional or
184 translational level under low magnesium stress. Indeed, *yobF* expression is induced post-
185 transcriptionally during heat shock response [22]. The expression of *yobF* under magnesium
186 limitation may be controlled via a similar post-transcriptional regulatory mechanism.

187 To delve deeper into the transcriptional control mechanism of the small proteins we sought to:
188 1) identify the regulatory regions upstream of each sORF, and 2) determine if the expression is
189 PhoQ-dependent. To identify the regions containing the putative promoters of low $Mg^{2+}$-induced
190 small proteins, we carefully selected ~200 to 500 base pairs upstream of each sORF (Table 2).
191 In general, we did not include any annotated full-length ORFs or non-coding RNAs occurring
192 within the regulatory region being tested, to avoid interference from the ectopic expression of
193 the corresponding product. In cases where a sORF appeared to be in the middle of an operon,
194 we selected two regions to test: one upstream of the entire operon and another immediately
195 upstream of the sORF of interest. We designed transcriptional reporter constructs to measure

196 the activity of each putative regulatory region, as shown in the schematic (Figure 3A). To
197 analyze which of these sORFs are regulated by the PhoQP two-component system, we
198 measured the transcriptional reporter activities in a *phoQ* deletion strain and compared them to
199 that of the wild type (Figure 3B).
200
201 Consistent with our RNA-seq data, we saw an increase in the transcriptional activity for
202 regulatory regions corresponding to 11 sORFs with this upregulation under low $Mg^{2+}$ condition
203 being PhoQ-dependent (Figure 3B). Two sets of overlapping (out-of-frame) sORFs including
204 *mgtS-mgtT* and *yriA-yriB*, strongly suggest their association within the same operon. Three
205 other genes, *yadW, ymiC,* and *ydgU* are likely regulated as part of the operons, *yadX-clcA-*
206 *yadW*, *ymiA-yciX-ymiC*, and *asr-ydgU*, respectively. For all the sORFs occurring within an
207 established or putative operon, the region upstream of the operon showed a higher
208 transcriptional reporter activity in response to stress, while a second region immediately
209 upstream of the given sORF had negligible activity (Table 2, Figure 3B). Based on the reporter
210 assay, the transcriptional activity for the 11 sORFs (*mgrB*, *mgtS*, *mgtT*, *ymiA*, *ymiC*, *yddY*, *yriA*,
211 *yriB, yadX*, *yadW*, and *ydgU*) peaks at ~6-10 hours. The RNA-Seq data represent
212 transcriptomic abundances at a given time point of growth (early exponential phase). This
213 transcriptional reporter assay captures temporal changes in the reporter activity and serves as a
214 complementary approach to RNA-Seq, where changes in low-abundance transcripts would be
215 missed. For instance, we did not observe a significant upregulation of *yadX* and *yadW* in the
216 RNA-Seq data, but we see a PhoQ-dependent increase in the reporter activity for the putative
217 regulatory region $P_{yadX\text{-}clcA\text{-}yadW}$ region under low magnesium stress. Conversely, for *pmrR* and
218 *yqhI*, while the RNA-Seq data suggested upregulation, we did not detect a significant increase
219 in the transcriptional reporter activity under stress suggesting that there may be distal or
220 additional regulatory factors, outside of our reporter construct, involved in controlling their
221 transcription. Indeed, *pmrR* is shown to be transcriptionally activated by the PmrA-PmrB
222 signaling system during magnesium limitation through the PhoQP-regulated connector protein
223 PmrD in *Salmonella enterica* [33] . This connection between the PhoQ-PhoP and PmrA-PmrB
224 signaling pathways is also active in *E. coli* under specific conditions including high stimulation of
225 the PhoQ-PhoP system [35,46]. We did not observe a reporter activity for *dinQ, ykgS, yobF*, and
226 *yoaI* in either the wild-type or *ΔphoQ* cells, consistent with the results from the RNA-Seq.
227
228 In summary, our RNA-Seq and transcriptional reporter assays reveal transcriptional
229 upregulation of 13 of the 17 small proteins, of which PhoQ regulates at least 11 under
230 magnesium starvation.
231
232 **Regulation of small membrane protein YoaI under $Mg^{2+}$ stress.**
233 YoaI is known to be regulated by the PhoRB two-component system [47–49], which responds to
234 phosphate starvation [39]. PhoRB signaling is also activated under low magnesium stress due to
235 the slowdown of protein synthesis and reduction of cytoplasmic phosphate levels [50].
236 Consistently, we noticed a 10-fold increase in reads mapping to the PhoB translation start site
237 under magnesium stress (Figure S2D). We then tested our transcriptional reporter for *yoaI*
238 ($P_{yoaI}$-YFP) in a low-phosphate medium and saw increased transcriptional activity for $P_{yoaI}$ when
239 compared to no-stress condition, in a PhoB-dependent manner (Figure 4A). This transcriptional

240 activation is PhoQ-independent as we see an amplification of $P_{yoaI}$ reporter in Δ*phoQ* cells as
241 well (Figure 4B). Taken together, these results show that *yoaI* transcription is controlled by
242 PhoB, and there is no significant effect of low magnesium stress on *yoaI* transcription based on
243 RNA-Seq and transcriptional reporter data (Figures 2, 3B). Yet YoaI protein levels increase
244 under low magnesium conditions, and we wondered if PhoQ controls YoaI abundance. To test
245 this possibility, we examined YoaI protein expression in wild-type and Δ*phoQ* cells in high and
246 low magnesium conditions by western blotting. Our results demonstrate that YoaI's expression
247 remains magnesium-dependent in a Δ*phoQ* strain, mirroring the pattern seen in the wild type
248 (Figure 4C), suggesting that PhoQ does not affect YoaI levels. Therefore, YoaI expression is
249 induced in a PhoQ-independent manner under magnesium limitation potentially via a post-
250 transcriptional regulatory mechanism that enhances translation initiation.
251

252 **About half of the low $Mg^{2+}$ stress-induced small proteins localize to the membrane.**

253 As a first step to classifying the 17 stress-induced small proteins, we checked if a given small
254 protein is likely associated with the membrane or cytoplasm. Most of these proteins have limited
255 or no documented information, so their cellular localization can provide insights into their
256 potential mechanisms of action and interactions within the cell. Using bioinformatic tools
257 TMHMM [51], TMPred [52], and Phobius [53] to predict membrane helices, we find that at least 9 of
258 our candidates are putative membrane proteins. Three of them, MgrB, MgtS, and DinQ, were
259 previously shown to localize to the membrane in *E. coli* [21,45]. Additionally, PmrR from *S. enterica*
260 was shown to be membrane-bound [33]. Our bioinformatic analyses predict that small proteins
261 YdgU, YmiA, YmiC, YoaI, and YobF also localize to the membrane (Table S6).
262

263 Next, to confirm the membrane association and visualize the small protein localization we used
264 epitope-tagging with GFP. Taking into account the predicted orientation of the putative
265 transmembrane protein, we created either an N- or C-terminal fusion of GFP by tagging the end
266 that is expected to face the cytoplasm (Figure S5A, Table S6) to ensure proper folding of GFP
267 [54]. Accordingly, YdgU, YmiA, and YmiC were tagged at the N-terminus, and YoaI was tagged at
268 the C-terminus. Upon observation by fluorescence microscopy, cells expressing GFP-tagged
269 YdgU, YmiA, YmiC, and YoaI revealed bright fluorescence at the cell periphery indicative of
270 membrane localization, similar to the known membrane protein, MgrB (Figure S5B). As a
271 control, cells expressing GFP alone showed uniform fluorescence indicative of cytoplasmic
272 localization.
273

274 For PmrR, we constructed an N-terminal fusion with GFP, where the tag was expected to
275 localize to the cytoplasm. However, we did not observe membrane localization (Figure S5B).
276 Considering the predicted membrane helices, this suggests that the tag interferes with PmrR
277 localization. Alternately, we tagged the C-terminus of *E. coli* PmrR with a hexahistidine (6XHis)
278 tag (Figure S5C) and performed western blotting using membrane and cytoplasmic fractions.
279 PmrR-6XHis strongly associated with the membrane fraction (Figure S5D), consistent with the
280 bioinformatic prediction and data from *S. enterica* PmrR. As in the case of PmrR, YobF-GFP
281 localized to the cytoplasm, which was inconsistent with its predicted membrane localization
282 (Table S6). Therefore, we used a 6XHis-tagged version of YobF, which showed a greater

283 association with the membranes than the cytoplasmic fraction (Figure S5D). Overall, among the
284 17 small proteins induced under low $Mg^{2+}$, we find that 9 of them are membrane proteins.
285

286 **Three small proteins exhibit stress-specific growth defects upon gene deletion.**

287 To identify potential defects in growth and cellular morphology caused by the absence of each
288 small protein in the cell, we utilized single gene deletions of *mgtS*, *mgtT*, *pmrR*, *yadW*, *yadX*,
289 *yddY*, *ykgS*, *ymiC*, *yqhI*, *yobF, dinQ*, *ydgU*, *ymiA*, and *yoaI* in the *E. coli* genome. *mgtT* lies in an
290 operon with *mgtS* [38], with an out-of-frame overlap between the stop codon of MgtS and the start
291 codon of MgtT. Therefore, we carefully generated an *mgtS* deletion without affecting the start
292 codon of MgtT, and similarly, an *mgtT* deletion while keeping the stop codon for MgtS intact (for
293 details see materials and methods, Table SI). In the case of *yriAB*, the two small proteins YriA
294 and YriB have overlapping open reading frames, where ~80% of the *yriB* gene overlaps with that
295 of *yriA* (Figure 6C, schematic), so, we first deleted the combined *yriAB* ORF to see if there is a
296 phenotype. 12 out of the 17 small proteins displayed no discernible growth defects upon deletion
297 relative to the wild-type strain when grown under magnesium limitation. However, four mutants –
298 namely *ΔpmrR, ΔyobF, ΔyqhI,* and *ΔyriAB* – exhibit reduced growth yields when grown over 24
299 hours (Figure 5). The cells carrying these deletions entered the stationary phase earlier than the
300 wild type. Notably, PmrR and YobF are membrane-bound proteins, while YqhI, YriA, and YriB are
301 putative soluble proteins (Figure S5D, Table S6).
302

303 To determine whether these growth defects are specifically related to the loss of these small
304 proteins, we complemented the deletion strains with plasmids encoding the corresponding small
305 proteins and induced with IPTG. Successful rescue of growth is observed for *ΔpmrR*, and *ΔyobF*
306 (Figure 6A, B; top panel). To confirm that this complementation is specific to the small protein and
307 not due to a cryptic ORF or regulatory element present within the small protein coding region, we
308 prepared plasmids carrying *pmrR* and *yobF* where their start codons are mutated to stop codons.
309 When tested for complementation in *ΔpmrR* and *ΔyobF*, respectively, the start codon mutants
310 retained the growth defect similar to that observed for the empty vector (Figure 6A, B; top panel),
311 reinforcing that the growth phenotype is specific to the small proteins themselves. In addition, we
312 investigated whether the growth defect observed with *pmrR* and *yobF* deletions is specific to low
313 magnesium stress. Our results indicate that deletions of *pmrR* and *yobF* do not cause growth
314 defects in the absence of stress (Figure 6A, B; bottom panel), and the phenotype is specific to
315 magnesium-limited conditions. Intriguingly, expression of plasmid-encoded PmrR in the absence
316 of stress resulted in a growth defect (Figure 6A, bottom panel), suggesting that increased
317 expression of PmrR under no-stress conditions may be detrimental.
318

319 Given the growth phenotype observed for Δ*yriAB*, we performed complementation with either
320 plasmid-encoded YriA and/or YriB to establish if the loss of either protein is responsible for the
321 growth defect. Intriguingly, complementation with either YriA or YriB alone failed to restore growth
322 but a plasmid expressing the region from *yriB* to *yriA,* mimicking the native genomic arrangement
323 (*yriAB*), partially rescued the growth defect (Figure 6C, top panel). In our plasmid construct
324 encoding YriB and YriAB, there is a possibility of a spurious small protein produced due to the
325 intact, out-of-frame YriA start codon within the *yriB* ORF (Figure 6C, schematic) that potentially
326 interferes with the complementation. To address this issue, we created a modified *yriB* construct

327 where YriA start codon ATG is mutated to TAA, this substitution changes codons 4 (Asp) and 5
328 (Val) in YriB to 4 (Ile) and 5 (Ile). This variant of YriB confers full complementation (Figure 6C, top
329 panel), indicating that loss of YriB contributes to the growth phenotype, at least in part. In addition,
330 we see that the growth defect associated with *yriAB* deletion is specific to low magnesium stress
331 condition (Figure 6C, bottom panel).
332
333 Finally, the growth defect observed in *ΔyqhI* is not complemented with a plasmid encoding YqhI
334 (Figure 6D), which suggests that this phenotype is not directly related to the YqhI protein itself.
335 Intriguingly, we did not see a growth defect in *ΔmgtS* strain when grown in a low magnesium
336 medium (Figure 5), contrasting with the previous report [31]. This discrepancy might be due to
337 differences in strain construction and/or growth media. Together, our results underscore the
338 complexities in studying overlapping small ORFs and their phenotypes.
339

340 **Seven small proteins affect growth and cell morphology upon overexpression.**

341 As a parallel approach to analyzing loss-of-function phenotypes, we explored the phenotypes
342 associated with the overexpression of small proteins. We cloned the genes corresponding to the
343 untagged small proteins into either an IPTG-inducible (all except DinQ as we were unable to
344 generate a DinQ clone in the IPTG-inducible pEB52 background) or arabinose-inducible (DinQ)
345 vector. Upon induction, slow growth or a prolonged lag phase is observed for 7 out of the 17 small
346 proteins tested: MgtS, MgrB, PmrR, YmiA, YoaI, YkgS, and DinQ (Figure 7). Notably, six of these
347 proteins are membrane-bound (MgtS, MgrB, PmrR, YmiA, YoaI, and DinQ). In the case of MgtS,
348 MgrB, PmrR, YmiA, and YoaI, induction of expression with IPTG leads to an extended lag phase
349 lasting for ~8-10 hours, after which the cells grow exponentially at growth rates similar to that of
350 control cells carrying empty vector, eventually reaching saturation at comparable levels.
351 Interestingly, cells expressing small proteins YkgS and DinQ did not display a long lag phase but
352 grew at a slower rate, eventually catching up to the same growth yield as the control cells. The
353 growth defect due to DinQ overexpression aligns with previous studies indicating that its
354 overexpression disrupts membrane potential and depletes intracellular ATP levels [45]. It is worth
355 noting that overexpression of the other 10 small proteins, including 3 membrane proteins YdgU,
356 YmiC, and YobF had a negligible impact on cell growth under the same condition, suggesting that
357 cells may tolerate high amounts of these proteins (Figure 7). More importantly, the lack of a
358 phenotype for most of these small proteins indicates that the growth defects observed here are
359 not due to a generic burden on the cell from plasmid-driven protein overexpression.
360
361 To be cautious in interpreting the overexpression data, we considered the possibility that the
362 observed growth defects might be attributed to a cryptic small open reading frame or regulatory
363 element within the small ORF being overexpressed. To check if the growth defects are indeed
364 small protein-dependent, we prepared plasmid constructs containing variants of the small protein
365 where the start codon (ATG) is substituted with a stop codon (TAA). For all 7 small proteins
366 displaying overexpression phenotypes, we repeated the growth assay with the start codon
367 mutants of each small protein. Expression of the mutant small proteins rescued the growth defect
368 with the cells exhibiting similar growth patterns to those carrying the empty vector (Figure 8A),
369 reinforcing that the observed growth defects are specific to the overexpression of these small
370 proteins.

371
372 In addition to the impact on growth, we explored whether overexpression of these 7 small proteins
373 (MgtS, MgrB, PmrR, YmiA, YoaI, YkgS, and DinQ) influences cell size and morphology, especially
374 given the delayed growth (Figures 7, 8A). We hypothesized that cells overexpressing these small
375 proteins may undergo morphological changes as part of adaptation during the extended lag and
376 log phases of growth. Using phase contrast microscopy, we imaged cells induced for expression
377 of the small proteins during the lag and exponential growth phases. As controls, we used wild-
378 type cells carrying either an empty vector or a plasmid containing a variant of the small ORF
379 where its start codon (ATG) is mutated to a stop (TAA). The control cells exhibited a roughly
380 uniform cell size with volumes around 1.1-1.3 fL and 1.2-1.4 fL in lag and log phases, respectively.
381 Intriguingly, overexpression of small proteins MgtS, MgrB, PmrR, YkgS, YoaI, and YmiA causes
382 distinct changes in cell size (Figures 8B, S6). Specifically, overexpression of MgtS results in
383 smaller cell size (Figure 8B), with a reduction in cellular volume to ~30-36% of the control cells
384 carrying either empty vector or start codon mutants in both lag and log phases (Figure S6).
385 Similarly, overexpression of PmrR and YoaI leads to a ~29% decrease in cell size and volume
386 during the lag phase, however, the cell size reverts to that of control cells during the exponential
387 phase (Figures 8B, S6). In contrast, overexpression of MgrB leads to an increase in cell size, with
388 an average volume of 2.2 fL, ~1.6-fold larger than the controls in the lag phase (Figures 8B, S6),
389 akin to the Δ*phoQ* cells grown in low magnesium conditions (Figure S7). This finding is remarkable
390 because MgrB is known to inhibit PhoQ [26,27], consistently, plasmid overexpression of MgrB likely
391 leads to strong inhibition of PhoQ, resulting in a cellular morphology similar to that of Δ*phoQ*.
392 These cells eventually return to normal size (cell volume of 1.2 fL) in the exponential phase.
393 Overexpression of YkgS and YmiA causes varying extents of cell elongation affecting cell size
394 and volume (Figures 8B, S6). Cells overexpressing DinQ did not show a significant change in cell
395 size.
396
397 Overall, the slow or delayed growth observed here along with the diverse morphological
398 phenotypes at distinct growth stages reflects how cells adapt in response to the overexpression
399 of small proteins mentioned above.
400

401 **Small protein YoaI connects distinct signaling systems – PhoQ-PhoP, PhoR-PhoB, and**
402 **EnvZ-OmpR.**

403 We wondered whether the growth delay observed upon overexpression of the 7 small proteins
404 described above is PhoQ-dependent, given the pivotal role of PhoQ in low magnesium stress. To
405 explore this, we evaluated the effects of overexpressing these proteins in a Δ*phoQ* strain under
406 magnesium limitation. Notably, the growth phenotype associated with protein overexpression is
407 retained in the Δ*phoQ* cells, similar to those observed in the wild-type strain for 6 out of 7
408 candidates – MgrB, MgtS, PmrR, YmiA, YkgS, and DinQ (Figures 8C), indicating that these
409 effects are PhoQ-independent. Interestingly, in the case of YoaI overexpression, the extended
410 lag phase observed in wild-type cells is completely abolished in the Δ*phoQ* cells, suggesting a
411 direct or indirect link between PhoQ and YoaI where PhoQ functions upstream of YoaI in this
412 regulatory pathway.
413

To check if YoaI and PhoQ physically interact with each other, we employed a bacterial two-hybrid (BACTH) assay based on reconstituting split adenylyl cyclase (CyaA) [55,56]. In this system, CyaA activity is restored when the two fragments T18 and T25 come close leading to an increase in cyclic AMP (cAMP) levels and subsequent expression of β-galactosidase (β-gal) from the *lac* promoter. We fused the T18 fragment to YoaI and tested it against T25-PhoQ. We included the T18-MgrB and T25-PhoQ pair as a positive control and two other histidine kinases, PhoR and EnvZ, each fused to the T25 fragment as additional controls. In this experiment, YoaI did not show an interaction with either PhoQ or PhoR, however, to our surprise there was a strong signal between YoaI and EnvZ that is comparable to the positive control (Figure 9A). EnvZ is primarily known to be an osmosensor, integral to the EnvZ-OmpR two-component system, which regulates porins in response to changes in osmolarity, pH, temperature, and growth phase [40]. Several small membrane proteins are known to modulate the activities of sensor kinases [14]. A 127-amino acid protein, MzrA regulates EnvZ resulting in higher levels of phosphorylated OmpR [57]. Based on the BACTH interaction between YoaI and EnvZ, we suspected YoaI might influence the activity of the EnvZ-OmpR signaling system. To address this possibility, we utilized an EnvZ-OmpR-regulated transcriptional reporter strain with chromosomal fusion of mScarlet to $P_{omrB}$ [58] and measured *omrB* promoter activity in cells grown in low magnesium vs. no-stress media. Interestingly, we observe an increase of 2.5-fold in EnvZ-regulated transcription under stress in wild-type cells (Figure 9B). The significantly high activity of *omrB* reporter in low $Mg^{2+}$ conditions suggests that upregulation of YoaI protein levels may mediate this effect (Figures 4C, S4). Upon deletion of *yoaI*, the *omrB* transcription reduced by ~1.4-1.5-fold in both low and high $Mg^{2+}$ media, indicating that YoaI affects EnvZ-OmpR activity regardless of stress. Together with our observation that YoaI-SPA levels increase under low $Mg^{2+}$ stress (Figures 4C, S4B), the higher transcriptional activity of the EnvZ-regulated promoter can be attributed to the positive interaction of YoaI with EnvZ. To further support the idea that an increase in YoaI levels is responsible for modulating the activity of the EnvZ-OmpR system, we examined *omrB* transcription upon plasmid overexpression of YoaI in wild-type *E. coli* cells. We observed a greater than 6-fold increase in $P_{omrB}$-*lacZ* reporter activity in cells expressing YoaI on a plasmid (Figure S8A) relative to the control cells carrying an empty vector. We also tested two other reporters to genes *ompF*, $P_{ompF}$-YFP and *ompC*, $P_{ompC}$-CFP [59], and found a ~2-fold change in their transcriptional activities (Figures S8B, C), consistent with the activation of EnvZ [40,60,61]. In summary, these findings suggest that YoaI interacts with and stimulates EnvZ activity, potentially enhancing OmpR-P levels.

## Discussion

In this study, we identified 17 small proteins (≤50 amino acids) induced by low magnesium stress from approximately 150 documented small proteins in *E. coli*, using Ribo-RET [37,38]. Only 3 of these proteins, MgrB, MgtS, and PmrR were previously studied in the context of magnesium starvation [27,31,33]. For all the stress-induced small proteins except one (YoaI), expression from the genomic locus was verified *in vivo* (Table S5). In a previous report when cells were grown in a rich medium, expression of YoaI tagged with SPA epitope from a genomic translation fusion was undetected [21]. Interestingly, our observation of cells grown in low $Mg^{2+}$ detected a robust expression of YoaI expression using the same construct, highlighting the condition-specific expression of this protein (Figures 4C, S4B). Using RNA-Seq, we found that

458 many of these stress-induced proteins are transcriptionally activated in low magnesium media.
459 Further, we identified the regions upstream of these small ORFs responsible for transcriptional
460 regulation using operon fusions and reporter assays. Few hits, including YoaI and YobF, do not
461 show a change in transcription levels under low $Mg^{2+}$, suggesting that they are regulated post-
462 transcriptionally.
463
464 Lacking any functional or phenotypic information for most of these stress-induced proteins, we
465 began their characterization by predicting their subcellular localization using bioinformatic tools
466 (Tables 1, S6). By epitope tagging and imaging or western blotting, we empirically determined
467 that 9 of the 17 shortlisted stress-induced small proteins localize to the membrane (Figure S5).
468 These membrane-bound small proteins may interact with, stabilize, or fine-tune the activities of
469 large transmembrane proteins, such as sensor kinases, channel proteins, and drug efflux pumps,
470 thereby mediating cellular adaptation and stress responses [14]. Among the 9 candidates, three
471 proteins – MgrB, MgtS, and PmrR are shown to have specific membrane protein targets, as
472 described earlier. To further investigate their biological roles, we performed targeted deletion and
473 protein overexpression analysis.
474
475 Loss-of-function analysis of small proteins can be a useful approach to understanding their
476 physiological roles. For example, deleting *mgrB* causes hyperactivation of the PhoQP two-
477 component system, leading to cell division inhibition and filamentation of cells grown under low
478 magnesium stress [28]. In clinical isolates of *Klebsiella pneumoniae,* the absence of MgrB-mediated
479 PhoQ inhibition has been linked to acquired colistin resistance [30,62]. In the current work, we found
480 deletion phenotypes associated with the following small proteins—PmrR, YobF, YriA/B, and YqhI
481 —leading to an early entry into the stationary phase and reduced yield at saturation under
482 magnesium limitation. Based on plasmid complementation, growth defects caused by PmrR and
483 YobF are specific to the respective small proteins. The overlapping ORFs of YriA and YriB present
484 a unique challenge in interpreting the Δ*yriAB* growth phenotype observed under low magnesium
485 stress. While expressing the native *yriAB* region partially rescues the defect, individual expression
486 of YriA or YriB fails to do so; however, modifying YriB by mutating the out-of-frame YriA start
487 codon fully restores growth, emphasizing that the loss of YriB is a critical factor in the observed
488 phenotype. In the case of YqhI, the deletion phenotype could not be fully complemented by
489 plasmid-encoded small protein, pointing to putative cryptic ORF or regulatory factors within the
490 small ORF that warrant further investigation.
491
492 We also analyzed overexpression phenotypes associated with each of the stress-induced small
493 proteins to gain insights into cellular pathways or components functionally linked to these proteins.
494 For instance, overexpression of MgtS is shown to activate the PhoRB two-component system by
495 regulating the phosphate transporter, PitA [32]. Similarly, DinQ overexpression disrupts membrane
496 potential and depletes intracellular ATP levels [45]. We observed overexpression phenotypes for 7
497 of the 17 small proteins induced under magnesium stress—MgtS, MgrB, PmrR, YmiA, YoaI,
498 YkgS, and DinQ—resulting in either a long lag phase or slow growth (Figure 7). These
499 overexpression phenotypes are specific to each small protein as we see control plasmids carrying
500 a mutated start codon do not cause growth defects (Figure 8A). Analysis of the cell morphology
501 during the lag and exponential phases of growth revealed interesting variations in cell sizes and

volumes that reflect how cells adapt to the overexpression of these small proteins. Remarkably for one of the small proteins, PmrR, both the deletion and overexpression caused growth defects under low magnesium stress. It is unclear how cells balance small protein levels when needed during specific conditions vs. when not needed, say in the absence of stress. In this context, complementation of the *ΔpmrR* strain with plasmid-encoded PmrR restored normal growth under magnesium limitation but caused a growth defect under no-stress condition (Figure 6A). This suggests that PmrR levels may be controlled precisely in cells undergoing stress, as both its absence and its overexpression disrupt the balance necessary for cellular homeostasis.

In *Salmonella enterica,* PmrR has been shown to inhibit the inner membrane protein LpxT, which plays a role in lipopolysaccharide modification [33,34,36]. We explored whether the growth defects associated with PmrR deletion and overexpression in *E. coli* are mediated through its interaction with LpxT. Interestingly, expressing PmrR in a Δ*lpxT* background did not alleviate the growth defects regardless of stress (Figure S9A). It is possible that higher LpxT levels, resulting from the absence of PmrR, could lead to growth defects. However, both single deletions (*ΔlpxT* and *ΔpmrR*) and the double deletion (*ΔpmrR ΔlpxT*) exhibited growth defects under magnesium stress (Figure S9B). This result suggests that the growth defect upon *pmrR* deletion is independent of PmrR's interaction with LpxT. PmrR may be involved in other pathways or regulatory mechanisms where it has additional interacting partners. It is not uncommon for small proteins to have multiple binding partners, as seen with MgtS, which interacts with both MgtA and PitA [31,32]. Whether PmrR associates with other targets contributing to phenotypes observed here warrants further investigation.

Finally, we would like to discuss the interesting case of the small membrane protein YoaI, whose transcription is controlled by the PhoR-PhoB signaling system [47–49]. YoaI levels are quite low or undetectable when cells are grown in a rich medium or specific stress conditions [21,22]. However, we find that YoaI protein levels strongly increase under magnesium limitation and it becomes detectable (Figure 4C). Overexpression of YoaI leads to a long delay in growth (Figures 7, 8A, S4B). This phenotype is abolished in a *phoQ* mutant (Figure 8C), hinting at an unknown PhoQ-dependent factor that may contribute to the growth defect observed upon YoaI overexpression. Through a bacterial two-hybrid assay, we found a direct interaction of YoaI with the EnvZ sensor kinase (Figure 9A), which controls osmoregulation [40] suggesting that this small protein acts as a connector between the PhoR-PhoB and EnvZ-OmpR signaling networks. Activation of EnvZ by YoaI is supported by the data from our transcriptional reporter analysis of promoters regulated by the EnvZ-OmpR system (Figures 9B, S8). Modulation of sensor kinases via small protein connectors appears to be a general theme that many small membrane proteins of unknown function may fall under [14]. For instance, under acidic conditions, a 65-amino acid protein SafA is activated by the EvgS-EvgA two-component system, which subsequently interacts with and activates the PhoQ-PhoP system [63]. In a second example, an 88-amino acid protein PmrD connects the PmrB-PmrA and PhoQ-PhoP signaling systems in *Salmonella* [64,65]. Another 127-amino acid protein MzrA is known to bind and activate EnvZ, which links the CpxA-CpxR and EnvZ-OmpR pathways in *E. coli* [57]. Taken together, our findings outlining the transcriptional regulation of YoaI by PhoB (Figure 4A), PhoQ-dependent growth phenotype upon YoaI overexpression (Figure 8C), and YoaI's physical interaction with EnvZ and

546 modulation of EnvZ-regulated promoter activity (Figures 9B, S8) reveal how this 34-amino acid
547 small protein acts as a connector between distinct two-component signaling systems – PhoRB,
548 PhoQP, and EnvZ-OmpR to integrate diverse stress responses (Figure 9C).
549
550 Most small proteins (≤50 amino acids in prokaryotes) are of unknown function and little is known
551 about when/if they are expressed in the cell and what their physiological relevance is. Small
552 proteins are thought to fine-tune the activity and/or stability of larger target molecules in the cell,
553 adding a layer of gene regulation. This type of conditional regulation by small proteins may be
554 especially important when cells are grown in non-ideal or stressful environments. Overall, our
555 work describing the identification of condition-specific small proteins and targeted phenotypic
556 characterization provides a deeper understanding of small protein regulation and the
557 physiological consequences of altering their expression levels, laying a foundation for
558 deciphering their functions and regulatory mechanisms under relevant stress conditions.
559
560

## 561 Materials and methods

562

563 **Media and growth conditions.**
564 Bacterial cultures were grown in either Luria-Bertani (LB) Miller medium (IBI Scientific) or
565 minimal A medium [66] supplemented with 0.2% glucose, 0.1% casamino acids, and the indicated
566 concentration of $MgSO_4$, with aeration at 37°C, unless otherwise specified. In general, overnight
567 cultures are grown in supplemented minimal A medium containing 1 mM $MgSO_4$ and
568 antibiotic(s) as applicable. Saturated cultures are diluted 1:500 into fresh medium. For low $Mg^{2+}$
569 stress, no $Mg^{2+}$ was added when overnight cultures were diluted into fresh medium. Media
570 containing 10 mM $Mg^{2+}$ was used as the no-stress condition. For phosphate stress experiments,
571 MOPS minimal medium (Teknova) supplemented with 0.2% glucose, 0.1% casamino acids, and
572 either 1 mM $K_2HPO_4$ (no-stress) or no $K_2HPO_4$ (phosphate stress). For routine growth on solid
573 medium, LB containing 1.5% bacteriological-grade agar (VWR Lifesciences) was used. For
574 antibiotic selection, carbenicillin, kanamycin, and chloramphenicol were added at a final
575 concentration of 50-100 µg $ml^{-1}$, 25- 50 µg $ml^{-1}$, and 6-25 µg $ml^{-1}$. b-isopropyl-D-thiogalactoside
576 (IPTG) was used at a final concentration of 500 µM, unless otherwise specified. Arabinose was
577 used at final concentrations of 0.5% and 30 mM for pBAD24-based vectors and pMR120-based
578 vectors, respectively, to induce protein expression when needed.
579

580 **Strains, plasmids, and cloning.**
581 See supplemental information for details of the strains (Table S1), plasmids (Table S2), and
582 primers (Table S3) used in this study. All the strains used were derived from *Escherichia coli K-*
583 *12* MG1655. Strain JW2162 was a gift from Dr. Bryce Nickels; plasmids pEB52, pAL38, pAL39,
584 pSMART, pMR120 and strains AML67, MDG147, TIM92, TIM100, and TIM202 were gifts from
585 Dr. Mark Goulian. Strains GSO195, GSO219, GSO225, GSO232, and GSO317 were gifts from
586 Dr. Gisela Storz. Strains JM2110 and JM2113 were kind gifts from Dr. Maude Guillier.
587
588 A modified version of the method described by [67] was used to generate in-frame gene deletions
589 corresponding to each small protein. Briefly, the entire small open reading frame (sORF)

590 (including the stop codon) was deleted from the MG1655 genome and substituted with a
591 kanamycin resistance cassette. While constructing the gene deletions, we avoided deleting any
592 overlapping annotated ORFs, non-coding RNAs, or putative regulatory regions in the vicinity of
593 the target gene. In the case of *yriA-yriB (yriAB),* the two small protein ORFs significantly
594 overlapped; therefore, we deleted the combined *yriAB* ORF. Detailed information on the
595 genomic coordinates of deleted regions can be found in Table S1. Genomic deletions and
596 reporter constructs carrying the kanamycin resistance cassettes were transferred between
597 strains using $P1_{vir}$ transduction [66] and validated by PCR. When necessary, the kanamycin
598 cassette was excised from the chromosome by FLP-mediated recombination using pCP20, as
599 previously described [68]. PCR and loss of antibiotic resistance confirmed the excision of the
600 kanamycin cassette.
601
602 Plasmids expressing translational fusions of GFP-A206K to the small open reading frames
603 (sORFs), specifically pPJ1-13 and pSV25, were generated through inverse PCR [69] using pAL39
604 as a template. Plasmids encoding C-terminally 6XHis-tagged-YobF and -PmrR (sORF-GGSG
605 linker-6XHis) were created using inverse PCR with pEB52 as a template, resulting in pSV14
606 and pSV26, respectively. Plasmids encoding untagged small proteins (pSV30-pSV37, pSV58,
607 pSV60, and pJS1-pJS7) were also generated by inverse PCR with pEB52 as a template. pSV54
608 was generated by inverse PCR using pBAD24 as a template. Plasmids pSV38-pSV45, pSV55,
609 pSV59, and pSV61, encoding variants of sORFs with start codon substitutions to stop codons
610 (TAA), were generated by site-directed mutagenesis with inverse PCR using templates pSV35,
611 pSV34, pJS7, pJS4, pSV36, pJS5, pSV54, pSV37, and pSV60 as applicable. For pSV39-
612 pSV42, another in-frame start codon within five amino acids of the annotated start was also
613 substituted to TAA. All constructs were verified by Sanger sequencing. To generate pSV47, *yoaI*
614 was PCR amplified from the MG1655 genome, digested with *XbaI/EcoRI* restriction enzymes,
615 and then cloned into pUT18C at *XbaI/EcoRI* sites.
616
617 To examine the transcriptional regulation of the sORFs and identify the putative regulatory
618 regions, ~200-500 bp upstream region of the start codon of each sORF was selected for cloning
619 (see details in Table 2). If a given sORF was suspected to be part of an operon, two putative
620 regions were chosen for analysis, the first directly upstream of the gene and a second region
621 upstream of the entire operon. Each DNA segment was amplified from MG1655 genomic DNA
622 by PCR and inserted upstream of the *yfp* reporter gene in pMR120 into the restriction sites
623 (*XhoI/BamHI* to construct pSV16, while *EcoRI-BamHI* sites were used for the remaining
624 constructs). The pMR120 vector also includes a *cfp* reporter regulated by a constitutive *tetA*
625 promoter, serving as an internal plasmid control. The resulting plasmids (pPJ14, pPJ16-pPJ20,
626 pPJ23, pSV16-21, pSV24, pSV28, pSV29) were confirmed by Sanger sequencing and
627 transformed into MG1655 and TIM202 (*ΔphoQ)*. Note that pSMART (Lucigen), pMR120, and
628 the derivatives are single-copy plasmids when transformed into *E. coli* [70]. *E. cloni* replicator cells
629 (Lucigen) are transformed with these plasmids and cultured with arabinose induction to increase
630 the copy number for plasmid isolation.
631
632 **Translation initiation profiling (Ribo-RET) and RNA-Seq.**

633 Overnight cultures of wild-type *E. coli* grown in supplemented minimal A medium and 1 mM
634 $MgSO_4$ were diluted 1:500 in 100 ml of fresh medium and the specified concentrations of
635 $MgSO_4$. Once the cultures reached an OD600 of ~0.4, they were split into two 50 ml conical
636 tubes. Cells from one tube were pelleted and submitted to Genewiz for RNA-Seq, while the cells
637 from the second tube were used for Ribo-RET. For Ribo-RET, cells were treated with
638 retapamulin at a final concentration of 100 µg $ml^{-1}$ for 5 minutes at 37°C with continuous
639 shaking. After retapamulin treatment, cells were filtered through a nitrocellulose membrane with
640 a pore size of 0.45 µm, quickly scraped off the surface, and flash-frozen in liquid nitrogen. The
641 resulting samples were processed, and libraries were prepared as described previously [41] with
642 the following modifications. Specifically, RNA fragments of 15-30 nucleotides (nt) in length were
643 isolated by performing a tight gel size selection, and rRNA depletion was performed using the
644 RiboCop for Gram-negative bacteria kit (Lexogen). The resulting RNA fragments were then
645 pooled, and libraries were prepared, with a final library structure consisting of a 5' adapter – 4
646 random bases – insert – 5 random bases – sample barcode – 3' adapter. The randomized
647 bases serve as Unique Molecular Identifiers (UMIs) for deduplication. The multiplexed library
648 was sequenced on an Illumina HiSeq 4000 with a paired end reading of 150 bases (PE150
649 runs) at a sequencing depth of 40-60 million raw reads per sample.
650
651 **Sequencing data analysis.**
652 The raw sequencing data for this project has been deposited in the GEO database with the
653 accession number GSE276379. An R package with codes for data processing and analysis has
654 been made available on GitHub (https://github.com/yadavalli-lab/Small-proteins-induced-under-
655 low-magnesium-stress-in-E.coli). The raw sequencing data was first demultiplexed, and the
656 adaptors were removed using cutadapt [71]. The reads were then depleted of rRNA and tRNA and
657 deduplicated using umi_tools dedup [72]. The Ribo-RET reads were aligned to the *E. coli* MG1655
658 genome NC_000913.3 (RefSeq assembly accession: GCF_000005845.2) using hisat2 [73], and
659 the ribosome density was assigned to the 3' end of the reads. Initiation peak density was
660 calculated for the annotated translation start sites by summing up the normalized reads (reads
661 per million, RPM) within 4 to 20 nt downstream of the first nucleotide in the start codon. For
662 transcript quantification of RNA-Seq reads, Kallisto [74] was used. DESeq2 [75] was used for the
663 differential expression analysis of gene expression in the RNA-Seq data. Normalization of the
664 data for differential expression was carried out using the "apeglm" method [76]. Fold-changes
665 were estimated by comparing two replicates of the low $Mg^{2+}$ dataset to two replicates of the no-
666 stress dataset, with filtering criteria set at more than two-fold changes and a p-value below 0.05.
667
668 **Measurement of growth (optical density) and fluorescence using a microplate reader.**
669 The optical density ($OD_{600}$) measurements for small protein overexpression and deletion
670 constructs were performed in a clear flat bottom 96-well microplate (Corning) containing 150 µL
671 culture per well using a microplate reader (Agilent BioTek Synergy Neo2S). Fluorescence
672 measurements for transcriptional reporters were carried out similarly, using black-walled, clear-
673 flat bottom 96-well microplates (Corning). Saturated cultures grown in supplemented minimal A
674 or MOPS minimal medium were normalized to the same initial $OD_{600}$ values across all samples
675 and diluted 1:50 in fresh medium containing specified concentrations of $MgSO_4$ or $K_2HPO_4$,
676 along with appropriate antibiotics and inducers, as indicated. The microplates were incubated at

677 37 °C with double orbital shaking before the real-time measurements of optical density (at 600
678 nm), YFP (excitation: 500 nm; emission: 540 nm), or CFP (excitation: 420 nm; emission: 485
679 nm) were acquired every hour for 20-24 hours.
680
681 **Microscopy, and image analysis.**
682 For localization of GFP-tagged small proteins, cells were grown to an $OD_{600}$ of ~0.2 (~3 hours)
683 and then rapidly cooled in an ice slurry. Streptomycin was added to a final concentration of 250
684 μg $ml^{-1}$. GFP fluorescence was captured with a 475 nm excitation wavelength and a 540 nm
685 emission filter, with an exposure time of 30 ms and 20% intensity. While the exposure times
686 were typically set to these specified values, slight variations were occasionally made to optimize
687 imaging based on the levels of fluorescence expression observed.
688
689 For overexpression analysis, overnight cultures were diluted 1:500 into supplemented minimal
690 medium containing no added $MgSO_4$, 50 μg $ml^{-1}$ carbenicillin, and either 500 μM IPTG or 0.5%
691 arabinose, as indicated. Cells were grown to the lag phase ($OD_{600}$ ~0.005), then rapidly cooled
692 in an ice slurry before phase contrast microscopy. For empty vector control and start codon
693 variants, we captured lag phase micrograph images approximately 30-40 minutes post-
694 inoculation and -induction. For MgtS, MgrB, PmrR, YoaI, and YmiA overexpression, lag phase
695 measurements were performed at 2-3 hours, and for YkgS and DinQ, at 1-hour post-inoculation
696 and -induction. To concentrate the cells, 1 mL of the culture was pelleted and resuspended in
697 30-50 μL minimal A salt solution. For exponential phase analysis ($OD_{600}$ between 0.2-0.4) in
698 cultures carrying empty vector control and start codon variants images were taken at ~3-4
699 hours. In the case of cells expressing MgtS, MgrB, PmrR, YoaI, and YmiA, images were taken
700 at 16-18 hours, and YkgS and DinQ at 6-8 hours. Microscope slides were prepared using 1%
701 agarose pads as described previously [28], with approximately 5-7 μL of the resuspended cells. A
702 40 ms exposure time and 20% intensity were applied to capture the phase-contrast images.
703
704 For single-cell fluorescence measurements of wild type and Δ*yoaI* cells carrying $P_{omrB}$-*mScarlet*
705 reporter, overnight cultures were diluted 1:500 into fresh supplemented minimal A medium
706 containing either 10 mM or no added $MgSO_4$. Cells were grown to exponential ($OD_{600}$ ~0.3 for
707 both stress and no stress conditions) and stationary phase ($OD_{600}$ ~1.0 for stress condition and
708 ~3.5 for no stress condition), and then rapidly cooled in an ice slurry. Streptomycin was added
709 to a final concentration of 250 μg $ml^{-1}$. Fluorescence was measured using the mCherry channel
710 with an excitation wavelength of 570 nm and an emission filter of 645 nm. The exposure time
711 was set to 100 ms, with an intensity of 20%. Background fluorescence was determined by
712 imaging MG1655 cells grown under the same conditions.
713
714 For single-cell fluorescence measurements upon YoaI overexpression (to measure reporter
715 activities of $P_{ompF}$-*yfp* and $P_{ompC}$-*cfp*), the overnight cultures were diluted 1:500 into fresh
716 supplemented minimal A medium containing 10 mM $MgSO_4$. Cells were grown to exponential
717 phase ($OD_{600}$ between 0.2-0.4), then rapidly cooled in an ice slurry, and streptomycin was added
718 at 250 μg $ml^{-1}$. YFP fluorescence was measured using a 500 nm excitation wavelength and a
719 535 nm emission filter. CFP fluorescence was measured using a 435 nm excitation wavelength
720 and a 480 nm emission filter. The exposure time for YFP and CFP measurements was set to 50

721 ms, respectively, with an intensity of 20%. The background fluorescence was determined by
722 imaging MG1655/pEB52 cells grown under the same conditions.
723
724 Image visualization and acquisition were performed using a Nikon Ti-E epifluorescence
725 microscope equipped with a TI2-S-HU attachable mechanical stage. The images were captured
726 with a Prime 95B sCMOS camera from Teledyne Photometrics with 1x1 binning. All image
727 acquisition was managed using Metamorph software (Molecular Devices), version 7.10.3.279. A
728 minimum of 50 cells per replicate were analyzed for cell volume and single-cell fluorescence
729 quantification. The distributions of cellular volume were assumed to follow the sphero-cylindrical
730 shape of *E. coli.* The volume was calculated using the formula $V = \frac{pi}{4} * W^2 * \left(L - \frac{W}{3}\right)$. Images
731 were analyzed, and the cellular length, width, and fluorescence intensity were quantified using
732 ImageJ [77] and MicrobeJ plugin [78].
733
734 **Preparation of membrane and cytoplasmic fractions.**
735 Membrane and cytoplasmic protein fractions were prepared as described previously [26]. Briefly,
736 saturated cultures of MG1655/pSV14 (PmrR-GGSG-6XHis), MG1655/pSV26 (YobF-GGSG-
737 6XHis), and MG1655/pEB52 (empty vector) were diluted 1:500 in 4 ml of LB media containing
738 100 µg $ml^{-1}$ carbenicillin and grown at 37 °C. After 4 hours of growth, 0.5 mM IPTG was added
739 to the cultures, and the cells were harvested after 2 hours of induction. Cell pellets were
740 resuspended in 50 µl of cold resuspension buffer containing 20% sucrose, 30 mM Tris pH 8.0,
741 and 1X protease inhibitor cocktail (Sigma, cOmplete, EDTA-free). Then, 50 µl of 10 mg $ml^{-1}$
742 lysozyme, freshly prepared in 0.1 M EDTA pH 7.0, was added to the cell suspension, and the
743 mixture was incubated on ice for 30 minutes. Next, 1 ml of 3 mM EDTA pH 7.5 was added to
744 each sample, followed by sonication (10s pulse, 10s gap, 6 times) using VCX-130 Vibra-Cell
745 Ultrasonic sonicator (Fisher Scientific). Samples were briefly centrifuged at 6,000 rpm for 10
746 minutes at 4 °C to remove cellular debris, and the supernatant was collected and spun at
747 21,000 ×g for 30 minutes at 4 °C. The supernatant from this step is separated and stored as the
748 cytoplasmic fraction. The pellet, representing the membrane fraction, was resuspended in a
749 storage buffer containing 20 mM Tris pH 8.0/20% glycerol. For strains carrying genomic YoaI-
750 SPA translational fusion, cultures were grown to an $OD_{600}$ of ~0.2-0.4 before harvesting, and
751 membrane and cytoplasmic fractions were prepared as mentioned above.
752
753 **Western blot analysis.**
754 The membrane and cytoplasmic fractions were resuspended in 4X Laemmli sample buffer
755 containing 5% 2-mercaptoethanol and no dyes. The samples were heated at 70 °C for 10
756 minutes and run on a 12% Bis-Tris gel (NuPage, Invitrogen) using MES running buffer
757 (Invitrogen) at 160V for 80 minutes. After electrophoresis, proteins were transferred to a PVDF
758 membrane (Amersham™ Hybond™) with a 0.2 µm pore size using a semi-dry transfer cell (Bio-
759 Rad Trans-Blot SD). The membranes were blocked with 5% w/v milk in Tris-buffered saline, pH
760 7.4, with 1% Tween 20 (TBS-T). Primary antibodies – mouse M2 anti-FLAG (Sigma-Aldrich) and
761 rabbit anti-6XHis tag antibody (Rockland) were used at 1:1000 dilution to detect SPA- and
762 6XHis-tagged constructs, respectively. IRDye 800CW goat anti-mouse and IRDye 680RD
763 donkey anti-rabbit antibodies (LiCOR) were used for secondary detection. SeaBlue™ Plus2 Pre-

764 stained Protein Standard (Invitrogen) was used as a ladder to visualize lower molecular weight
765 protein bands. The proteins were visualized using a LI-COR Odyssey imager.
766
767 **Bacterial two-hybrid and β-galactosidase reporter gene assays.**
768 For the bacterial two-hybrid assay, several clones from the transformation plate were picked to
769 reduce heterogeneity [55] and inoculated in LB containing 100 µg $ml^{-1}$ ampicillin and 50 µg $ml^{-1}$
770 kanamycin. Cultures were grown overnight at 30°C with shaking. The cultures were then diluted
771 1:1000 into LB supplemented with 500 µM IPTG and grown at 30°C until $OD_{600}$ reached
772 between 0.2-0.4, after which β-galactosidase activities (Miller units) were measured as
773 previously described [79].
774
775 For the β-galactosidase reporter gene assay, strains carrying $P_{omrB}$-*lacZ* with either pSV34
776 (pYoaI) or pEB52 (empty vector) were grown overnight in LB medium with 100 µg $ml^{-1}$
777 ampicillin. The next day, the cultures were diluted 1:100 in the same medium and grown at 37
778 °C. After 3 hours of growth, 0.5 mM IPTG was added to the cultures, and the cells were
779 harvested after 2 hours of induction. For high-throughput measurements in a 96-well format, the
780 protocol was modified as previously described [79].
781
782 Resource availability
783
784 Lead contact
785 Further information and requests for resources and reagents should be directed to and will be
786 fulfilled by the lead contact, Srujana S. Yadavalli (sam.yadavalli@rutgers.edu).
787
788 Materials availability
789 Requests for strains and plasmids generated in this study should be directed to and will be
790 fulfilled by the lead contact, Srujana S. Yadavalli (sam.yadavalli@rutgers.edu).
791
792 Data and code availability
793 Next-generation sequencing data generated in this study are deposited at Gene Expression
794 Omnibus (GEO) with accession number GSE276379. All data generated or analyzed during this
795 study are included in the manuscript and its supporting files. Source data files for all figures
796 have been provided. The code used for data processing and analysis is available in a series of
797 R Markdown documents hosted on GitHub (https://github.com/yadavalli-lab/Small-proteins-
798 induced-under-low-magnesium-stress-in-E.coli).
799
800
801 Acknowledgments
802 The authors would like to thank Drs. Mark Goulian, Bryce Nickels, Gisela Storz, and Maude
803 Guillier for generously sharing strains and plasmids. We thank the past and present members of
804 the Yadavalli, Storz, and Shah Labs for their helpful discussions. We also thank Drs. Gisela
805 Storz and Mark Goulian for critical feedback on the manuscript.
806 Funding: S.S.Y. is supported by the National Institutes of Health - National Institute of General
807 Medical Sciences (NIH-NIGMS) ESI-MIRA R35 GM147566 and institutional start-up funds from
808 Rutgers. P.S. was supported by NIH/NIGMS grant R35 GM124976 and start-up funds from the
809 Human Genetics Institute of New Jersey at Rutgers University. S.V. is supported by the
810 Waksman Institute Busch Predoctoral fellowship (2022-24). The funders did not play any role in

the study design, data collection and analysis, decision to publish, or preparation of the manuscript.

## Author contributions

S.V., P.S., and S.S.Y. conceived the experiments. All authors planned the experiments, designed the methodology, and performed data analysis. S.V., P.S., and S.S.Y. wrote the initial draft of the manuscript, P.S. contributed to revisions and editing, and all authors reviewed the final manuscript.

## Declaration of interests

S.S.Y. consults for and collaborates with Designs for Vision, Inc. P.S. a director at an RNA-therapeutics startup, and consults for Designs for Vision, Inc. S.V. declared that no competing interests exist.

## References


1. Carlberg, C., and Molnar, F. (2016). Mechanisms of Gene Regulation 2nd ed. (Springer).

2. Goulian, M. (2010). Two-component signaling circuit structure and properties. Curr. Opin. Microbiol. *13*, 184–189.

3. Stock, A.M., Robinson, V.L., and Goudreau, P.N. (2000). Two-component signal transduction. Annu. Rev. Biochem. *69*, 183–215.

4. Laub, M.T. (2014). The role of two-component signal transduction systems in bacterial stress responses. In Bacterial Stress Responses (ASM Press), pp. 45–58.

5. Baumberg, S. ed. (1999). Prokaryotic Gene Expression. Preprint at Oxford University PressOxford, https://doi.org/10.1093/oso/9780199636044.001.0001 https://doi.org/10.1093/oso/9780199636044.001.0001.

6. Banerjee, T. (2022). Regulation of Gene Expression in Prokaryotes. In Genetics Fundamentals Notes (Springer Nature Singapore), pp. 569–596.

7. Tollerson, R., 2nd, and Ibba, M. (2020). Translational regulation of environmental adaptation in bacteria. J. Biol. Chem. *295*, 10434–10445.

8. Cain, J.A., Solis, N., and Cordwell, S.J. (2014). Beyond gene expression: the impact of protein post-translational modifications in bacteria. J. Proteomics *97*, 265–286.

9. Gottesman, S. (2019). Trouble is coming: Signaling pathways that regulate general stress responses in bacteria. J. Biol. Chem. *294*, 11685–11700.

10. Storz, G., Vogel, J., and Wassarman, K.M. (2011). Regulation by small RNAs in bacteria: expanding frontiers. Mol. Cell *43*, 880–891.

850 11. Seshasayee, A.S.N., Sivaraman, K., and Luscombe, N.M. (2011). An overview of
851 prokaryotic transcription factors : a summary of function and occurrence in bacterial
852 genomes. Subcell. Biochem. *52*, 7–23.

853 12. Burton, A.T., Zeinert, R., and Storz, G. (2024). Large Roles of Small Proteins. Annu. Rev.
854 Microbiol. https://doi.org/10.1146/annurev-micro-112723-083001.

855 13. Hemm Matthew R., Weaver Jeremy, Storz Gisela, Lovett Susan T., and Hinton Deborah
856 (2020). Escherichia coli Small Proteome. EcoSal Plus *9*.
857 https://doi.org/10.1128/ecosalplus.ESP-0031-2019.

858 14. Yadavalli, S.S., and Yuan, J. (2022). Bacterial Small Membrane Proteins: the Swiss Army
859 Knife of Regulators at the Lipid Bilayer. J. Bacteriol. *204*, e0034421.

860 15. Gray, T., Storz, G., and Papenfort, K. (2022). Small Proteins; Big Questions. J. Bacteriol.
861 *204*, e0034121.

862 16. Pueyo, J.I., Magny, E.G., and Couso, J.P. (2016). New peptides under the s(ORF)ace of
863 the genome. Trends Biochem. Sci. *41*, 665–678.

864 17. Patraquim, P., Mumtaz, M.A.S., Pueyo, J.I., Aspden, J.L., and Couso, J.-P. (2020).
865 Developmental regulation of canonical and small ORF translation from mRNAs. Genome
866 Biol. *21*, 128.

867 18. Sberro, H., Fremin, B.J., Zlitni, S., Edfors, F., Greenfield, N., Snyder, M.P., Pavlopoulos,
868 G.A., Kyrpides, N.C., and Bhatt, A.S. (2019). Large-Scale Analyses of Human Microbiomes
869 Reveal Thousands of Small, Novel Genes. Cell *178*, 1245-1259.e14.

870 19. Kastenmayer, J.P., Ni, L., Chu, A., Kitchen, L.E., Au, W.-C., Yang, H., Carter, C.D.,
871 Wheeler, D., Davis, R.W., Boeke, J.D., et al. (2006). Functional genomics of genes with
872 small open reading frames (sORFs) in S. cerevisiae. Genome Res. *16*, 365–373.

873 20. Steinberg, R., and Koch, H.-G. (2021). The largely unexplored biology of small proteins in
874 pro- and eukaryotes. FEBS J. *288*, 7002–7024.

875 21. Hemm, M.R., Paul, B.J., Schneider, T.D., Storz, G., and Rudd, K.E. (2008). Small
876 membrane proteins found by comparative genomics and ribosome binding site models.
877 Mol. Microbiol. *70*, 1487–1501.

878 22. Hemm, M.R., Paul, B.J., Miranda-Ríos, J., Zhang, A., Soltanzad, N., and Storz, G. (2010).
879 Small stress response proteins in Escherichia coli: proteins missed by classical proteomic
880 studies. J. Bacteriol. *192*, 46–58.

881 23. Groisman, E.A., and Chan, C. (2021). Cellular Adaptations to Cytoplasmic Mg2+ Limitation.
882 Annu. Rev. Microbiol. *75*, 649–672.

883 24. Groisman, E.A., Duprey, A., and Choi, J. (2021). How the PhoP/PhoQ System Controls
884 Virulence and Mg2+ Homeostasis: Lessons in Signal Transduction, Pathogenesis,
885 Physiology, and Evolution. Microbiol. Mol. Biol. Rev. *85*, e0017620.

886 25. Groisman, E.A. (2001). The pleiotropic two-component regulatory system PhoP-PhoQ. J.
887 Bacteriol. *183*, 1835–1842.

26. Yadavalli Srujana S., Goh Ted, Carey Jeffrey N., Malengo Gabriele, Vellappan Sangeevan, Nickels Bryce E., Sourjik Victor, Goulian Mark, Yuan Jing, and Silhavy Thomas J. (2020). Functional Determinants of a Small Protein Controlling a Broadly Conserved Bacterial Sensor Kinase. J. Bacteriol. *202*, e00305-20.

27. Lippa, A.M., and Goulian, M. (2009). Feedback inhibition in the PhoQ/PhoP signaling system by a membrane peptide. PLoS Genet. *5*, e1000788.

28. Yadavalli, S.S., Carey, J.N., Leibman, R.S., Chen, A.I., Stern, A.M., Roggiani, M., Lippa, A.M., and Goulian, M. (2016). Antimicrobial peptides trigger a division block in Escherichia coli through stimulation of a signalling system. Nat. Commun. *7*, 1–10.

29. Patel, V., and Matange, N. (2021). Adaptation and compensation in a bacterial gene regulatory network evolving under antibiotic selection. Elife *10*. https://doi.org/10.7554/eLife.70931.

30. Cannatelli, A., Giani, T., D'Andrea, M.M., Di Pilato, V., Arena, F., Conte, V., Tryfinopoulou, K., Vatopoulos, A., Rossolini, G.M., and COLGRIT Study Group (2014). MgrB inactivation is a common mechanism of colistin resistance in KPC-producing Klebsiella pneumoniae of clinical origin. Antimicrob. Agents Chemother. *58*, 5696–5703.

31. Wang, H., Yin, X., Wu Orr, M., Dambach, M., Curtis, R., and Storz, G. (2017). Increasing intracellular magnesium levels with the 31-amino acid MgtS protein. Proc. Natl. Acad. Sci. U. S. A. *114*, 5689–5694.

32. Yin, X., Wu Orr, M., Wang, H., Hobbs, E.C., Shabalina, S.A., and Storz, G. (2019). The small protein MgtS and small RNA MgrR modulate the PitA phosphate symporter to boost intracellular magnesium levels. Mol. Microbiol. *111*, 131–144.

33. Kato, A., Chen, H.D., Latifi, T., and Groisman, E.A. (2012). Reciprocal control between a bacterium's regulatory system and the modification status of its lipopolysaccharide. Mol. Cell *47*, 897–908.

34. Hong, X., Chen, H.D., and Groisman, E.A. (2018). Gene expression kinetics governs stimulus-specific decoration of the *Salmonella* outer membrane. Sci. Signal. *11*. https://doi.org/10.1126/scisignal.aar7921.

35. Chen, A.I., Albicoro, F.J., Zhu, J., and Goulian, M. (2021). Effects of regulatory network organization and environment on PmrD connector activity and polymyxin resistance in Klebsiella pneumoniae and Escherichia coli. Antimicrob. Agents Chemother. *65*. https://doi.org/10.1128/AAC.00889-20.

36. Tian, X., Manat, G., Gasiorowski, E., Auger, R., Hicham, S., Mengin-Lecreulx, D., Boneca, I.G., and Touzé, T. (2021). LpxT-Dependent Phosphorylation of Lipid A in Escherichia coli Increases Resistance to Deoxycholate and Enhances Gut Colonization. Front. Microbiol. *12*, 676596.

37. Meydan, S., Marks, J., Klepacki, D., Sharma, V., Baranov, P.V., Firth, A.E., Margus, T., Kefi, A., Vázquez-Laslop, N., and Mankin, A.S. (2019). Retapamulin-Assisted Ribosome Profiling Reveals the Alternative Bacterial Proteome. Mol. Cell *74*, 481-493.e6.

927 38. Weaver, J., Mohammad, F., Buskirk, A.R., and Storz, G. (2019). Identifying Small Proteins
928 by Ribosome Profiling with Stalled Initiation Complexes. MBio *10*.
929 https://doi.org/10.1128/mBio.02819-18.

930 39. Gardner, S.G., and McCleary, W.R. (2019). Control of the phoBR Regulon in Escherichia
931 coli. EcoSal Plus *8*. https://doi.org/10.1128/ecosalplus.ESP-0006-2019.

932 40. Kenney, L.J., and Anand, G.S. (2020). EnvZ/OmpR Two-Component Signaling: An
933 Archetype System That Can Function Noncanonically. EcoSal Plus *9*.
934 https://doi.org/10.1128/ecosalplus.ESP-0001-2019.

935 41. Cope, A.L., Vellappan, S., Favate, J.S., Skalenko, K.S., Yadavalli, S.S., and Shah, P.
936 (2022). Exploring Ribosome-Positioning on Translating Transcripts with Ribosome Profiling.
937 Methods Mol. Biol. *2404*, 83–110.

938 42. Glaub, A., Huptas, C., Neuhaus, K., and Ardern, Z. (2020). Recommendations for bacterial
939 ribosome profiling experiments based on bioinformatic evaluation of published data. J. Biol.
940 Chem. *295*, 8999–9011.

941 43. Kato, A., Tanabe, H., and Utsumi, R. (1999). Molecular characterization of the PhoP-PhoQ
942 two-component system in Escherichia coli K-12: identification of extracellular Mg2+-
943 responsive promoters. J. Bacteriol. *181*, 5516–5520.

944 44. Hobbs, E.C., Astarita, J.L., and Storz, G. (2010). Small RNAs and small proteins involved in
945 resistance to cell envelope stress and acid shock in Escherichia coli: analysis of a bar-
946 coded mutant collection. J. Bacteriol. *192*, 59–67.

947 45. Weel-Sneve, R., Kristiansen, K.I., Odsbu, I., Dalhus, B., Booth, J., Rognes, T., Skarstad,
948 K., and Bjørås, M. (2013). Single transmembrane peptide DinQ modulates membrane-
949 dependent activities. PLoS Genet. *9*, e1003260.

950 46. Rubin, E.J., Herrera, C.M., Crofts, A.A., and Trent, M.S. (2015). PmrD is required for
951 modifications to escherichia coli endotoxin that promote antimicrobial resistance.
952 Antimicrob. Agents Chemother. *59*, 2051–2061.

953 47. Fitzgerald, D.M., Stringer, A.M., Smith, C., Lapierre, P., and Wade, J.T. (2023). Genome-
954 Wide Mapping of the Escherichia coli PhoB Regulon Reveals Many Transcriptionally Inert,
955 Intragenic Binding Sites. MBio *14*, e0253522.

956 48. Yoshida, Y., Sugiyama, S., Oyamada, T., Yokoyama, K., and Makino, K. (2012). Novel
957 members of the phosphate regulon in Escherichia coli O157:H7 identified using a whole-
958 genome shotgun approach. Gene *502*, 27–35.

959 49. Chekabab, S.M., Jubelin, G., Dozois, C.M., and Harel, J. (2014). PhoB activates
960 Escherichia coli O157:H7 virulence factors in response to inorganic phosphate limitation.
961 PLoS One *9*, e94285.

962 50. Pontes, M.H., and Groisman, E.A. (2018). Protein synthesis controls phosphate
963 homeostasis. Genes Dev. *32*, 79–92.

964 51. Möller, S., Croning, M.D., and Apweiler, R. (2001). Evaluation of methods for the prediction
965 of membrane spanning regions. Bioinformatics *17*, 646–653.

966 52. Ikeda, M., Arai, M., Okuno, T., and Shimizu, T. (2003). TMPDB: a database of
967 experimentally-characterized transmembrane topologies. Nucleic Acids Res. *31*, 406–409.

968 53. Käll, L., Krogh, A., and Sonnhammer, E.L.L. (2004). A combined transmembrane topology
969 and signal peptide prediction method. J. Mol. Biol. *338*, 1027–1036.

970 54. Feilmeier, B.J., Iseminger, G., Schroeder, D., Webber, H., and Phillips, G.J. (2000). Green
971 fluorescent protein functions as a reporter for protein localization in Escherichia coli. J.
972 Bacteriol. *182*, 4068–4076.

973 55. Battesti, A., and Bouveret, E. (2012). The bacterial two-hybrid system based on adenylate
974 cyclase reconstitution in Escherichia coli. Methods *58*, 325–334.

975 56. Karimova, G., Pidoux, J., Ullmann, A., and Ladant, D. (1998). A bacterial two-hybrid system
976 based on a reconstituted signal transduction pathway. Proc. Natl. Acad. Sci. U. S. A. *95*,
977 5752–5756.

978 57. Gerken, H., Charlson, E.S., Cicirelli, E.M., Kenney, L.J., and Misra, R. (2009). MzrA: a
979 novel modulator of the EnvZ/OmpR two-component regulon. Mol. Microbiol. *72*, 1408–
980 1422.

981 58. Bastet, L., Korepanov, A.P., Jagodnik, J., Grondin, J.P., Lamontagne, A.-M., Guillier, M.,
982 and Lafontaine, D.A. (2024). Riboswitch and small RNAs modulate btuB translation
983 initiation in Escherichia coli and trigger distinct mRNA regulatory mechanisms. Nucleic
984 Acids Res. *52*, 5852–5865.

985 59. Batchelor, E., Silhavy, T.J., and Goulian, M. (2004). Continuous control in bacterial
986 regulatory circuits. J. Bacteriol. *186*, 7618–7625.

987 60. Alphen, W.V., and Lugtenberg, B. (1977). Influence of osmolarity of the growth medium on
988 the outer membrane protein pattern of Escherichia coli. J. Bacteriol. *131*, 623–630.

989 61. Batchelor, E., Walthers, D., Kenney, L.J., and Goulian, M. (2005). The Escherichia coli
990 CpxA-CpxR envelope stress response system regulates expression of the porins ompF and
991 ompC. J. Bacteriol. *187*, 5723–5731.

992 62. Olaitan, A.O., Morand, S., and Rolain, J.-M. (2014). Mechanisms of polymyxin resistance:
993 acquired and intrinsic resistance in bacteria. Front. Microbiol. *5*, 643.

994 63. Eguchi, Y., Itou, J., Yamane, M., Demizu, R., Yamato, F., Okada, A., Mori, H., Kato, A., and
995 Utsumi, R. (2007). B1500, a small membrane protein, connects the two-component
996 systems EvgS/EvgA and PhoQ/PhoP in *Escherichia coli*. Proc. Natl. Acad. Sci. U. S. A.
997 *104*, 18712–18717.

998 64. Kox, L.F., Wösten, M.M., and Groisman, E.A. (2000). A small protein that mediates the
999 activation of a two-component system by another two-component system. EMBO J. *19*,
1000 1861–1872.

1001 65. Kato, A., and Groisman, E.A. (2004). Connecting two-component regulatory systems by a
1002 protein that protects a response regulator from dephosphorylation by its cognate sensor.
1003 Genes Dev. *18*, 2302–2313.

1004 66. Miller, J.H., and Others (1992). A Short Course in Bacterial Genetics: A Laboratory Manual
1005 and Handbook for Escherichia Coli and Related Bacteria (CSHL Press).

1006 67. Datsenko, K.A., and Wanner, B.L. (2000). One-step inactivation of chromosomal genes in
1007 Escherichia coli K-12 using PCR products. Proc. Natl. Acad. Sci. U. S. A. *97*, 6640–6645.

1008 68. Cherepanov, P.P., and Wackernagel, W. (1995). Gene disruption in Escherichia coli: TcR
1009 and KmR cassettes with the option of Flp-catalyzed excision of the antibiotic-resistance
1010 determinant. Gene *158*, 9–14.

1011 69. Ochman, H., Medhora, M.M., Garza, D., and Hartl, D.L. (1990). Amplification of flanking
1012 sequences by inverse PCR. PCR protocols: A guide to methods and applications, 219–227.

1013 70. Godiska R, Patterson M, Schoenfeld T, and Mead DA (2005). Beyond pUC: Vectors for
1014 Cloning Unstable DNA. In DNA Sequencing: Optimizing the Process and Analysis, J.
1015 Kieleczawa, ed. (Jones & Bartlett Learning), pp. 55–76.

1016 71. Martin, M. (2011). Cutadapt removes adapter sequences from high-throughput sequencing
1017 reads. EMBnet.journal *17*, 10–12.

1018 72. Smith, T., Heger, A., and Sudbery, I. (2017). UMI-tools: modeling sequencing errors in
1019 Unique Molecular Identifiers to improve quantification accuracy. Genome Res. *27*, 491–
1020 499.

1021 73. Kim, D., Paggi, J.M., Park, C., Bennett, C., and Salzberg, S.L. (2019). Graph-based
1022 genome alignment and genotyping with HISAT2 and HISAT-genotype. Nat. Biotechnol. *37*,
1023 907–915.

1024 74. Bray, N.L., Pimentel, H., Melsted, P., and Pachter, L. (2016). Near-optimal probabilistic
1025 RNA-seq quantification. Nat. Biotechnol. *34*, 525–527.

1026 75. Love, M.I., Huber, W., and Anders, S. (2014). Moderated estimation of fold change and
1027 dispersion for RNA-seq data with DESeq2. Genome Biol. *15*, 550.

1028 76. Zhu, A., Ibrahim, J.G., and Love, M.I. (2019). Heavy-tailed prior distributions for sequence
1029 count data: removing the noise and preserving large differences. Bioinformatics *35*, 2084–
1030 2092.

1031 77. Schneider, C.A., Rasband, W.S., and Eliceiri, K.W. (2012). NIH Image to ImageJ: 25 years
1032 of image analysis. Nat. Methods *9*, 671–675.

1033 78. Jiang, C., Brown, P.J.B., Ducret, A., and Brun, Y.V. (2014). Sequential evolution of bacterial
1034 morphology by co-option of a developmental regulator. Nature *506*, 489–493.

1035 79. Thibodeau, S.A., Fang, R., and Joung, J.K. (2004). High-throughput beta-galactosidase
1036 assay for bacterial cell-based reporter systems. Biotechniques *36*, 410–415.

1037

1038

1039

1040 Figures and tables

1041

1042

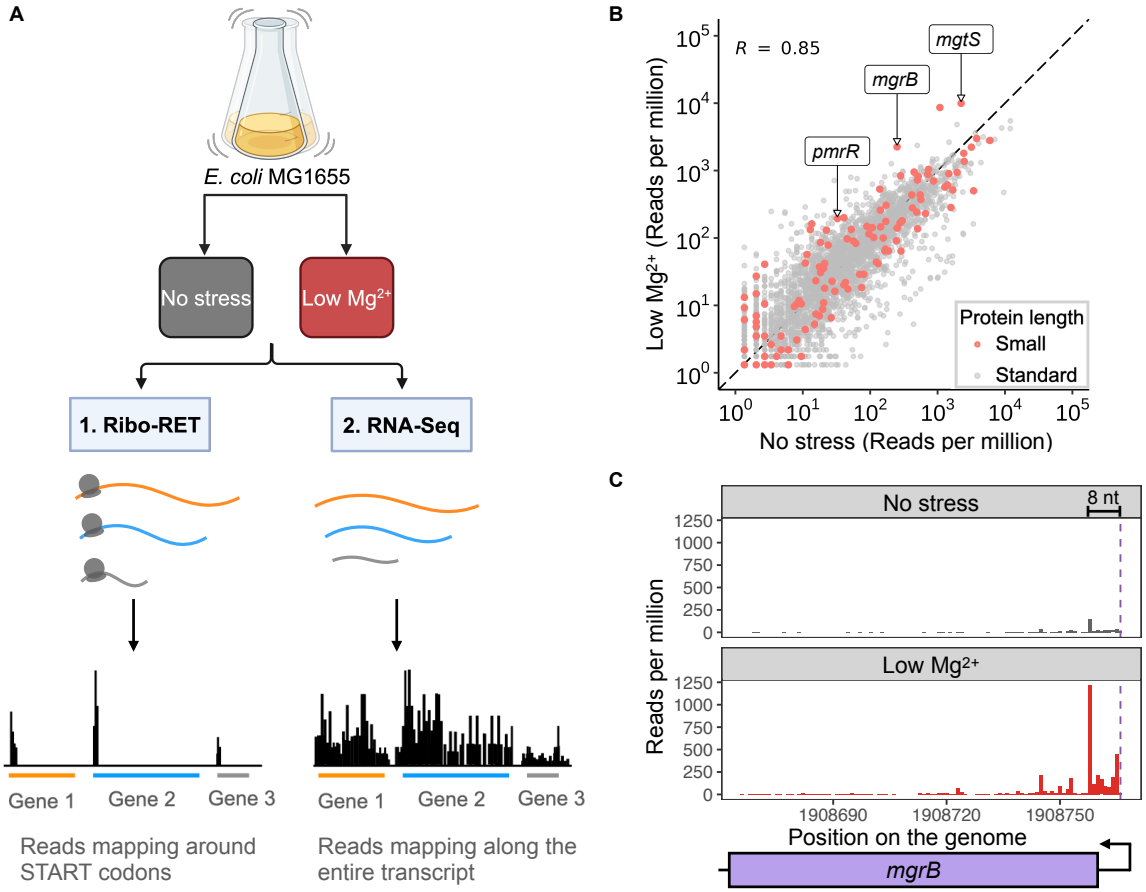


1043

1044

1045 **Figure 1. Identification of small proteins induced under low magnesium stress in *E. coli***
1046 **by translation-initiation profiling (Ribo-RET).** (A) Schematic diagram showing the Ribo-RET
1047 and RNA-Seq experimental setup used to identify small proteins induced by low magnesium
1048 stress. Wild-type *E. coli* K-12 MG1655 cells were grown in supplemented minimal A medium
1049 containing $MgSO_4$ at either 10 mM (no stress) or ~1 μM (no added magnesium, low $Mg^{2+}$
1050 stress). (B) Scatterplot showing the correlation between the Ribo-RET reads mapping to the
1051 annotated start sites of proteins expressed under low $Mg^{2+}$ stress and no stress. The red dots
1052 represent annotated small proteins of ≤ 50 amino acids in length, and the gray dots represent
1053 proteins > 50 amino acids long. Small proteins, MgrB, MgtS, and PmrR, known to be induced
1054 under magnesium starvation, are highlighted. Pearson's coefficient, r= 0.85. (C) Ribo-RET data
1055 for a representative small protein MgrB induced under low $Mg^{2+}$ stress. A purple dashed line
1056 indicates the translation start site, and the 8 nucleotide (nt) indicates the distance between the
1057 highest ribosome density peak and the first nucleotide of the start codon. (Also see Tables 1,
1058 S4, Figures S1 and S2)

1059

1060

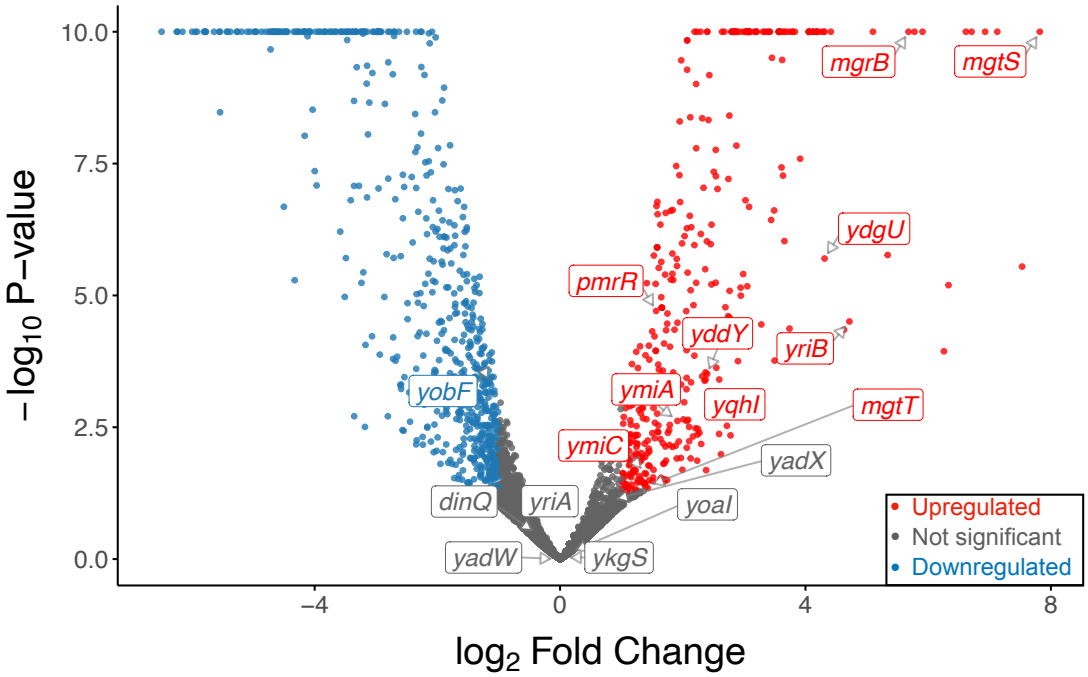


**Figure 2. RNA-Seq analysis of transcripts representing small proteins induced under low magnesium stress.** Volcano plot illustrating differential expression of small proteins induced under low magnesium stress from RNA-Seq data. Transcripts that are either upregulated or downregulated are highlighted in red or blue, respectively, and those with no significant change are represented in gray. The criteria for significance include a fold change threshold of >2 and a p-value of <0.05. The -$\log_{10}$ P-value of *mgrB* and *mgtS* were 75 and 140 respectively. To prevent distortion from their exceptionally high values dominating the plot, the transformed p-values were capped at 10 to enhance visualization. Data represent differential expression analysis from two independent replicates. (Also see Tables 2, S4, and Figure S3)

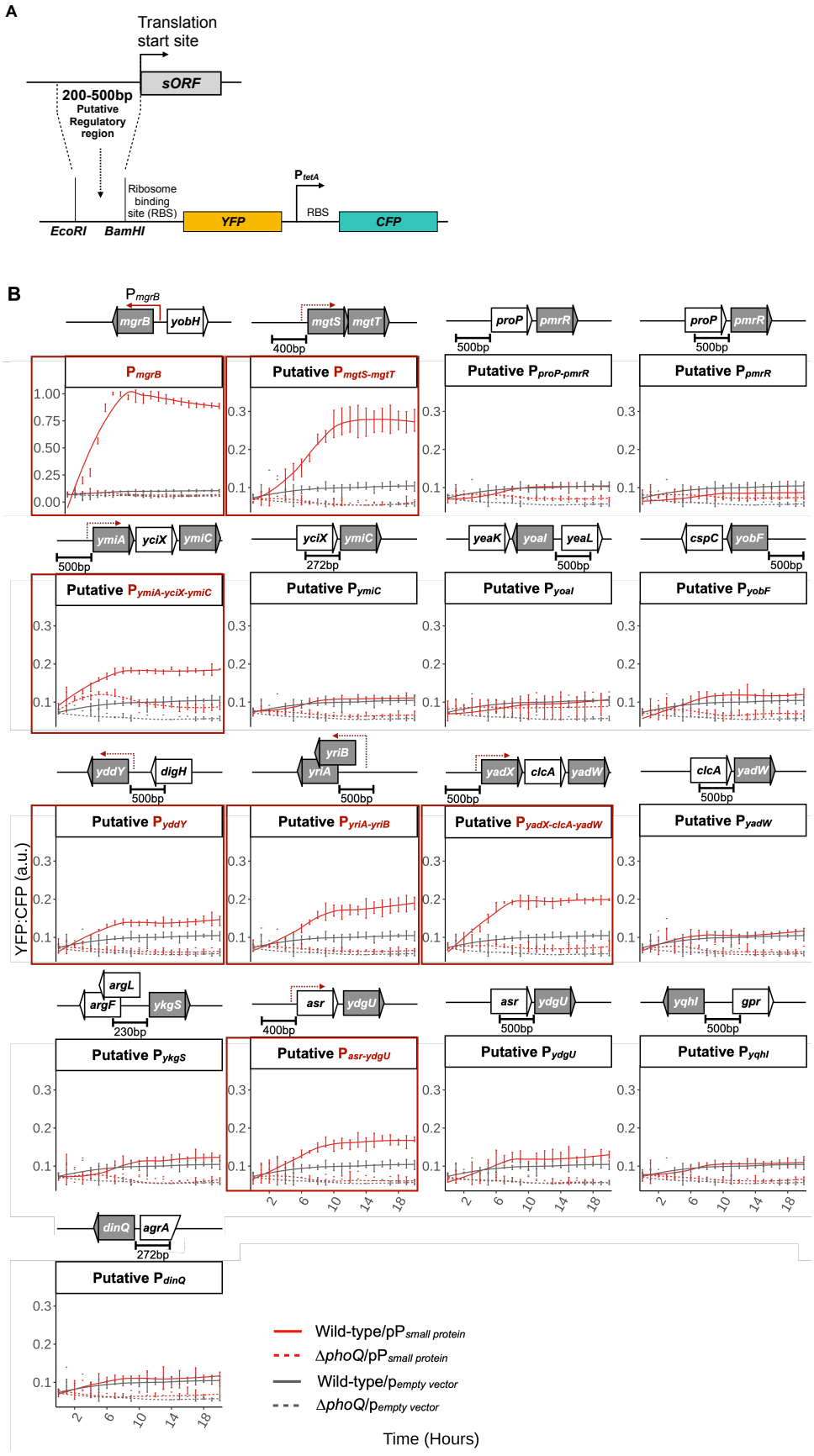
A
Translation start site
sORF
200-500bp
Putative Regulatory region
Ribosome binding site (RBS)
EcoRI
BamHI
YFP
P tetA
RBS
CFP
B
P mgrB
mgrB
yobH
mgtS
mgtT
400bp
proP
pmrR
500bp
Putative P mgtS-mgtT
Putative P proP-pmrR
Putative P pmrR
ymiA
yciX
ymiC
272bp
yeaK
yoaI
yeaL
cspC
yobF
Putative P ymiA-yciX-ymiC
Putative P ymiC
Putative P yoaI
Putative P yobF
yddY
digH
yriB
yriA
yadX
clcA
yadW
Putative P yddY
Putative P yriA-yriB
Putative P yadX-clcA-yadW
Putative P yadW
YFP:CFP (a.u.)
argL
argF
ykgS
230bp
asr
ydgU
yqhI
gpr
Putative P ykgS
Putative P asr-ydgU
Putative P ydgU
Putative P yqhI
dinQ
agrA
Putative P dinQ
Wild-type/pP small protein
ΔphoQ/pP small protein
Wild-type/p empty vector
ΔphoQ/p empty vector
Time (Hours)

1085 **Figure 3. Transcriptional regulation of small proteins under low magnesium stress.** (A)
1086 Schematic representation of the transcriptional reporter fusion construct. Regions (200-500 bp)
1087 upstream of the small open reading frames of interest were amplified from the MG1655 genome
1088 and cloned into a YFP-encoding reporter plasmid (pMR120) resulting in plasmids pPJ14,
1089 pPJ16-pPJ20, pPJ23, pSV16-pSV21, pSV24, pSV28-pSV29 (See Table 2 for genomic
1090 coordinates of the regulatory regions tested here and Table S2 for plasmid details). (B)
1091 Measurement of transcriptional reporter activity (YFP:CFP) for the indicated small proteins
1092 under low $Mg^{2+}$ (no added magnesium). The solid and dashed lines represent the wild-type *E.*
1093 *coli* MG1655 and Δ*phoQ* cells, respectively, harboring plasmids with either transcriptional fusion
1094 for a putative regulatory region of a small protein with *yfp* (red line) or *yfp* only (gray line). The
1095 schematic above each plot depicts the arrangement of the small protein-encoding genes (shown
1096 in gray), including the putative regulatory regions and operons where applicable. Transcriptional
1097 reporters showing an increased activity compared to the empty vector control (pMR120) are
1098 highlighted in red. The cultures were grown in a supplemented minimal medium with 6 μg $ml^{-1}$
1099 chloramphenicol. The data represent averages and standard errors of the means for four
1100 independent replicates. (Also see Table 2)
1101
1102
1103
1104
1105

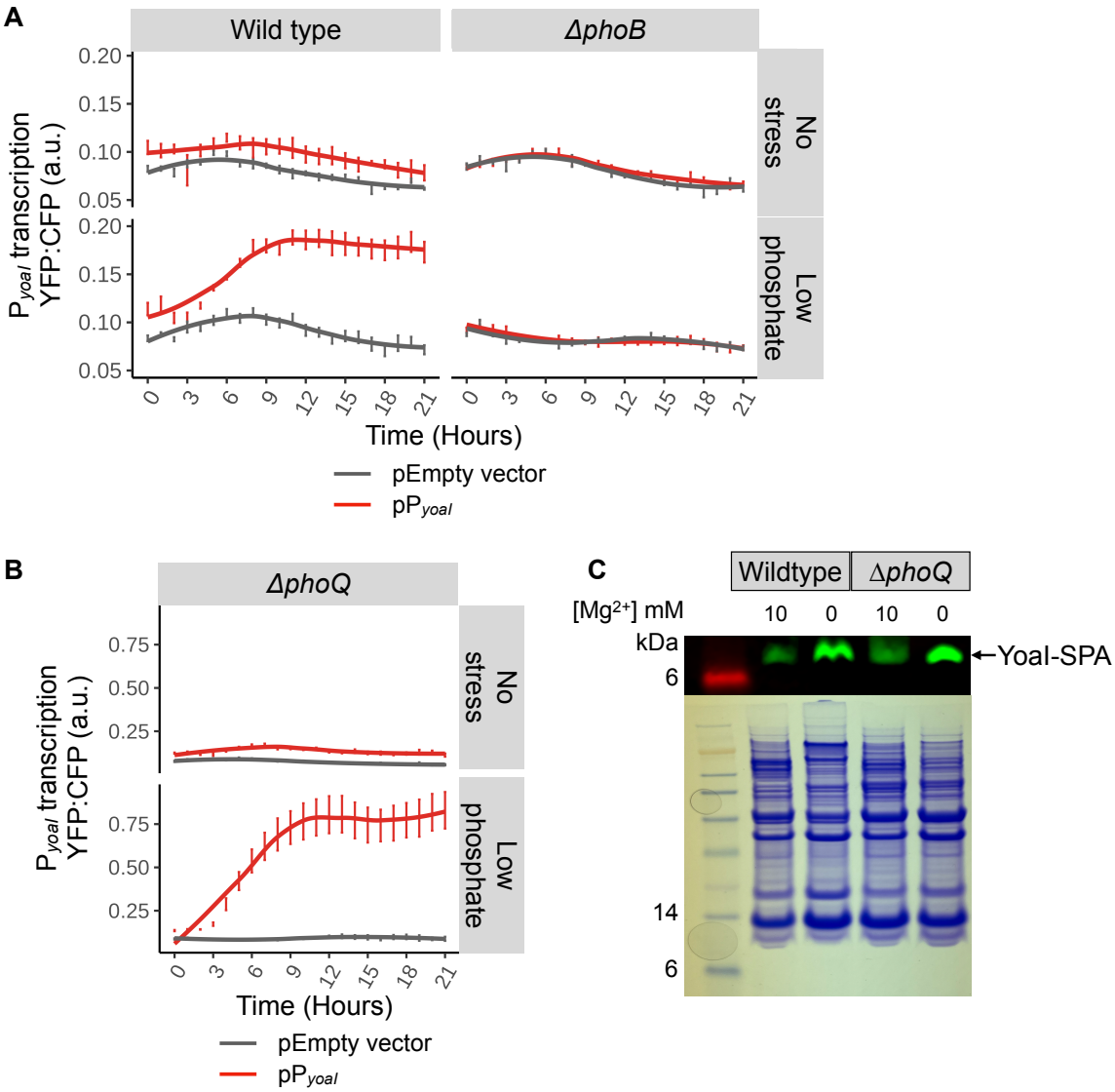


**Figure 4. Regulation of YoaI expression during magnesium limitation.** (A-B) Transcriptional activity of *yoaI* was measured as a function of YFP reporter fluorescence in *E. coli* MG1655, Δ*phoB* (SV48), and Δ*phoQ* (TIM100) strains under phosphate stress as indicated. The red and gray lines represent cells carrying plasmid-encoded $P_{yoaI}$-*yfp* transcriptional reporter (pPJ18) and *yfp*-only control vector (pMR120), respectively. The cultures were grown in a supplemented MOPS minimal medium with 6 μg $ml^{-1}$ chloramphenicol with either 1 mM $K_2HPO_4$ for no stress condition, or no added $K_2HPO_4$ for phosphate stress. The data illustrate average YFP:CFP fluorescence with standard error of the means, derived from four independent replicates. (C) Detection of YoaI protein in *E. coli* wild-type (GSO317) and Δ*phoQ* (SV60) strains containing *yoaI-SPA* genomic translational fusion. Cells were grown in supplemented minimal A medium, with $MgSO_4$ added at the specified concentration (10mM or no added $MgSO_4$). Membrane fractions were analyzed by western blotting using M2 anti-FLAG antibodies (top) and by Coomassie Brilliant Blue staining (bottom). The data represent results from two independent replicates.

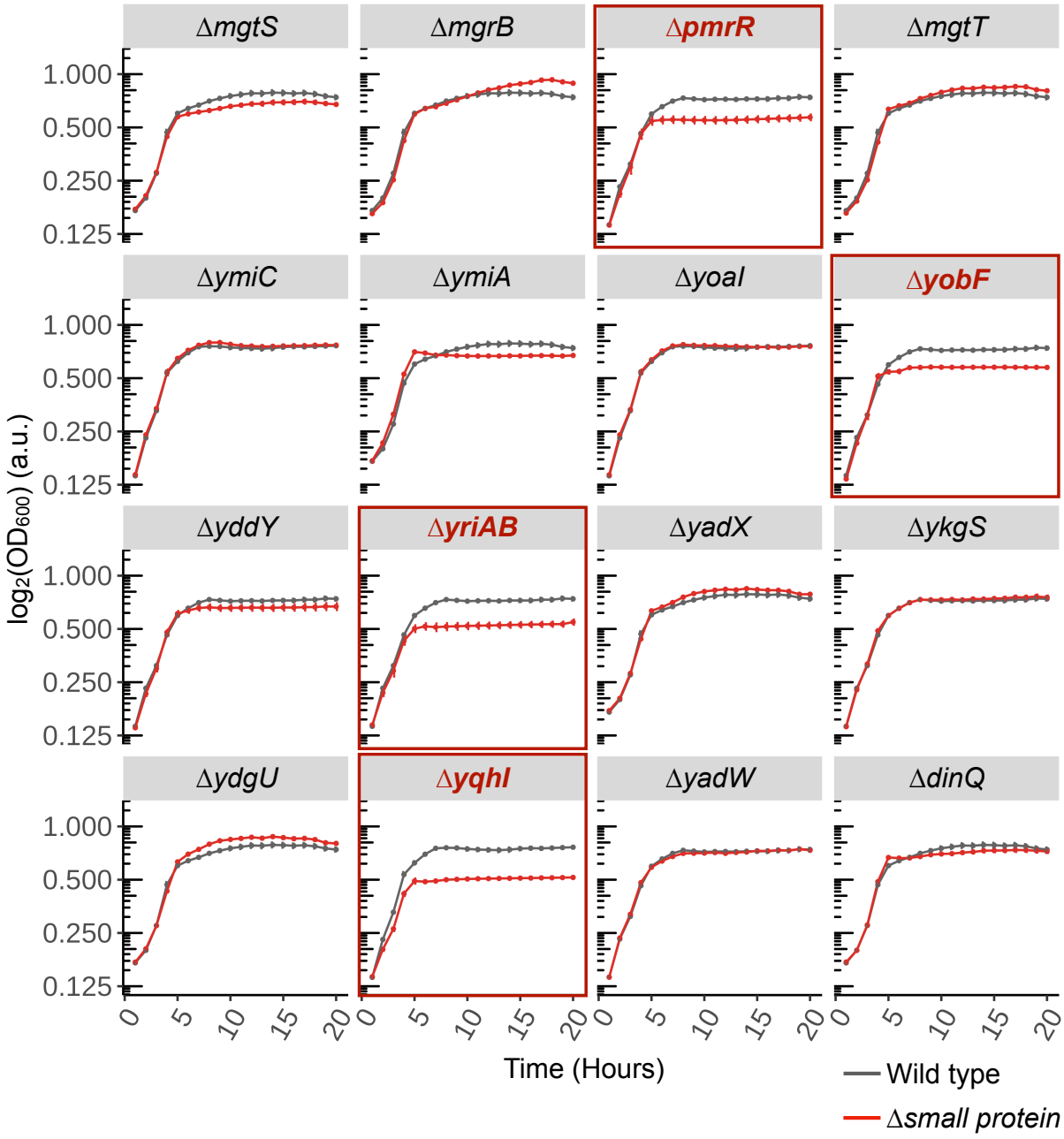


**Figure 5. Effect of deleting genes encoding low $Mg^{2+}$ stress-induced small proteins on bacterial growth.** Growth curves of wild-type *E. coli* MG1655 (gray) and mutants corresponding to the deletions of small protein-encoding genes (red) (strains SV64, AML67, SV35, SV31, SV41, SV57, SV59, SV33, SV29, SV25, SV39, SV43, SV58, SV37, SV27, and SV56, please see Table S1 and methods for strain details). Deletion mutants showing reduced growth yield compared to wild-type cells are highlighted in red. The cultures were grown in supplemented minimal A medium with no added magnesium and 50 μg $ml^{-1}$ carbenicillin. Data represent averages and standard errors of means for four independent cultures.

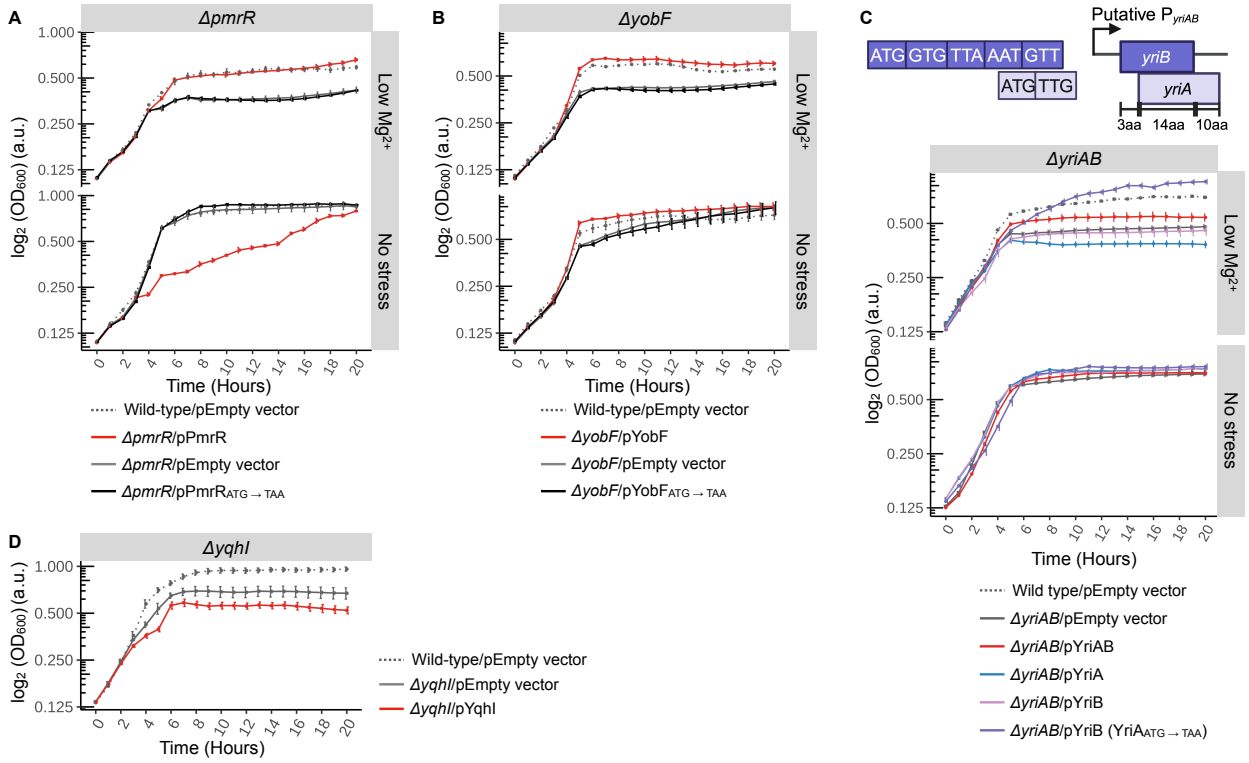


**Figure 6. Complementation of growth phenotypes associated with *pmrR,* and *yobF* deletions.** (A-B) Growth curves of Δ*pmrR* (SV35), and Δ*yobF* (SV34) deletion strains carrying an empty vector (pEB52, solid gray line) or complemented with plasmids encoding small proteins pPmrR (pSV35) and pYobF (pJS5) (red line) or their variants $pPmrR_{ATG\rightarrow TAA}$ (pSV38), and $pYobF_{ATG\rightarrow TAA}$ (pSV45) (black line), as indicated. Wild-type MG1655 cells containing the empty vector are included as a control (dashed gray line). (C) Schematic of the overlapping genes *yriAB* followed by the growth curves of gene deletion *ΔyriAB* (SV25) complemented with pYriAB (pSV58), pYriA (pJS1), pYriB (pSV37), pYriB ($YriA_{ATG\rightarrow TAA}$) (pSV59), or an empty vector (pEB52, as indicated. (D) Growth curves of gene deletion *ΔyqhI* (SV37) carrying an empty vector (pEB52), or complemented with a plasmid encoding YqhI. Wild-type cells containing an empty vector (pEB52, dashed gray line) are included as a control. For panels A-D, cultures were grown in supplemented minimal A medium containing 50 μg $ml^{-1}$ carbenicillin and either no added magnesium or 10 mM $MgSO_4$ as indicated. 500 μM IPTG was used for induction, except for PmrR derivatives (pSV35 and pSV38), where 12.5 μM IPTG was used. Data represent averages and standard errors of means for four independent cultures.

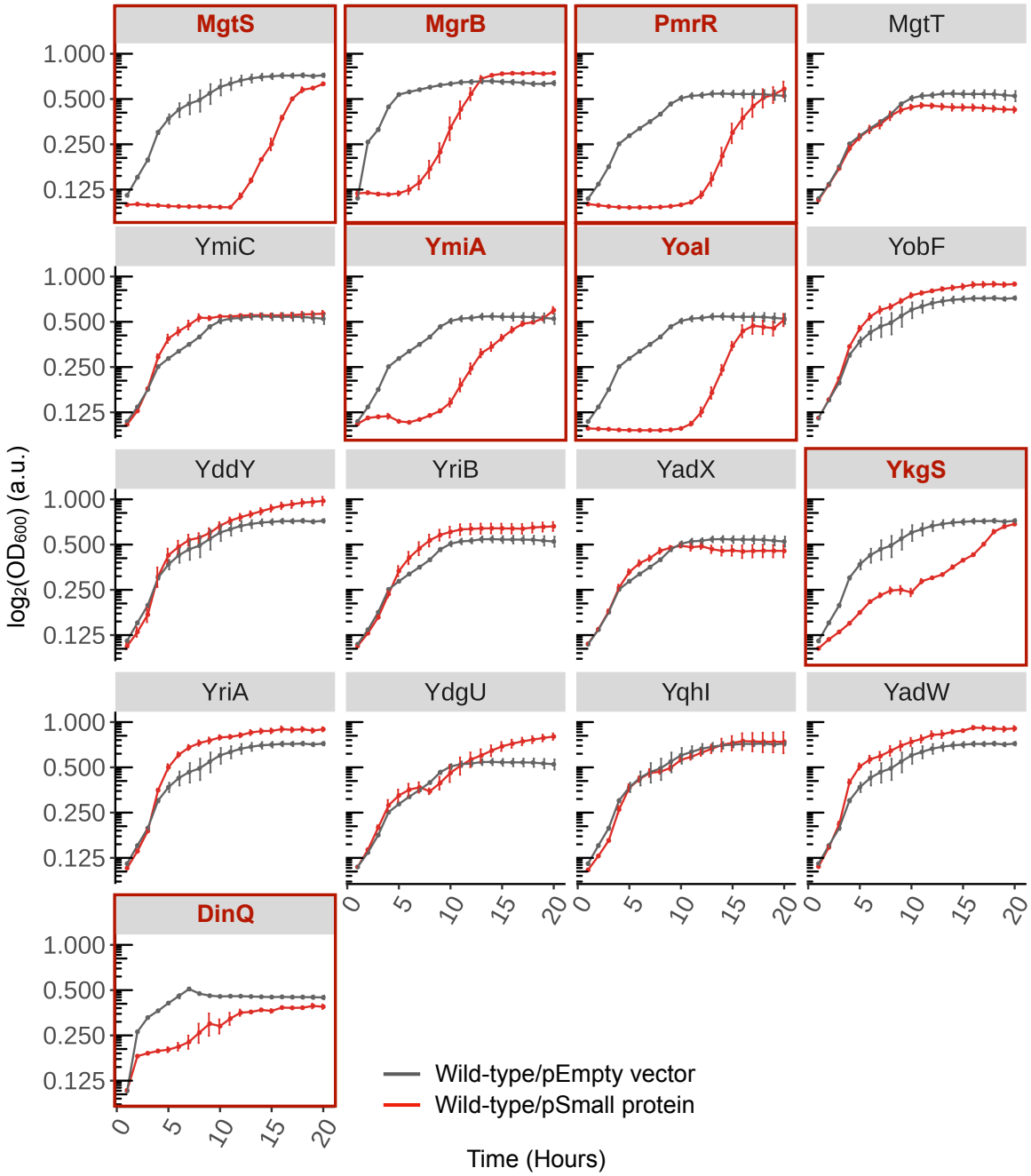


**Figure 7. Effect of overexpression of low $Mg^{2+}$ stress-induced small proteins on growth**. Growth curves of *E. coli* MG1655 cells expressing each of the 17 stress-specific small proteins (encoded by plasmids pSV30-37, pSV54, pSV60, or pJS1-7; please see Table S2 for details) are represented in red, while cells carrying the empty vector (pEB52 and pBAD24) are shown in gray. The cells were grown under low $Mg^{2+}$ stress (no added magnesium). Small proteins whose expression causes a growth defect or delay are highlighted in red. The cultures were grown in supplemented minimal A medium with 50 µg $ml^{-1}$ carbenicillin. 500 µM IPTG was used as an inducer for all $P_{trc}$-based vectors, in the case of pSV54and pBAD24, 0.5% arabinose was used. Data represent averages and standard error of means for four independent cultures.

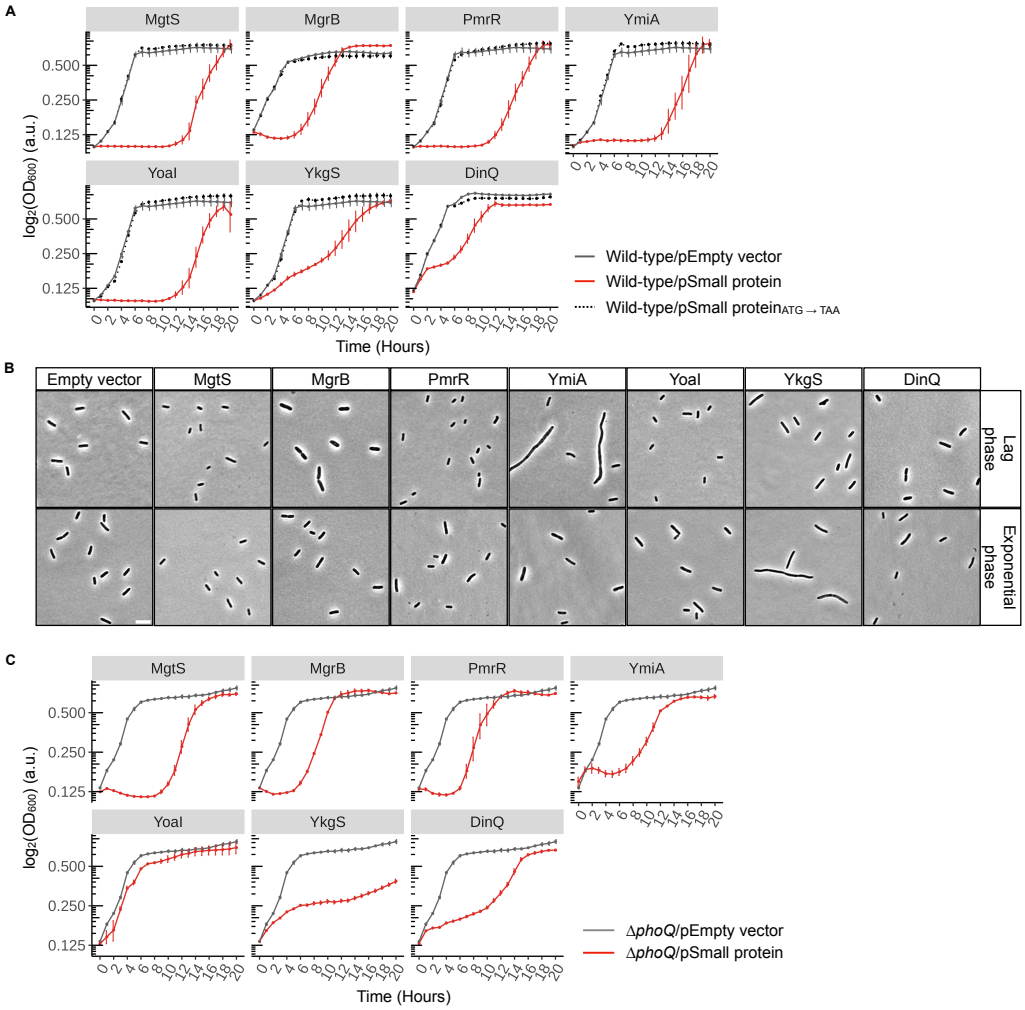


**Figure 8. Analysis of growth defect and cell size changes associated with overexpression of small proteins, MgtS, MgrB, PmrR, YkgS, YoaI, YmiA and DinQ.** (A) Growth curves of *E. coli* MG1655 cells expressing the indicated small proteins (red line) and empty vector control (pEB52 or pBAD24, gray line). The start codon (ATG) of each small protein is mutated to a stop codon (TAA), and the growth curves of cells expressing these constructs are depicted in dotted black. Plasmids pSV34-36, pSV38-42, pSV54-55, pSV60-61, or pJS4, pJS7 were used as applicable, please see Table S2 for details. Data represent averages and standard error of means for four independent cultures. (B) Representative phase contrast micrographs of the cells expressing small proteins during lag (top panel) and exponential phase (bottom panel) after induction, scale bar = 5 μm. Data is representative of three independent cultures. (C) Growth curves of Δ*phoQ* (TIM202) cells expressing the indicated small proteins (red line) and empty vector control (pEB52 or pBAD24, gray line). Plasmids pSV34-36, pSV54, pSV60, pJS4, and pJS7 were used as applicable, please see Table S2 for details. Data represent averages and standard error of means for four independent cultures. For panels A-C, the cultures were grown in supplemented minimal A medium containing no added magnesium, 50 μg $ml^{-1}$ carbenicillin, and 500 μM IPTG for all $P_{trc}$-based vectors, except for pSV54 and pBAD24, where 0.5% arabinose was utilized instead. (Also see Figures S6 and S7)

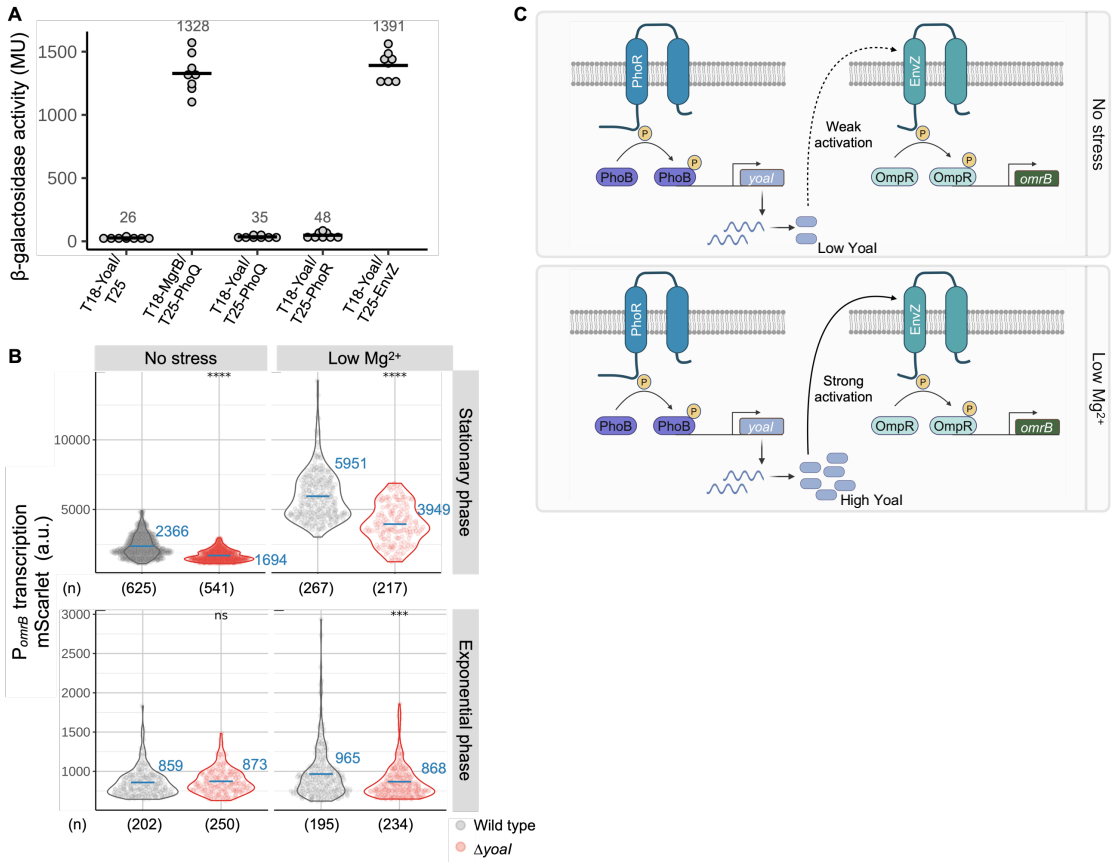


**Figure 9. Effect of YoaI expression on the EnvZ-OmpR system.** (A) BACTH assays were conducted using cells harboring T18 and T25 fusion proteins of *B. pertussis* adenylyl cyclase, in a *cyaA* mutant BACTH host strain, SAM85, which contains *lacI*$^q$. β-gal activity was measured to assess interactions between T18-YoaI (pSV47) and T25-linked PhoQ (pAL27), PhoR (pSY68), or EnvZ (pKK14). T25 alone was used as a negative control, and T18-MgrB (pAL33) combined with T25-PhoQ (pAL27) was used as a positive control. The cultures were grown in LB medium containing 50 μg ml$^{-1}$ kanamycin, 100 μg ml$^{-1}$ carbenicillin, and 500 μM IPTG. Each circle represents a biological replicate, with the mean values from two independent experiments indicated, expressed in Miller units (MU). (B) Transcriptional activity of *omrB* was measured as a function of mScarlet reporter fluorescence in *E. coli* MG1655 (SV97), and Δ*yoaI* (SV95) strains at the stationary phase (top panel) and exponential phase (bottom panel). Each circle corresponds to a single cell. Δ*yoaI* cells are depicted in red, while wild-type cells are in gray. The cultures were grown in supplemented minimal A medium containing either 10mM (no stress) or no added magnesium ($Mg^{2+}$ stress). Data are derived from three independent replicates and the number of cells analyzed is indicated by (n). Mean fluorescence is shown with blue bars and is noted in blue text. P-values indicate the results of a t-test when Δ*yoaI* cells were compared to the wild-type cells, ****P ≤ 0.0001, ***P ≤ 0.001, and "ns" = P > 0.05. (C) Schematic representation of small membrane protein YoaI as a connector of the two-component systems, PhoR-PhoB and EnvZ-OmpR. YoaI is transcriptionally controlled by the PhoR-PhoB system, under low $Mg^{2+}$ YoaI protein levels increase and it binds sensor kinase EnvZ and modulates signaling through the EnvZ-OmpR pathway. (Also see Figure S9)

1207 **Table 1. Summary of the 17 small proteins induced under low magnesium stress in *E. coli*.** Small proteins with at least a 3-fold increase in
1208 reads mapping to the translation initiation site under low $Mg^{2+}$ relative to no stress are indicated below. The analysis of transcriptional regulation,
1209 localization, and characterization of deletion and overexpression phenotypes is summarized.
1210

| Small protein | Transcriptional Regulation | | Membrane localization | Phenotypic characterization | |
|---|---|---|---|---|---|
| | | | | Deletion | Overexpression |
| MgtS | + | PhoQP-dependent, in an operon *mgtS-mgtT* | Y | No effect | Growth defect (prolonged lag phase) & decrease in cell size during lag and exponential phase |
| MgrB | + | PhoQP-dependent | Y | Increase in cell length, and change in colony morphology (larger, rough, translucent colonies)[28] | Growth defect (prolonged lag phase) & increase in cell size during lag phase |
| PmrR | + | BasSR-dependent [33,35] | Y | Growth defect (lower yield at saturation) | Growth defect (prolonged lag phase) & decrease in cell size during lag phase |
| MgtT | + | PhoQP-dependent, in an operon *mgtS-mgtT* | N | No effect | No effect |
| YmiC | + | PhoQP-dependent, in an operon *ymiA-yciX-ymiC* | Y | No effect | No effect |
| YmiA | + | | Y | No effect | Growth defect (prolonged lag phase) & increase in cell length during lag phase |
| YoaI | - | PhoRB-dependent [47–49] | Y | No effect | Growth defect (prolonged lag phase) & decrease in cell size during lag phase |
| YobF | - | | Y | Growth defect (lower yield at saturation) | No effect |
| YddY | + | PhoQP-dependent | N | No effect | No effect |
| YriB | + | PhoQP-dependent, in an operon *yriA-yriB* | N | Growth defect (lower yield at saturation) | No effect |
| YadX | + | PhoQP-dependent, in an operon *yadX-clcA-yadW* | N | No effect | No effect |
| YkgS | - | | N | No effect | Growth defect (slow growth) & increase in cell length during exponential phase |
| YriA | + | PhoQP-dependent, in an operon *yriA-yriB* | N | No effect | No effect |
| YdgU | + | PhoQP-dependent, in an operon *asr-ydgU* | Y | No effect | No effect |
| YqhI | + | | N | No effect | No effect |
| YadW | + | PhoQP-dependent, in an operon *yadX-clcA-yadW* | N | No effect | No effect |
| DinQ | - | | Y | No effect | Growth defect (slow growth) |

1211 + indicates transcriptional upregulation under magnesium stress vs. no stress; - indicates no change in transcriptional activity under magnesium stress vs. no stress; 'Y'
1212 indicates proteins predicted to contain membrane helices using TMHMM [51] and Phobius [53] and shown to localize to the membrane; 'N' indicates a lack of membrane
1213 helices based on bioinformatic prediction

1214 **Table 2. Analysis of transcriptional regulation of low magnesium stress-induced small proteins.** Putative regulatory regions
1215 corresponding to the stress-induced small proteins and their dependence on PhoQ-PhoP signaling system.
1216
1217
1218
1219

| Small protein | Putative region(s) of interest | Length of region (bp) | Genomic location in *E. coli* MG1655 | PhoQP-dependence | Low $Mg^{2+}$ stress-specific expression reported in |
|---|---|---|---|---|---|
| MgrB | $P_{mgrB}$ | 500 | 1908767 - 1909266 | Yes | [27] |
| MgtS, MgtT | $P_{mgtS\text{-}mgtT}$ | 405 | 1622241 - 1622645 | Yes | [31], This study |
| ProP, PmrR | $P_{proP\text{-}pmrR}$ | 500 | 4330002 - 4330501 | No | This study |
| PmrR | $P_{pmrR}$ | 500 | 4331616 - 4332115 | No | This study |
| YmiA, YmiC | $P_{ymiA\text{-}yciX\text{-}ymiC}$ | 500 | 1334648 - 1335147 | Yes | This study |
| YmiC | $P_{ymiC}$ | 272 | 1335300 - 1335571 | No | This study |
| YoaI | $P_{yoaI}$ | 500 | 1874183 - 1874682 | No | This study |
| YobF | $P_{yobF}$ | 500 | 1907592 - 1908091 | No | This study |
| YddY | $P_{yddY}$ | 500 | 1567220 - 1567719 | Yes | This study |
| YriA | $P_{yriA\text{-}yriB}$ | 500 | 3640697 - 3641196 | Yes | This study |
| YriB | | | | | |
| YadX, YadW | $P_{yadX\text{-}clcA\text{-}yadW}$ | 500 | 174548 - 175047 | Yes | This study |
| YadW | $P_{yadW}$ | 500 | 176052 - 176551 | No | This study |
| YkgS | $P_{ykgS}$ | 230 | 290280 - 290509 | No | This study |
| YdgU | $P_{asr\text{-}ydgU}$ | 400 | 1670976 - 1671375 | Yes | This study |
| | $P_{ydgU}$ | 500 | 1671277 - 1671776 | No | This study |
| YqhI | $P_{yqhI}$ | 500 | 3147741 - 3148240 | No | This study |
| DinQ | $P_{dinQ}$ | 272 | 3647789- 3648060 | No | This study |

Supporting Information (Vellappan *et al.*, 2024)

**Table S1. List of strains used in the study**

| Strain | Genotype | Source or Reference |
|---|---|---|
| AML67 | MG1655 *ΔmgrB*::(FRT-kan-FRT) *ΔlacZ* $\lambda_{att}$::($P_{mgtA}$-*lacZ cat*) | [1] |
| *E. cloni* | $F^-$ *mcrA Δ(mrr-hsdRMS-mcrBC) endA1 recA1 φ80lacZΔM15 ΔlacX74 araD139 Δ(ara-leu)7697 galU galK rpsL nupG tonA (attL araC-PBAD-trfA250 bla attR) λ−* | Lucigen Corporation |
| *E. coli K-12 MG1655* | F- λ- ilvG- rfb-50 rph-1 | *E. coli* Genetic Stock Center, CGSC# 7740 |
| GSO195 | MG1655 *ΔdinQ*::(FRT-kan-FRT) | [2] |
| GSO219 | MG1655 *ΔydgU*::(FRT-kan-FRT) | [2] |
| GSO225 | MG1655 *ΔymiA*::(FRT-kan-FRT) | [2] |
| GSO232 | MG1655 Δ*yoaI*::(FRT-kan-FRT) | [2] |
| GSO317 | MG1655 *yoaI*-SPA::kan | [3] |
| JM2110 | MG1508 *mhpR*-$P_{LtetO\text{-}1\text{-}omrB\text{-}104+8}$-*lacZ*$_{+28}$ *Δmini-λ-Tet* | Guillier lab stock (unpublished) |
| JM2113 | OK510 *argG*-[TT1-$P_{LtetO\text{-}1\text{-}omrB\text{-}104+8}$-mScarlet$_{+4}$-FRT-*nptII*-FRT-TT2]-*yhbX*, *Δmini-λ-Tet* | Guillier lab stock (unpublished) |
| JW2162 | BW25113 Δ*lpxT*::(FRT-kan-FRT) | [4] |
| MDG147 | MG1655 (seq) Φ(*ompF*$^+$-*yfp*$^+$)30 Φ(*ompC*$^+$-*cfp*$^+$)31 | [5] |
| MG1508 | MG1655 *mal::lacI*$^q$, *mini- λ-Tet*, *mhpR*-$P_{LtetO\text{-}1}$-*cat-sacB-lacZ* | [6] |
| OK510 | MG1432 *argG*-[TT1-$P_{LtetO\text{-}}$1(no -10)-*sacB-cat*-mScarlet(no ATG)- FRT-*nptII*-FRT-TT2]-*yhbX* | [7] |
| SAM85 | F+ *lacI*$^q$*ZΔM15* Tn*10*(Tet$^R$), *cya-99 araD139 galE15 galK16 rpsL1* (Str$^R$) *hsdR2 mcrA1 mcrB1*. Strain prepared by conjugation: BTH101 (F-) x XL1-Blue (F+). | [8] |
| SV25 | MG1655 *ΔyriAB*::(FRT-kan-FRT), coordinates deleted: 3,640,612 - 3,640,699 | This study |
| SV27 | MG1655 *ΔyadW*::(FRT-kan-FRT), coordinates deleted: 176,552 - 176,594 | This study |
| SV29 | MG1655 *ΔyddY*::(FRT-kan-FRT), coordinates deleted: 1,567,219 - 1,567,178 | This study |
| SV31 | MG1655 *ΔmgtT*::(FRT-kan-FRT), coordinates deleted: 1,622,742 - 1,622,816 | This study |

| | | |
|---|---|---|
| SV33 | MG1655 *ΔyobF*::(FRT-kan-FRT), coordinates deleted: 1,907,451 - 1,907,573 | This study |
| SV35 | MG1655 *ΔpmrR*::(FRT-kan-FRT), coordinates deleted: 4,332,116 - 4,332,178 | This study |
| SV37 | MG1655 *ΔyqhI*::(FRT-kan-FRT), coordinates deleted: 3,147,597 - 3,147,740 | This study |
| SV39 | MG1655 *ΔyadX*::(FRT-kan-FRT), coordinates deleted: 175,048 - 175,077 | This study |
| SV41 | MG1655 *ΔymiC*::(FRT-kan-FRT), coordinates deleted: 1,335,572 - 1,335,667 | This study |
| SV43 | MG1655 *ΔykgS*::(FRT-kan-FRT), coordinates deleted: 290,510 - 290,641 | This study |
| SV47 | MG1655 Δ*lpxT*::(FRT-kan-FRT) | This study |
| SV50 | MG1655 *ΔpmrR* | This study |
| SV54 | MG1655 *ΔlpxT*::(FRT-kan-FRT) *ΔpmrR* | This study |
| SV56 | MG1655 *ΔdinQ*::(FRT-kan-FRT) | This study |
| SV57 | MG1655 *ΔymiA*::(FRT-kan-FRT) | This study |
| SV58 | MG1655 *ΔydgU*::(FRT-kan-FRT) | This study |
| SV59 | MG1655 *ΔyoaI*::(FRT-kan-FRT) | This study |
| SV60 | MG1655 *yoaI*-SPA-kan *ΔlacZ ΔphoQ* | This study |
| SV64 | MG1655 *ΔmgtS*::(FRT-kan-FRT), coordinates deleted: 1,622,646 - 1,622,735 | This study |
| SV91 | MG1655 Δ*yoaI* | This study |
| SV95 | MG1655 *argG*-[TT1-$P_{LtetO-1-omrB-104+8}$-mScarlet$_{+4}$-FRT-*nptII*-FRT-TT2]-*yhbX*, *Δmini-λ-Tet* | This study |
| SV97 | MG1655 *argG*-[TT1-$P_{LtetO-1-omrB-104+8}$-mScarlet$_{+4}$-FRT-*nptII*-FRT-TT2]-*yhbX*, *Δmini-λ-Tet* Δ*yoaI* | This study |
| TIM92 | MG1655 $\lambda_{att}$::($P_{mgrB-yfp}$) $HK_{att}$::($P_{tetA-cfp}$) | [9] |
| TIM100 | MG1655 *ΔphoQ* $\lambda_{att}$::($P_{mgrB-yfp}$) $HK_{att}$::($P_{tetA-cfp}$) | [9] |
| TIM202 | MG1655 Δ*lacZ*::FRT Δ*phoQ*::FRT | [10] |
| TOP10 | *F– mcrA Δ(mrr-hsdRMS-mcrBC) φ80lacZΔM15 ΔlacX74 recA1 araD139 Δ(ara-leu)7697 galU galK λ– rpsL(StrR) endA1 nupG* | Invitrogen |
| XL1-Blue | *recA1 endA1 gyrA96 thi-1 hsdR17 supE44 relA1 lac [F´ proAB lacIqZΔM15 Tn10 (Tetr)]* | [11] |

Φ and Ψ denote transcriptional and translational fusions, respectively

**Table S2. List of plasmids used in the study**

| Plasmid | Relevant genotype | Source or reference |
|---|---|---|
| pAL27 | pKT25 $P_{lac}$-*cyaA*$_{T25}$-*phoQ*, Kan$^R$ | [1] |
| pAL33 | pUT18C $P_{lac}$-*cyaA*$_{T18}$-*mgrB*, Amp$^R$ | [1] |
| pAL38 | pEB52 $P_{trc}$-*gfpA206K-mgrB*, Amp$^R$ | [1] |
| pAL39 | pEB52 $P_{trc}$-*gfpA206K*, Amp$^R$ | [1] |
| pBAD24 | pMB1-derived plasmid, *araBAD,* Amp$^R$ | [12] |
| pCP20 | ori(pSC101) *rep101(ts) bla* λ$P_R$-FLP λcI(ts) cat. Amp$^R$, Cam$^R$ | [13] |
| pEB52 | pTrc99a with the NcoI site removed, Amp$^R$ | Goulian lab collection |
| pJS1 | pEB52 $P_{trc}$-*yriA*. Amp$^R$ | This study |
| pJS2 | pEB52 $P_{trc}$-*yadW*. Amp$^R$ | This study |
| pJS3 | pEB52 $P_{trc}$-*yqhI*. Amp$^R$ | This study |
| pJS4 | pEB52 $P_{trc}$-*ykgS*. Amp$^R$ | This study |
| pJS5 | pEB52 $P_{trc}$-*yobF*. Amp$^R$ | This study |
| pJS6 | pEB52 $P_{trc}$-*yddY*. Amp$^R$ | This study |
| pJS7 | pEB52 $P_{trc}$-*mgtS*. Amp$^R$ | This study |
| pKD13 | ori(R6K) FRT-kan-FRT, Amp$^R$ | [14] |
| pKD46 | ori(pSC101) *rep101*(*ts*) $P_{araB}$-*gam-betexo araC*, Amp$^R$ | [14] |
| pKK14 | pKT25 $P_{lac}$-*cyaA*$_{T25}$-EnvZ, Kan$^R$ | Goulian lab collection |
| pKT25 | *ori*$_{p15A}$ $P_{lac}$-*cyaA*$_{T25}$-MCS, Kan$^R$ | Euromedex |
| pMR120 | A derivative of pSMART VC (Lucigen) containing two copies of the *rrnB* transcription terminator, $P_{putative\ promoter}$-*yfpA206K*-$P_{tetA}$-*cfp*, Cam$^R$ | Goulian lab collection |
| pPJ1 | pEB52 $P_{trc}$-*gfpA206K-mgtT*, Amp$^R$ | This study |
| pPJ2 | pEB52 $P_{trc}$-*gfpA206K-pmrR*, Amp$^R$ | This study |
| pPJ3 | pEB52 $P_{trc}$-*gfpA206K-ydgU*, Amp$^R$ | This study |
| pPJ4 | pEB52 $P_{trc}$-*yoaI-gfpA206K*, Amp$^R$ | This study |
| pPJ5 | pEB52 $P_{trc}$-*gfpA206K-yqhI*, Amp$^R$ | This study |
| pPJ6 | pEB52 $P_{trc}$-*gfpA206K-yobF*, Amp$^R$ | This study |
| pPJ7 | pEB52 $P_{trc}$-*gfpA206K-yriA*, Amp$^R$ | This study |
| pPJ8 | pEB52 $P_{trc}$-*gfpA206K-yddY*, Amp$^R$ | This study |

| | | |
|---|---|---|
| pPJ9 | pEB52 $P_{trc}$-*gfpA206K-yadW*, $Amp^R$ | This study |
| pPJ10 | pEB52 $P_{trc}$-*gfpA206K-yadX*, $Amp^R$ | This study |
| pPJ11 | pEB52 $P_{trc}$-*gfpA206K-yriB*, $Amp^R$ | This study |
| pPJ12 | pEB52 $P_{trc}$-*gfpA206K-ymiA*, $Amp^R$ | This study |
| pPJ13 | pEB52 $P_{trc}$-*gfpA206K-ymiC*, $Amp^R$ | This study |
| pPJ14 | pMR120 putative $P_{pmrR}$-*yfp*, $Cam^R$ | This study |
| pPJ16 | pMR120 putative $P_{asr\text{-}ydgU}$-*yfp*, $Cam^R$ | This study |
| pPJ17 | pMR120 putative $P_{ydgU}$-*yfp*, $Cam^R$ | This study |
| pPJ18 | pMR120 putative $P_{yoaI}$-*yfp*, $Cam^R$ | This study |
| pPJ19 | pMR120 putative $P_{yqhI}$-*yfp*, $Cam^R$ | This study |
| pPJ20 | pMR120 putative $P_{yriA\text{-}yriB}$-*yfp*, $Cam^R$ | This study |
| pPJ23 | pMR120 putative $P_{yadX\text{-}clcA\text{-}yadW}$-*yfp,* $Cam^R$ | This study |
| pSMART | pSMART VC *BamHI* (BAC) with single-copy replication origin *ori2 repE IncC parABC*, *oriV cat* $Cam^R$ | Lucigen Corporation |
| pSV14 | pEB52 $P_{trc}$-*yobF*-GGSG-6XHis, $Amp^R$ | This study |
| pSV16 | pMR120 putative $P_{ykgS}$-*yfp*, $Cam^R$ | This study |
| pSV17 | pMR120 putative $P_{proP\text{-}pmrR}$-*yfp*, $Cam^R$ | This study |
| pSV18 | pMR120 putative $P_{yadW}$-*yfp*, $Cam^R$ | This study |
| pSV19 | pMR120 putative $P_{ymiC}$-*yfp*, $Cam^R$ | This study |
| pSV20 | pMR120 putative $P_{ymiA\text{-}yciX\text{-}ymiC}$-*yfp*, $Cam^R$ | This study |
| pSV21 | pMR120 putative $P_{dinQ\text{-}}$*yfp*, $Cam^R$ | This study |
| pSV24 | pMR120 putative $P_{yobF}$-*yfp*, $Cam^R$ | This study |
| pSV25 | pEB52 $P_{trc}$-*gfpA206K-ykgS*, $Amp^R$ | This study |
| pSV26 | pEB52 $P_{trc}$-*pmrR*-GGSG-6XHis, $Amp^R$ | This study |
| pSV28 | pMR120 putative $P_{yddY}$-*yfp*, $Cam^R$ | This study |
| pSV29 | pMR120 putative $P_{mgtS\text{-}mgtT}$-*yfp*, $Cam^R$ | This study |
| pSV30 | pEB52 $P_{trc}$-*mgtT*. $Amp^R$ | This study |
| pSV31 | pEB52 $P_{trc}$-*ydgU*. $Amp^R$ | This study |
| pSV32 | pEB52 $P_{trc}$-*yadX*. $Amp^R$ | This study |
| pSV33 | pEB52 $P_{trc}$-*ymiC*. $Amp^R$ | This study |
| pSV34 | pEB52 $P_{trc}$-*yoaI*. $Amp^R$ | This study |
| pSV35 | pEB52 $P_{trc}$-*pmrR*. $Amp^R$ | This study |
| pSV36 | pEB52 $P_{trc}$-*ymiA*. $Amp^R$ | This study |

| | | |
|---|---|---|
| pSV37 | pEB52 $P_{trc}$-*yriB*. $Amp^R$ | This study |
| pSV38 | pEB52 $P_{trc}$-$pmrR_{ATG\text{->}TAA}$ where the start codon ATG is substituted with a stop TAA, $Amp^R$ | This study |
| pSV39 | pEB52 $P_{trc}$-$yoaI_{ATG\text{->}TAA}$ where the start codon ATG is substituted with a stop TAA, $Amp^R$ | This study |
| pSV40 | pEB52 $P_{trc}$-$mgtS_{ATG\text{->}TAA}$ where the start codon ATG is substituted with a stop TAA, $Amp^R$ | This study |
| pSV41 | pEB52 $P_{trc}$-$ykgS_{ATG\text{->}TAA}$ where the start codon ATG is substituted with a stop TAA, $Amp^R$ | This study |
| pSV42 | pEB52 $P_{trc}$-$ymiA_{ATG\text{->}TAA}$ where the start codon ATG is substituted with a stop TAA, $Amp^R$ | This study |
| pSV45 | pEB52 $P_{trc}$-$yobF_{ATG\text{->}TAA}$ where the start codon ATG is substituted with a stop TAA, $Amp^R$ | This study |
| pSV47 | pUT18C $P_{lac}$-$cyaA_{T18}$-*yoaI*, $Amp^R$ | This study |
| pSV54 | pBAD24 $P_{araBAD}$-*dinQ,* $Amp^R$ | This study |
| pSV55 | pBAD24 $P_{araBAD}$-$dinQ_{ATG\text{->}TAA}$ where the start codon ATG is substituted with a stop TAA, $Amp^R$ | This study |
| pSV58 | pEB52 $P_{trc}$-*yriAB,* $Amp^R$ | This study |
| pSV59 | pEB52 $P_{trc}$-$yriB_{ATG\text{->}TAA}$ where the start codon ATG is substituted with a stop TAA, $Amp^R$ | This study |
| pSV60 | pEB52 $P_{trc}$-*mgrB,* $Amp^R$ | This study |
| pSV61 | pEB52 $P_{trc}$-$mgrB_{ATG\text{->}TAA}$ where the start codon ATG is substituted with a stop TAA, $Amp^R$ | This study |
| pSY68 | pKT25 $P_{lac}$-$cyaA_{T25}$-*phoR*, $Kan^R$ | [8] |
| pTrc99a | $lacI^q$, $P_{trc}$-MCS, $Amp^R$ | [15] |
| pUT18C | pUC19 $P_{lac}$-$cyaA_{T18}$-MCS, $Amp^R$ | Euromedex |

$Amp^R$ = carries a carbenicillin/ampicillin-resistance marker; $Cam^R$ = carries a chloramphenicol-resistance marker; $Kan^R$ = carries a kanamycin-resistance marker

**Table S3. List of primers used in the study**

| Primer | Sequence (5'-> 3') | Use |
|---|---|---|
| C-term-pmrR-F1 | AGCTTTCTTTATATCTGGTTTGCCACGTACGGCGGCAGCGGCCACCATCACCATCACCATTAAGCTTAATTAGCTGACCTACTAGAGTCG | Cloning of pSV26 |
| C-term-pmrR-R1 | GCTGACCACCAGCACGCTGAACACGGTAGTTAAACTTTCATAAACACGGTTTTTCATGCTTAATTTCTCCTCTTTAATTCTAGGTACCCG | Cloning of pSV26 |
| dinQ_del_screen_1 | aagatgggggcaaccaaaaaag | Validation of GSO195 |
| dinQ_del_screen_2 | ttcactctggcaatgcgcata | Validation of GSO195 |
| dinQ_F1 | ATATGAATTCCATCAATGCTAATACCATACTGAAACTATTGCA | Cloning of pSV21 |
| dinQ_R1 | ATATGGATCCCCGTTTTCTCCATGCGATGGAG | Cloning of pSV21 |
| dinQ_pBAD_R | CAGCGCAATTAACGCCCCTAGAACGATGATTGCTTTATCAATcatTGAATTCCTCCTGCTAGCCCAAA | Cloning of pSV54 |
| dinQ_pBAD_F | CTGGAACTGATCCGCTTTCTGCTTCAGCTTCTGAACTAAGGTACCCGGGGATCCTCTAG | Cloning of pSV54 |
| dinQ_stop_F | TAAATTGATAAAGCAATCATCGTTCTAGGGG | Cloning of pSV55 |
| dinQ_stop_R | TGAATTCCTCCTGCTAGCCCA | Cloning of pSV55 |
| F_yoaI_BATCH | ACTGTCTAGAGatgAACGATCAAATGTTTGTCGAGACAC | Cloning of pSV47 |
| Fp_Inv_PCR_yobF | TAAGCTTAATTAGCTGACCTACTAGAGTCGAC | Cloning of pSV14 |
| JA1 | GCGTACGCAATCAAAATCCCCAGCCAATACAAcatTTAACACCATgcttaatttctcctctttaattctaggtacccg | Cloning of pSV58 |
| JA2 | AGACCGTAGGCCAGATAAGGTGTTTACGCTGATCAGGtaaGCTTAATTAGCTGACCTactagagtcgac | Cloning of pSV58 |
| JS4 | taaTTGTATTGGCTGGGGATTTTGATTGC | Cloning of pSV59 |
| lpxT_del_F | gacagccgtattgagctgatttcc | Validation of JW2162 |
| lpxT_del_R | aaagtgatacagaaagttaataagcgggg | Validation of JW2162 |
| mgrB_forward | atgaaaaagtttcgatgggtcgttct | Cloning of pSV60 |
| mgrB_stop3 | TAAaaaaagtttcgatgggtcgttctg | Cloning of pSV61 |

| | | |
|---|---|---|
| MgtS_del_F | AAAATTAAGGTAAGCGAGGAAACACACCACACCATAAACGGAGGCAAATAattccggggatccgtcgacctgcagttcgaagttcctatt | Construction of SV64 |
| MgtS_del_R | AACTGTAACAAGGGGCCGGTTAGGTGAGGGATTATCTCCGTTcatTAGTCtgtaggctggagctgcttcgaagttcctatact | Construction of SV64 |
| mgtS_del_screen_1 | cccgcgctttgttgatttaagtc | Validation of SV64 together with primer mgtT_del_screen2 |
| mgtS_forward_2_correct | TCTGGTTTTCTGGCCGCGTATTTCAGCCACAAATGGGATGACtaaTAAGCTTAATTAGCTGACCTactagagtcgac | Cloning of pJS7 |
| mgtS_reverse | AAATAAAATTATTCCCAGTACGGCCATAAAAACATTCATATTACCCAGcatgcttaatttctcctctttaattctaggtacccg | Cloning of pJS7 |
| mgtS_stop | TAACTGGGTAATTAAAATGTTTTTATGGCCGTACTGGGAATAATTTTATTTTCTGG | Cloning of pSV40 |
| mgtT_del_F | TATTTTCTGGTTTTCTGGCCGCGTATTTCAGCCACAAATGGGATGACTAAattccggggatccgtcgacc | Construction of SV31 |
| mgtT_del_R | CAAATCTATCCATGCAAGCATtcaCCGCCGGTTTACTGGCGGTTTTTTTTtgtaggctggagctgcttcg | Construction of SV31 |
| mgtT_del_screen1 | CACACCACACCATAAACGGAGG | Validation of SV31 |
| mgtT_del_screen2 | ACCGGAAGAAATCGCTGCATG | Validation of SV31 |
| mgtT_F | GAGAATTCTCAGCTGCGGTATTTACTGTCGG | Cloning of pSV29 |
| mgtT_R | GGGGATCCTAGTCATCCCATTTGTGGCTGAAATACG | Cloning of pPJ1 |
| mgtT_R1 | ATATGGATCCTATTTGCCTCCGTTTATGGTGTGGTG | Cloning of putative pSV29 |
| mgtT-forward | ATGAACGGAGATAATCCCTCACCTAAC | Cloning of pSV30 |
| N_term_pmrR_forward | ATGAAAAACCGTGTTTATGAAAGTTTAACTACCG | Cloning of pSV35 |
| pEB52-rev | GCTTAATTTCTCCTCTTTAATTCTAGGTACCCG | When targeting N-terminal-tagged small proteins, this primer, along with a small protein-specific forward primer, removes the tags by binding to the pEB52 backbone |

| | | |
|---|---|---|
| phoB_del_F | cgaaaaagcatgggcgcgatta | Validation of JW0389 |
| phoB_del_R | agggcaggtaaccaaaaaatgcac | Validation of JW0389 |
| pmrR Primer 1 | CTGGTGGTCAGCAGCTTTCTTTATATCTGGTTTGCCACGTACTGATAAGCTTAATTAGCTGACCTactagagt | Cloning of pPJ2 |
| pmrR Primer 2 | CACGCTGAACACGGTAGTTAAACTTTCATAAACACGGTTTTTCATtttgtatagttcatccatgccatgtg | Cloning of pPJ2 |
| pmrR_del_F | CTTAATCTCTGACGCGCATACTCTCCTCCAGGTTAACGGAGGAGAGTGCAattccggggatccgtcgacc | Construction of SV35 |
| pmrR_del_R | GCCTGGGTACGGCTGAAGAAAGAtcaGTACGTGGCAAACCAGATATAAGtgtaggctggagctgcttcg | Construction of SV35 |
| pmrR_del_screen1 | GCGAATTGATGAATAAGCTGAAACGG | Validation of SV35 |
| pmrR_del_screen2 | CGTTTGTACGTATGGACAGCCG | Validation of SV35 |
| pmrR_stop | TAaAAAAACCGTGTTTATGAAAGTTTAACTACCG | Cloning of pSV38 |
| pmrR1_F | GAGAATTCTGGCTTCTACCTTGCCAGCG | Cloning of pPJ14 |
| pmrR1_R | GGGGATCCTGCACTCTCCTCCGTTAACCTG | Cloning of pPJ14 |
| pmrR2_F | GAGAATTCCCGACCACGCGTCACTATTACC | Cloning of pSV17 |
| pmrR2_R | GGGGATCCAGCTTTCCTCGCAGAGTTGG | Cloning of pSV17 |
| pSMART SV_19 | GACCATAACCGAAAGTAGTGAC | Sequencing primer for pMR120 based vectors |
| R_yoaI_BATCH | TACTGAATTCctaGCCGGTCCGTTCGATAAGAAG | Cloning of pSV47 |
| Rp_Inv_PCR_yobF | ATGGTGATGGTGATGGTGGCCGCTGCCGCCGATTGTTTTCTTCGCCCGCAGG | Cloning of pSV14 |
| SA26R | CATCCGCCAAAACAGCCAAG | Sequencing primer for pEB52 based vectors |
| yadW Primer 1 | TGCCGATGTCGTTTGGAGCAAAATATGAGTGATAAGCTTAATTAGCTGACCTactagagt | Cloning of pPJ9 |
| yadW Primer 2 | ATTGGGCAAATTCTAACCCAATAATAATCGCCATtttgtatagttcatccatgccatgtg | Cloning of pPJ9 |
| yadW_del_F | GCCGCATCAGCCAGCGAGAATACTTGAACGAAATACCAGGGTATTAGATAattccggggatccgtcgacc | Construction of SV27 |
| yadW_del_R | TCGGTAAACTCCAGCGGCAGTGCTACGTCAtcaCTCATATTTTGCTCCAAACGtgtaggctggagctgcttcg | Construction of SV27 |

| | | |
|---|---|---|
| yadW_del_screen1 | CGGGAAACCGCTATACTCGG | Validation of SV27 |
| yadW_del_screen2 | GGTGAAACCATACTGGAAGCCG | Validation of SV27 |
| yadW_forward | atgGCGATTATTATTGGGTTAGAATTTGCC | Cloning of pJS2 |
| yadW1_F | GAGAATTCTTCCATTTCGGTTGGTGCACCAA | Cloning of pSV18 |
| yadW1_R | GGGGATCCCCAATGATCACTTATTGGTCATACAAATAAGATGAC | Cloning of pSV18 |
| yadW2_F | GAGAATTCACCATGCGCACCATATCCATGG | Cloning of pPJ23 |
| yadW2_R | GGGGATCCGAAAATCCTTTGCAAAGCGTAATGTTTCAAAT | Cloning of pPJ23 |
| yadX Primer 1 | TCATCTTATTTGTATGACCAATAATAAGCTTAATTAGCTGACCTactagagt | Cloning of pPJ10 |
| yadX Primer 2 | CGGCATTTTACTCGCACGTTCCATtttgtatagttcatccatgccatgtg | Cloning of pPJ10 |
| yadX_del_F | AGTATAAAAGTTTTGTGCATTTGAAACATTACGCTTTGCAAAGGATTTTCattccggggatccgtcgacc | Construction of SV39 |
| yadX_del_R | AGAGGGAGTATCAGTTTTCATCCAATGATCACttaTTGGTCATACAAATAtgtaggctggagctgcttcg | Construction of SV39 |
| yadX_del_screen1 | CATGGAGGGTTCCTGATTCGTAG | Validation of SV39 |
| yadX_del_screen2 | GCCATAAACAAAATGGCTAACGGG | Validation of SV39 |
| yadX-forward | ATGGAACGTGCGAGTAAAATGC | Cloning of pSV32 |
| yddY Primer 1 | GCACGTTGCGTTTCATTTTGATAAGCTTAATTAGCTGACCTactagagt | Cloning of pPJ8 |
| yddY Primer 2 | GAGATCGACTAACTGCACCATtttgtatagttcatccatgccatgtg | Cloning of pPJ8 |
| yddY_del_F | GTCCTAAATCGCTTATTTCTTTTCAGTATATCTTCATATTTCAGGAGAATattccggggatccgtcgacc | Construction of SV29 |
| yddY_del_R | AATACATCTCCATAATTCACACCCTTATAAGGCTGGGAAATCAGACGGAAtgtaggctggagctgcttcg | Construction of SV29 |
| yddY_del_screen1 | CATACGATATTCGCTGTCACCG | Validation of SV29 |
| yddY_del_screen2 | CCGCGGCTTTAGCACGAAT | Validation of SV29 |
| yddY_F | GAGAATTCCTGTATATCGGTATCGCCTTCTATAAAGTGG | Cloning of pSV28 |

| | | |
|---|---|---|
| yddY_forward | ATGGTGCAGTTAGTCGATCTCG | Cloning of pJS6 |
| yddY_R | GGGGATCCATTCTCCTGAAATATGAAGATATACTGAAAAG | Cloning of pSV28 |
| ydgU Primer 1 | ATTTTATGCGCACTGATTACCGCCCGTTTTTATCTTTCCTGATAAGCTTAATTAGCTGACCTactagagt | Cloning of pPJ3 |
| ydgU Primer 2 | AAGGATGATCAGAATGAACTCAAAGCGATAACGGCCCACCATtttgtatagttcatccatgccatgtg | Cloning of pPJ3 |
| ydgU_del_screen_1 | gcagcgaagaaacacgccaa | Validation of GSO219 |
| ydgU_del_screen_2 | caaaagcagacgtcaaactaattgca | Validation of GSO219 |
| ydgU-forward | ATGGTGGGCCGTTATCGCTT | Cloning of pSV31 |
| ydgU1_F | ACTCGAGAATTCGAAACCAACCACTCACGGAAGTCTG | Cloning of pPJ17 |
| ydgU1_R | CCGGGGATCCACTACCCTCCGCTAAAGGCG | Cloning of pPJ17 |
| ydgU2_F | ACTCGAGAATTCATACCCGTCCGGACTTATTGCC | Cloning of pPJ16 |
| ydgU2_R | GGGGATCCTGTCATACCCTCAATTTGTTTTTTCATTTAACCC | Cloning of pPJ16 |
| ykgS_del_F2 | CAGAAGCAGAAAGACATTGGATCGAATTCTACAACCAGGTCGAGTCAGAaattccggggatccgtcgacctgcagttcgaagttcctatt | Construction of SV43 |
| ykgS_del_R2 | CAAAGTCATCGGGCATTATCTGAACATAAAACACTATCAATAAGTTGGAGtgtaggctggagctgcttcgaagttcctatact | Construction of SV43 |
| ykgS_del_screen1 | GGCAAACCCGTCCGTGTG | Validation of SV43 |
| ykgS_del_screen2 | AAGTCGCTGTCGTTCTCAAA | Validation of SV43 |
| ykgS_F | ATATCTCGAGAAGTGTTTTTTGTATAAATCGGACATTTTATCCTCG | Cloning of pSV25 |
| ykgS_F1 | ATATCTCGAGAAGTGTTTTTTGTATAAATCGGACATTTTATCCTCG | Cloning of pSV16 |
| ykgS_forward | ATGAGAATGATTGGCCTTCTTTATGATTTTAAGG | Cloning of pJS4 |
| ykgS_R | ATATGGATCCTTCTGACTCGACCTGGTTGTAGAATTCG | Cloning of pSV25 |
| ykgS_R1 | ATATGGATCCTTCTGACTCGACCTGGTTGTAGAATTCG | Cloning of pSV16 |
| ykgS_stop | TAAAGATAAATTGGCCTTCTTTATGATTTTAAGGATTATGCT | Cloning of pSV41 |

| | | |
|---|---|---|
| ymiA Primer 1 | TGGCGGTTTTTCTTGGTTCTGCACTTTTCTGGGTGGTTGTCGCACTGCTGATTTGGAAAGTGTGGGGATAATAAGCTTAATTAGCTGACCTactagagt | Cloning of pPJ12 |
| ymiA Primer 2 | GCCAGGCTTTACGTTTTAATTCAGGATCGCGGCGGGGTTCCTGATTTCCAGAAGGCATTGCTAACCTCATtttgtatagttcatccatgccatgtg | Cloning of pPJ12 |
| ymiA_del_screen_1 | gattgaattattcactggagacgattcg | Validation of GSO225 |
| ymiA_del_screen_2 | tcatcttcagcaaacagttctataaaggc | Validation of GSO225 |
| ymiA_F1 | ATATGAATTCTCAGCCACAGTACAACCAAAATTGG | Cloning of pSV20 |
| ymiA_R1 | ATATGATCCATAATCGCCATCACTTATCAGCAAGAC | Cloning of pSV20 |
| ymiA_stop | TAAAGGTTAGCATAACCTTCTGGAAATCAGGAACCCC | Cloning of pSV42 |
| ymiA-forward | ATGAGGTTAGCAATGCCTTCTGGA | Cloning of pSV36 |
| ymiC Primer 1 | CTGTCGATGCTCTTCTGGGCCGAACTCCTCTGGATCATTACTCACTGATAAGCTTAATTAGCTGACCTactagagt | Cloning of pPJ13 |
| ymiC Primer 2 | AGAAAACGCGCCCATCCAGGACCAATATTTCATATTTGTGTTGATCATtttgtatagttcatccatgccatgtg | Cloning of pPJ13 |
| ymiC_del_F | ACAGCTTGAGTTATCTCAACACAAAATAATAACCGTTAAGGGTGTAGCCTattccggggatccgtcgacc | Construction of SV41 |
| ymiC_del_R | GAAACCTTGTGGCAAAGCAAATGACAACCCCGCCGCAGCGGGGTCAAGGAtgtaggctggagctgcttcg | Construction of SV41 |
| ymiC_del_screen1 | GATGATCAGCCGAAACAATAATTATCATCATTC | Validation of SV41 |
| ymiC_del_screen2 | AAGCCCTGATTCTCTTCAGGGT | Validation of SV41 |
| ymiC_F1 | ATATGAATTCCAGGAGCAACTGGAGTCGTC | Cloning of pSV19 |
| ymiC_R1 | ATATGGATCCAGGCTACACCCTTAACGGTTATTATTTTG | Cloning of pSV19 |
| ymiC-forward | ATGATCAACACAAATATGAAATATTGGTCCTGGA | Cloning of pSV33 |
| yoaI Primer 1 | ATTGCTGTTGTACTGGTTTTGTCCGTTCTTCTTATCGAACGGACCGGCcgtaaaggagaagaacttttcactgg | Cloning pPJ4 |
| yoaI Primer 2 | GGCAAAAAACGATGACGTGATAATCAGTGTCTCGACAAACATTTGATCGTTcatgcttaatttctcctctttaattctaggtac | Cloning pPJ4 |
| yoaI_del_screen_1 | tggttgccgaccctctactc | Validation of GSO232 |

| | | |
|---|---|---|
| yoaI_del_screen_2 | agcctgcttactttacgcttgc | Validation of GSO232 |
| yoaI_F | GAGAATTCGCGGCTGGCTGCCCATTAA | Cloning of pPJ18 |
| yoaI_R | GGGGATCCAGCATGCCCCCGGGAGATA | Cloning pPJ18 |
| yoaI_stop | taAAACGATCAATAATTTGTCGAGACACTGATTATCACGTCATCG | Cloning of pSV39 |
| yoaI-forward | TAAGCTTAATTAGCTGACCTACTAGAGTCGAC | Cloning of pSV34 |
| yoaI-rev | GCCGGTCCGTTCGATAAGAAGA | Cloning of pSV34 |
| yobF Primer 1 | CCTTATATTGGTGCCTCATGCAGTAATGTGTCAGTTTTATCTATGTTATGCCTGCGGGCGAAGAAAACAATCcgtaaaggagaagaacttttcactgg | Cloning of pPJ6 |
| yobF Primer 2 | CTCGGCAGAGAAGCGGTATTCAACGTCAACGTGTTTACTCAGGACTTCTTTACTGAAAATGCCACAcatgcttaatttctcctctttaattctaggtac | Cloning of pPJ6 |
| yobF_del_F | AAAGAAGTCCTGAGTAAACACGTTGACGTTGAATACCGCTTCTCTGCCGAattccggggatccgtcgacc | Construction of SV33 |
| yobF_del_R | TTGAACCACTTAACCTGACCTTTAATCTTTGCCATTTGAAAAATTCCttatgtaggctggagctgcttcg | Construction of SV33 |
| yobF_del_screen1 | GTGTGCAAAAAAAGTGGAAGACGT | Validation of SV33 |
| yobF_del_screen2 | CCATTACCCTGGATAGCGGAG | Validation of SV33 |
| yobF_F1 | ATATGAATTCTAATTTATTAGGATGTTTACATCGGATTTGTGATTAAGCG | Cloning of pSV24 |
| yobF_R1 | ATATGGATCCAAACAGAACTGTACCTCGTTTAACCC | Cloning of pSV24 |
| yobF_reverse | GATTGTTTTCTTCGCCCGCAGG | Cloning of pJS5 |
| yobF_stop | taaTGTGGCATTTTCAGTAAAGAAGTCCTG | Cloning of pSV45 |
| yqhI Primer 1 | ATCTCGAAACGTGAGTTCCTCAACCTTGCGGCGAAGTGCGGTAGGCGGGATGACGGCATTAGCGTTGTTTGATAAGCTTAATTAGCTGACCTactagagt | Cloning of pPJ15 |
| yqhI Primer 2 | TTTCCCGTGAGCGTAATAGTCATAGTAATCCAGCAACTCTTGTGGGAAATCTTTGGCGGTTAAACGCGGCATtttgtatagttcatccatgccatgtg | Cloning of pPJ15 |
| yqhI_del_F2 | AATACGTGCTTATGCTTTGCTTAAAAAAACACCAACTGAGGAGTGCAACGaattccggggatccgtcgacctgcagttcgaagttcctatt | Construction of SV37 |
| yqhI_del_R2 | GGTCGGTAAACTCTACCTGAGTCGCCAGCGCATAATTTGGCTTGAGCAAAtgtaggctggagctgcttcgaagttcctatact | Construction of SV37 |

| | | |
|---|---|---|
| yqhI_del_screen 1 | TGTTTCTAGTTTAGCGATTCGCCAG | Validation of SV37 |
| yqhI_del_screen 2 | GGGCTTCACCAGATAACCCC | Validation of SV37 |
| yqhI_F | GAGAATTCTATTTACGTGAACCGCCAGAGCC | Cloning of pPJ19 |
| yqhI_forward | ATGCCGCGTTTAACCGCC | Cloning of pJS3 |
| yqhI_R | GGGGATCCCGTTGCACTCCTCAGTTGGTG | Cloning of pPJ19 |
| yriA Primer 1 | GCAGACCGTAGGCCAGATAAGGTGTTTACGCTGAT CAGGTAATAAGCTTAATTAGCTGACCTactagagt | Cloning of pPJ7 |
| yriA Primer 2 | GTACGCAATCAAAATCCCCAGCCAATACAACATtttgta tagttcatccatgccatgtg | Cloning of pPJ7 |
| yriA_F | TCGAGAATTCAAATCAGGTCAGGCTTAAGTAGCGAC | Cloning of pPJ20 |
| yriA_forward | ATGTTGTATTGGCTGGGGATTTTGAT | Cloning of pJS1 |
| yriA_R | GGGGATCCTTAACACCATCATATTTTCCATCATTAG TGTGATC | Cloning of pPJ20 |
| yriAB_del_F | ACACTATTACAACAGAAAATAACCAGATGATCACAC TAATGATGGAAAATattccggggatccgtcgacc | Construction of SV25 |
| yriAB_del_R | TGTTCCTGAACGCCCGCATATGCGGGCGTTTTGCT TTTTGGCGCGCCTTGgtgtaggctggagctgcttc | Construction of SV25 |
| yriAB_del_scree n1 | GAACGCGTAAGGGATAACGC | Validation of SV25 |
| yriAB_del_scree n2 | CTGATCAACACCGTTCACGTTG | Validation of SV25 |
| yriB Primer 1 | GATTTTGATTGCGTACGCAGACCGtagTAAGCTTAAT TAGCTGACCTactagagt | Cloning of pPJ11 |
| yriB primer 2 | CCCAGCCAATACAACATTTAACACcattttgtatagttcatcca tgccatgtg | Cloning of pPJ11 |
| yriB-forward | atgGTGTTAAATGTTGTATTGGCTGGG | Cloning of pSV37 |

**Table S4. List of all proteins with ≥3-fold increase in read counts from Ribo-RET and differentially expressed transcripts from RNA-Seq.**

| Ribo-RET | | | | | RNA-Seq Differential Expression | | | | | |
|---|---|---|---|---|---|---|---|---|---|---|
| gene | size | no_ stress | low_ mg | fold_ change | gene | base_ Mean | log2Fold Change | lfcSE | pvalue | padj |
| *phnC* | standard | 0.68 | 79.66 | 117.25 | *mgtS* | 14972.46 | 7.82 | 0.31 | 2.11E-140 | 6.60E-137 |
| *iraM* | standard | 3.4 | 247.31 | 72.8 | *ymgL* | 17.66 | 7.53 | 2.75 | 2.84E-06 | 2.56E-05 |
| *phoR* | standard | 0.68 | 44.65 | 65.71 | *mgtA* | 3789.38 | 7.13 | 0.39 | 9.56E-75 | 9.97E-72 |
| *ptrA* | standard | 1.36 | 72.66 | 53.47 | *ymgK* | 236.85 | 6.93 | 0.62 | 6.26E-29 | 5.02E-27 |
| *phoE* | standard | 5.44 | 242.93 | 44.69 | *iraM* | 205.15 | 6.71 | 0.63 | 4.09E-27 | 2.78E-25 |
| *eptA* | standard | 5.44 | 232.43 | 42.76 | *mgtL* | 11342.3 | 6.61 | 0.43 | 1.18E-54 | 5.27E-52 |
| *ydeT* | standard | 4.76 | 148.38 | 31.2 | *ydeT* | 28.94 | 6.33 | 1.43 | 6.39E-06 | 5.33E-05 |
| *arnC* | standard | 0.68 | 20.13 | 29.64 | *ydeS* | 9.66 | 6.26 | 2.76 | 1.15E-04 | 7.48E-04 |
| *yciX* | standard | 1.36 | 38.96 | 28.67 | *asr* | 332.57 | 5.91 | 0.48 | 3.80E-35 | 4.96E-33 |
| *waaH* | standard | 2.04 | 58.22 | 28.56 | *ybjG* | 1315.13 | 5.78 | 0.35 | 4.37E-63 | 3.42E-60 |
| *rstB* | standard | 0.68 | 18.82 | 27.7 | *mgrB* | 6552.83 | 5.68 | 0.31 | 4.00E-76 | 6.25E-73 |
| *phoQ* | standard | 2.04 | 54.71 | 26.84 | *phnD* | 25.86 | 5.34 | 1.17 | 1.71E-06 | 1.61E-05 |
| *ugpB* | standard | 10.87 | 288.45 | 26.53 | *yebO* | 1871.52 | 5.1 | 0.33 | 1.23E-55 | 6.42E-53 |
| *phoB* | standard | 29.21 | 711.72 | 24.36 | *yriB* | 18.19 | 4.72 | 1.24 | 3.12E-05 | 2.30E-04 |
| *appC* | standard | 6.79 | 162.39 | 23.9 | *phnC* | 17.35 | 4.63 | 1.25 | 4.47E-05 | 3.18E-04 |
| *otsB* | standard | 0.68 | 14.88 | 21.9 | *pstS* | 274.79 | 4.41 | 0.41 | 1.93E-28 | 1.48E-26 |
| *argD* | standard | 10.87 | 199.6 | 18.36 | *yfeO* | 91.2 | 4.31 | 0.56 | 1.21E-15 | 2.81E-14 |
| *cysD* | standard | 20.38 | 358.92 | 17.61 | *ydgU* | 24.42 | 4.31 | 0.99 | 2.00E-06 | 1.85E-05 |
| *cbl* | standard | 2.04 | 35.02 | 17.18 | *dgcZ* | 61.86 | 4.29 | 0.64 | 3.40E-12 | 6.33E-11 |
| *ynaL* | standard | 1.36 | 21.01 | 15.46 | *pgpC* | 397.23 | 4.24 | 0.37 | 2.38E-31 | 2.26E-29 |
| *asr* | standard | 51.64 | 796.2 | 15.42 | *ygdR* | 155.39 | 4.19 | 0.46 | 9.92E-21 | 3.34E-19 |
| *yriA* | small | 2.72 | 40.71 | 14.98 | *alaV* | 973.94 | 4.18 | 0.36 | 2.73E-32 | 2.85E-30 |
| *glsA* | standard | 0.68 | 10.07 | 14.82 | *alaU* | 973.94 | 4.18 | 0.36 | 2.73E-32 | 2.85E-30 |
| *yciW* | standard | 8.15 | 119.06 | 14.6 | *alaT* | 973.94 | 4.18 | 0.36 | 2.73E-32 | 2.85E-30 |
| *yohC* | standard | 8.15 | 118.18 | 14.5 | *metZ* | 673.96 | 4.12 | 0.43 | 6.41E-23 | 2.87E-21 |
| *yeeE* | standard | 4.08 | 58.65 | 14.39 | *metW* | 673.96 | 4.12 | 0.43 | 6.41E-23 | 2.87E-21 |
| *sbp* | standard | 6.79 | 96.3 | 14.17 | *metV* | 673.96 | 4.12 | 0.43 | 6.41E-23 | 2.87E-21 |
| *ydgU* | small | 2.04 | 27.14 | 13.31 | *glyW* | 9479.84 | 4.06 | 0.33 | 1.60E-35 | 2.27E-33 |
| *narU* | standard | 1.36 | 17.95 | 13.21 | *glyV* | 9479.84 | 4.06 | 0.33 | 1.60E-35 | 2.27E-33 |
| *arnB* | standard | 11.55 | 151.45 | 13.11 | *glyX* | 9479.84 | 4.06 | 0.33 | 1.60E-35 | 2.27E-33 |
| *argA* | standard | 16.31 | 212.29 | 13.02 | *glyY* | 9479.84 | 4.06 | 0.33 | 1.60E-35 | 2.27E-33 |
| *ais* | standard | 9.51 | 123 | 12.93 | *ais* | 16.7 | 4.03 | 1.15 | 6.60E-05 | 4.54E-04 |
| *ycaP* | standard | 1.36 | 17.51 | 12.88 | *arnB* | 38.15 | 3.91 | 0.76 | 2.56E-08 | 3.31E-07 |
| *phoA* | standard | 12.23 | 156.26 | 12.78 | *ugpB* | 80.2 | 3.83 | 0.57 | 1.18E-12 | 2.26E-11 |
| *ydeQ* | standard | 1.36 | 17.07 | 12.56 | *alaX* | 648.46 | 3.79 | 0.38 | 2.29E-24 | 1.21E-22 |
| *yncG* | standard | 2.04 | 25.39 | 12.46 | *alaW* | 648.46 | 3.79 | 0.38 | 2.29E-24 | 1.21E-22 |

| | | | | | | | | | | |
|---|---|---|---|---|---|---|---|---|---|---|
| *ilvB* | standard | 1.36 | 16.2 | 11.92 | *rttR* | 21.62 | 3.74 | 1.06 | 4.26E-05 | 3.06E-04 |
| *yoaI* | small | 13.59 | 161.95 | 11.92 | *metY* | 276.5 | 3.73 | 0.43 | 6.96E-19 | 2.05E-17 |
| *cysP* | standard | 63.87 | 758.56 | 11.88 | *leuW* | 4113.99 | 3.68 | 0.35 | 1.34E-27 | 9.30E-26 |
| *yfcG* | standard | 4.08 | 48.15 | 11.81 | *arnC* | 29.57 | 3.66 | 0.82 | 9.33E-07 | 9.24E-06 |
| *lysA* | standard | 2.04 | 23.64 | 11.6 | *rstA* | 323.01 | 3.65 | 0.38 | 8.71E-23 | 3.84E-21 |
| *artP* | standard | 43.48 | 491.11 | 11.29 | *msrQ* | 38.7 | 3.63 | 0.72 | 5.34E-08 | 6.58E-07 |
| *yhbW* | standard | 1.36 | 15.32 | 11.27 | *arnF* | 56.91 | 3.62 | 0.61 | 3.42E-10 | 5.22E-09 |
| *dacD* | standard | 0.68 | 7.44 | 10.95 | *phoA* | 78.32 | 3.62 | 0.55 | 3.42E-12 | 6.33E-11 |
| *ruvC* | standard | 0.68 | 7.44 | 10.95 | *ymcF* | 40.82 | 3.61 | 0.71 | 3.74E-08 | 4.73E-07 |
| *ydbL* | standard | 1.36 | 14.88 | 10.95 | *dacC* | 178.45 | 3.59 | 0.42 | 1.11E-18 | 3.21E-17 |
| *argG* | standard | 20.38 | 217.98 | 10.69 | *ileV* | 995.19 | 3.57 | 0.34 | 3.75E-26 | 2.35E-24 |
| *argC* | standard | 6.11 | 64.78 | 10.59 | *ileU* | 995.19 | 3.57 | 0.34 | 3.75E-26 | 2.35E-24 |
| *ybhP* | standard | 0.68 | 7 | 10.31 | *ileT* | 995.19 | 3.57 | 0.34 | 3.75E-26 | 2.35E-24 |
| *yobF* | small | 12.91 | 132.63 | 10.27 | *phoQ* | 258.31 | 3.57 | 0.38 | 1.64E-21 | 6.11E-20 |
| *pstS* | standard | 48.92 | 490.68 | 10.03 | *phoB* | 66.9 | 3.56 | 0.57 | 4.75E-11 | 7.87E-10 |
| *nadD* | standard | 1.36 | 13.57 | 9.99 | *eptA* | 15.82 | 3.5 | 1.11 | 1.72E-04 | 0.001078186 |
| *gadE* | standard | 2.72 | 26.7 | 9.82 | *arnA* | 35.6 | 3.49 | 0.74 | 2.45E-07 | 2.70E-06 |
| *ydeS* | standard | 2.72 | 26.7 | 9.82 | *ydhI* | 62.43 | 3.45 | 0.58 | 3.12E-10 | 4.78E-09 |
| *bcsB* | standard | 0.68 | 6.57 | 9.66 | *pdeR* | 34.61 | 3.44 | 0.74 | 3.72E-07 | 3.97E-06 |
| *pcm* | standard | 0.68 | 6.57 | 9.66 | *pstC* | 127.36 | 3.42 | 0.46 | 7.14E-15 | 1.56E-13 |
| *yadW* | small | 1.36 | 13.13 | 9.66 | *secG* | 2556.53 | 3.41 | 0.38 | 2.56E-20 | 8.08E-19 |
| *pagP* | standard | 8.15 | 75.29 | 9.23 | *phoP* | 729.83 | 3.38 | 0.33 | 5.44E-25 | 3.27E-23 |
| *pstA* | standard | 2.04 | 18.82 | 9.23 | *slyB* | 3744.69 | 3.34 | 0.3 | 7.35E-30 | 6.39E-28 |
| *waaQ* | standard | 2.04 | 18.82 | 9.23 | *hokD* | 178.33 | 3.31 | 0.42 | 3.78E-16 | 8.96E-15 |
| *aroE* | standard | 0.68 | 6.13 | 9.02 | *pagP* | 21.67 | 3.28 | 0.91 | 3.55E-05 | 2.57E-04 |
| *mgrB* | small | 250.71 | 2248.97 | 8.97 | *yliM* | 5741.91 | 3.21 | 0.32 | 5.03E-24 | 2.58E-22 |
| *dtpD* | standard | 2.72 | 24.07 | 8.86 | *yjcB* | 202.42 | 3.2 | 0.4 | 7.82E-17 | 1.93E-15 |
| *tatD* | standard | 8.15 | 71.78 | 8.8 | *relE* | 150.84 | 3.19 | 0.44 | 6.33E-14 | 1.28E-12 |
| *bcr* | standard | 2.04 | 17.51 | 8.59 | *rstB* | 99.93 | 3.16 | 0.49 | 8.30E-12 | 1.48E-10 |
| *pstC* | standard | 44.16 | 377.31 | 8.54 | *ynfB* | 711.59 | 3.09 | 0.34 | 1.32E-20 | 4.34E-19 |
| *blc* | standard | 2.72 | 23.2 | 8.54 | *ybfA* | 383.07 | 3.09 | 0.38 | 3.59E-17 | 9.13E-16 |
| *nudL* | standard | 2.72 | 23.2 | 8.54 | *deoR* | 205.33 | 3.08 | 0.4 | 6.56E-16 | 1.54E-14 |
| *insQ* | standard | 6.79 | 56.9 | 8.38 | *sraG* | 43.7 | 3.08 | 0.65 | 2.09E-07 | 2.33E-06 |
| *cysJ* | standard | 60.47 | 504.25 | 8.34 | *valT* | 8108.95 | 3.08 | 0.33 | 7.92E-22 | 3.02E-20 |
| *pdeR* | standard | 8.15 | 67.41 | 8.27 | *valZ* | 8108.95 | 3.08 | 0.33 | 7.92E-22 | 3.02E-20 |
| *iaaA* | standard | 30.57 | 251.69 | 8.23 | *valU* | 8108.95 | 3.08 | 0.33 | 7.92E-22 | 3.02E-20 |
| *yhdN* | standard | 4.08 | 32.83 | 8.05 | *valX* | 8108.95 | 3.08 | 0.33 | 7.92E-22 | 3.02E-20 |
| *chaC* | standard | 5.44 | 43.33 | 7.97 | *valY* | 8108.95 | 3.08 | 0.33 | 7.92E-22 | 3.02E-20 |
| *mgtT* | small | 1082.31 | 8622.95 | 7.97 | *tqsA* | 29.99 | 3.05 | 0.76 | 6.71E-06 | 5.58E-05 |
| *gadX* | standard | 4.08 | 31.95 | 7.84 | *lysT* | 11718.26 | 3.05 | 0.33 | 3.00E-21 | 1.04E-19 |
| *rssB* | standard | 4.08 | 31.95 | 7.84 | *lysW* | 11718.26 | 3.05 | 0.33 | 3.00E-21 | 1.04E-19 |
| *hisG* | standard | 13.59 | 105.93 | 7.8 | *lysY* | 11718.26 | 3.05 | 0.33 | 3.00E-21 | 1.04E-19 |

| | | | | | | | | | | |
|---|---|---|---|---|---|---|---|---|---|---|
| *cysW* | standard | 0.68 | 5.25 | 7.73 | *lysZ* | 11718.26 | 3.05 | 0.33 | 3.00E-21 | 1.04E-19 |
| *glaR* | standard | 0.68 | 5.25 | 7.73 | *lysQ* | 11718.26 | 3.05 | 0.33 | 3.00E-21 | 1.04E-19 |
| *ibsD* | small | 0.68 | 5.25 | 7.73 | *lysV* | 11718.26 | 3.05 | 0.33 | 3.00E-21 | 1.04E-19 |
| *ibsE* | small | 0.68 | 5.25 | 7.73 | *appC* | 46.53 | 3.02 | 0.63 | 1.57E-07 | 1.80E-06 |
| *ybdR* | standard | 0.68 | 5.25 | 7.73 | *fabR* | 293.94 | 3.02 | 0.37 | 4.17E-17 | 1.05E-15 |
| *hisD* | standard | 9.51 | 73.1 | 7.68 | *csrC* | 1142.49 | 3 | 0.32 | 6.80E-22 | 2.80E-20 |
| *tqsA* | standard | 8.15 | 61.28 | 7.52 | *phoR* | 33.35 | 2.98 | 0.72 | 3.93E-06 | 3.47E-05 |
| *purF* | standard | 15.63 | 117.31 | 7.51 | *ygcN* | 30.28 | 2.95 | 0.75 | 1.01E-05 | 8.10E-05 |
| *glcD* | standard | 8.15 | 60.84 | 7.46 | *yfiS* | 34.41 | 2.94 | 0.74 | 7.12E-06 | 5.88E-05 |
| *speG* | standard | 26.5 | 196.53 | 7.42 | *queE* | 213.58 | 2.94 | 0.39 | 5.47E-15 | 1.21E-13 |
| *ftsQ* | standard | 1.36 | 10.07 | 7.41 | *yodB* | 20 | 2.9 | 0.92 | 1.76E-04 | 0.001100074 |
| *ygbE* | standard | 3.4 | 24.95 | 7.34 | *tadA* | 238.08 | 2.89 | 0.38 | 6.15E-15 | 1.36E-13 |
| *yqhI* | small | 2.04 | 14.88 | 7.3 | *arnD* | 13.79 | 2.89 | 1.12 | 0.001001481 | 0.005046111 |
| *miaA* | standard | 13.59 | 96.73 | 7.12 | *ybgS* | 71.99 | 2.87 | 0.54 | 1.44E-08 | 1.91E-07 |
| *speC* | standard | 19.7 | 140.07 | 7.11 | *metU* | 243.67 | 2.87 | 0.42 | 6.17E-13 | 1.21E-11 |
| *appB* | standard | 0.68 | 4.81 | 7.09 | *metT* | 243.67 | 2.87 | 0.42 | 6.17E-13 | 1.21E-11 |
| *argH* | standard | 2.72 | 19.26 | 7.09 | *serV* | 8051.92 | 2.86 | 0.35 | 2.19E-17 | 5.70E-16 |
| *artJ* | standard | 13.59 | 96.3 | 7.09 | *cspG* | 125.16 | 2.85 | 0.44 | 1.28E-11 | 2.26E-10 |
| *cobC* | standard | 2.72 | 19.26 | 7.09 | *ugpA* | 23.5 | 2.84 | 0.85 | 9.04E-05 | 6.07E-04 |
| *rcdA* | standard | 2.72 | 19.26 | 7.09 | *gltW* | 2671.27 | 2.83 | 0.34 | 1.73E-17 | 4.54E-16 |
| *ydgD* | standard | 4.76 | 33.7 | 7.09 | *gltU* | 2671.27 | 2.83 | 0.34 | 1.73E-17 | 4.54E-16 |
| *hrpB* | standard | 4.08 | 28.89 | 7.09 | *gltT* | 2671.27 | 2.83 | 0.34 | 1.73E-17 | 4.54E-16 |
| *ydgI* | standard | 29.21 | 204.85 | 7.01 | *gltV* | 2671.27 | 2.83 | 0.34 | 1.73E-17 | 4.54E-16 |
| *yodB* | standard | 5.44 | 37.64 | 6.93 | *speG* | 402.93 | 2.82 | 0.35 | 2.21E-16 | 5.39E-15 |
| *phoH* | standard | 16.99 | 116.87 | 6.88 | *glnW* | 5581.76 | 2.79 | 0.34 | 2.38E-17 | 6.10E-16 |
| *ydhJ* | standard | 23.78 | 163.27 | 6.87 | *glnU* | 5581.76 | 2.79 | 0.34 | 2.38E-17 | 6.10E-16 |
| *yebW* | standard | 7.47 | 50.77 | 6.79 | *phnF* | 9.4 | 2.78 | 1.4 | 0.004516358 | 0.018545518 |
| *dinQ* | small | 1.36 | 9.19 | 6.76 | *ydhJ* | 35.29 | 2.76 | 0.7 | 8.20E-06 | 6.70E-05 |
| *yfbP* | standard | 0.68 | 4.38 | 6.44 | *appB* | 29.37 | 2.76 | 0.75 | 2.63E-05 | 1.97E-04 |
| *insD2* | standard | 0.68 | 4.38 | 6.44 | *pstA* | 84.17 | 2.76 | 0.5 | 3.89E-09 | 5.37E-08 |
| *lhr* | standard | 0.68 | 4.38 | 6.44 | *phoH* | 157.53 | 2.74 | 0.55 | 6.19E-08 | 7.50E-07 |
| *nhoA* | standard | 0.68 | 4.38 | 6.44 | *glsA* | 31.04 | 2.74 | 0.74 | 2.48E-05 | 1.86E-04 |
| *recX* | standard | 0.68 | 4.38 | 6.44 | *ycgX* | 11.14 | 2.72 | 1.26 | 0.002969559 | 0.012959207 |
| *ugpA* | standard | 0.68 | 4.38 | 6.44 | *clcA* | 33.59 | 2.7 | 0.71 | 1.68E-05 | 1.29E-04 |
| *yacH* | standard | 0.68 | 4.38 | 6.44 | *relB* | 212.04 | 2.68 | 0.39 | 9.27E-13 | 1.79E-11 |
| *ycaC* | standard | 2.04 | 13.13 | 6.44 | *mlaF* | 310.63 | 2.64 | 0.36 | 2.15E-14 | 4.54E-13 |
| *yidD* | standard | 0.68 | 4.38 | 6.44 | *rhsC* | 20.37 | 2.59 | 0.88 | 3.93E-04 | 0.002230904 |
| *patA* | standard | 3.4 | 21.01 | 6.18 | *pmrD* | 10.57 | 2.59 | 1.28 | 0.004234691 | 0.017596745 |
| *yncJ* | standard | 50.28 | 310.34 | 6.17 | *ymdF* | 73.54 | 2.57 | 0.52 | 9.59E-08 | 1.12E-06 |
| *rseA* | standard | 205.86 | 1264.99 | 6.14 | *mlrA* | 23.28 | 2.55 | 0.82 | 2.35E-04 | 0.001436063 |
| *opgG* | standard | 13.59 | 83.17 | 6.12 | *mqsA* | 81.15 | 2.54 | 0.5 | 5.50E-08 | 6.75E-07 |
| *ybiO* | standard | 1.36 | 8.32 | 6.12 | *zntA* | 87.62 | 2.54 | 0.48 | 1.74E-08 | 2.26E-07 |

| | | | | | | | | | | |
|---|---|---|---|---|---|---|---|---|---|---|
| *yfeO* | standard | 1.36 | 8.32 | 6.12 | *mdfA* | 45.72 | 2.54 | 0.62 | 5.74E-06 | 4.90E-05 |
| *hemD* | standard | 2.04 | 12.26 | 6.01 | *mqsR* | 84.83 | 2.51 | 0.49 | 4.53E-08 | 5.69E-07 |
| *iscX* | standard | 12.23 | 73.54 | 6.01 | *thrV* | 83.75 | 2.47 | 0.53 | 4.55E-07 | 4.79E-06 |
| *mdlA* | standard | 2.04 | 12.26 | 6.01 | *slp* | 50.9 | 2.47 | 0.6 | 6.20E-06 | 5.20E-05 |
| *argR* | standard | 27.18 | 163.27 | 6.01 | *ycfJ* | 63.77 | 2.46 | 0.55 | 1.07E-06 | 1.04E-05 |
| *pmrR* | small | 32.61 | 193.91 | 5.95 | *thrU* | 145.51 | 2.43 | 0.42 | 6.65E-10 | 9.68E-09 |
| *yddY* | small | 22.42 | 130.88 | 5.84 | *ytjA* | 131.58 | 2.42 | 0.44 | 4.71E-09 | 6.41E-08 |
| *yeeD* | standard | 108.03 | 627.68 | 5.81 | *folA* | 228.35 | 2.4 | 0.38 | 5.26E-11 | 8.65E-10 |
| *apaH* | standard | 2.72 | 15.76 | 5.8 | *mlaE* | 239.82 | 2.4 | 0.37 | 1.49E-11 | 2.60E-10 |
| *folM* | standard | 3.4 | 19.7 | 5.8 | *yddY* | 25.91 | 2.4 | 0.79 | 3.10E-04 | 0.001817096 |
| *ibsA* | small | 0.68 | 3.94 | 5.8 | *ycaC* | 70.21 | 2.39 | 0.53 | 9.42E-07 | 9.30E-06 |
| *insD3* | standard | 0.68 | 3.94 | 5.8 | *appA* | 25.61 | 2.37 | 0.77 | 2.88E-04 | 0.001708407 |
| *insD4* | standard | 0.68 | 3.94 | 5.8 | *yadE* | 24.1 | 2.37 | 0.8 | 3.94E-04 | 0.002230904 |
| *insD5* | standard | 0.68 | 3.94 | 5.8 | *ykfI* | 55.47 | 2.37 | 0.56 | 3.18E-06 | 2.85E-05 |
| *insD6* | standard | 0.68 | 3.94 | 5.8 | *arfA* | 24.15 | 2.36 | 0.8 | 4.15E-04 | 0.002324926 |
| *mhpF* | standard | 0.68 | 3.94 | 5.8 | *ychS* | 106.85 | 2.34 | 0.47 | 9.09E-08 | 1.08E-06 |
| *xylB* | standard | 0.68 | 3.94 | 5.8 | *yohC* | 26.27 | 2.32 | 0.77 | 3.43E-04 | 0.00200324 |
| *ydcK* | standard | 1.36 | 7.88 | 5.8 | *yjbJ* | 153.23 | 2.32 | 0.42 | 4.38E-09 | 5.98E-08 |
| *btuE* | standard | 19.7 | 113.81 | 5.78 | *paoD* | 10.75 | 2.3 | 1.23 | 0.00655796 | 0.025024217 |
| *yjdC* | standard | 8.83 | 48.59 | 5.5 | *yiaG* | 86.74 | 2.3 | 0.5 | 6.84E-07 | 6.95E-06 |
| *glsB* | standard | 10.19 | 56.03 | 5.5 | *rmf* | 1448.26 | 2.29 | 0.32 | 2.75E-13 | 5.45E-12 |
| *recJ* | standard | 6.79 | 37.21 | 5.48 | *ycaP* | 13.38 | 2.27 | 1.07 | 0.004022703 | 0.01682759 |
| *dosC* | standard | 16.31 | 87.54 | 5.37 | *yjdN* | 14.7 | 2.25 | 1.02 | 0.003375377 | 0.01444809 |
| *yecE* | standard | 2.04 | 10.94 | 5.37 | *symR* | 13.43 | 2.24 | 1.08 | 0.004360634 | 0.01804818 |
| *cpxP* | standard | 86.29 | 461.35 | 5.35 | *hemL* | 436.05 | 2.23 | 0.35 | 1.79E-11 | 3.08E-10 |
| *ampH* | standard | 38.05 | 202.22 | 5.32 | *glk* | 152.05 | 2.22 | 0.42 | 1.62E-08 | 2.12E-07 |
| *ycgV* | standard | 13.59 | 71.78 | 5.28 | *arrS* | 71.94 | 2.22 | 0.54 | 5.76E-06 | 4.90E-05 |
| *ymgE* | standard | 19.02 | 100.24 | 5.27 | *ybjX* | 352.08 | 2.22 | 0.38 | 9.80E-10 | 1.41E-08 |
| *bepA* | standard | 20.38 | 105.49 | 5.18 | *yagP* | 15.62 | 2.21 | 0.99 | 0.003308268 | 0.014180234 |
| *ecpA* | standard | 1.36 | 7 | 5.15 | *yijD* | 302.74 | 2.19 | 0.35 | 8.95E-11 | 1.45E-09 |
| *rzoQ* | standard | 0.68 | 3.5 | 5.15 | *gadW* | 98.62 | 2.19 | 0.49 | 1.11E-06 | 1.08E-05 |
| *tfaP* | standard | 0.68 | 3.5 | 5.15 | *zraR* | 36.16 | 2.19 | 0.66 | 1.39E-04 | 8.84E-04 |
| *thiQ* | standard | 0.68 | 3.5 | 5.15 | *psiF* | 55.56 | 2.17 | 0.56 | 1.53E-05 | 1.19E-04 |
| *ybbA* | standard | 2.04 | 10.51 | 5.15 | *mgrR* | 14.06 | 2.17 | 1.04 | 0.004721938 | 0.019238208 |
| *ydbH* | standard | 0.68 | 3.5 | 5.15 | *ydgV* | 108.03 | 2.14 | 0.46 | 5.08E-07 | 5.30E-06 |
| *pgpC* | standard | 21.74 | 108.99 | 5.01 | *yohP* | 29.27 | 2.14 | 0.72 | 4.45E-04 | 0.002479686 |
| *yqgF* | standard | 2.72 | 13.57 | 4.99 | *ygiW* | 67.93 | 2.13 | 0.52 | 7.97E-06 | 6.53E-05 |
| *yeaY* | standard | 63.19 | 314.72 | 4.98 | *pgaD* | 9.14 | 2.13 | 1.38 | 0.012332021 | 0.042160671 |
| *waaO* | standard | 7.47 | 37.21 | 4.98 | *ytfK* | 199.14 | 2.12 | 0.38 | 4.18E-09 | 5.74E-08 |
| *ydcL* | standard | 16.99 | 84.04 | 4.95 | *sixA* | 116.56 | 2.12 | 0.44 | 3.09E-07 | 3.35E-06 |

| | | | | | | | | | | |
|---|---|---|---|---|---|---|---|---|---|---|
| *csdE* | standard | 6.11 | 30.2 | 4.94 | *yafW* | 13.72 | 2.1 | 1.05 | 0.005813937 | 0.022796754 |
| *yeeY* | standard | 2.04 | 10.07 | 4.94 | *yqhI* | 17.34 | 2.1 | 0.92 | 0.003119101 | 0.013443068 |
| *yggC* | standard | 4.08 | 20.13 | 4.94 | *ybaT* | 19.7 | 2.09 | 0.86 | 0.002281827 | 0.010453641 |
| *waaG* | standard | 2.04 | 10.07 | 4.94 | *opgB* | 81.48 | 2.08 | 0.49 | 3.69E-06 | 3.28E-05 |
| *rseB* | standard | 163.74 | 808.02 | 4.93 | *glnX* | 1680.13 | 2.07 | 0.34 | 1.46E-10 | 2.27E-09 |
| *ykgS* | small | 11.55 | 56.9 | 4.93 | *glnV* | 1680.13 | 2.07 | 0.34 | 1.46E-10 | 2.27E-09 |
| *yfhH* | standard | 16.31 | 80.1 | 4.91 | *holE* | 345.7 | 2.07 | 0.35 | 5.26E-10 | 7.79E-09 |
| *yodE* | small | 40.77 | 200.03 | 4.91 | *yhcN* | 112.26 | 2.07 | 0.44 | 5.33E-07 | 5.52E-06 |
| *artQ* | standard | 1.36 | 6.57 | 4.83 | *glcD* | 12.51 | 2.07 | 1.11 | 0.007735031 | 0.028847334 |
| *xynR* | standard | 1.36 | 6.57 | 4.83 | *yeeW* | 19.64 | 2.06 | 0.86 | 0.002416881 | 0.010944167 |
| *yfjF* | standard | 5.44 | 26.26 | 4.83 | *yciY* | 33.11 | 2.06 | 0.68 | 3.66E-04 | 0.002099702 |
| *waaP* | standard | 10.19 | 49.02 | 4.81 | *gadA* | 55 | 2.06 | 0.6 | 1.09E-04 | 7.20E-04 |
| *opgB* | standard | 25.14 | 119.5 | 4.75 | *kefB* | 29.32 | 2.06 | 0.71 | 6.02E-04 | 0.003210015 |
| *rmf* | standard | 499.37 | 2361.46 | 4.73 | *sibC* | 62.55 | 2.06 | 0.53 | 1.98E-05 | 1.51E-04 |
| *yafS* | standard | 4.08 | 19.26 | 4.72 | *corA* | 126.56 | 2.03 | 0.44 | 7.50E-07 | 7.55E-06 |
| *yegS* | standard | 8.15 | 38.52 | 4.72 | *ynfC* | 26.23 | 2.02 | 0.74 | 0.001064516 | 0.005332848 |
| *clcB* | standard | 4.76 | 22.32 | 4.69 | *yoaC* | 21.34 | 2.01 | 0.82 | 0.002245505 | 0.010302324 |
| *yhdV* | standard | 25.82 | 120.81 | 4.68 | *leuP* | 370.92 | 1.99 | 0.44 | 1.03E-06 | 1.01E-05 |
| *yriB* | small | 18.34 | 85.79 | 4.68 | *proP* | 542.82 | 1.97 | 0.33 | 3.48E-10 | 5.29E-09 |
| *tcyJ* | standard | 86.97 | 399.19 | 4.59 | *ecpA* | 34.9 | 1.97 | 0.66 | 4.90E-04 | 0.002672328 |
| *gsiA* | standard | 7.47 | 34.14 | 4.57 | *arnE* | 10.7 | 1.97 | 1.18 | 0.012091365 | 0.04162143 |
| *amyA* | standard | 15.63 | 71.35 | 4.57 | *hscA* | 342.73 | 1.96 | 0.4 | 1.70E-07 | 1.92E-06 |
| *hscA* | standard | 41.44 | 187.78 | 4.53 | *rpoE* | 319.84 | 1.95 | 0.35 | 5.02E-09 | 6.80E-08 |
| *cysI* | standard | 21.74 | 98.05 | 4.51 | *amiC* | 208.92 | 1.95 | 0.38 | 5.25E-08 | 6.52E-07 |
| *fepE* | standard | 0.68 | 3.06 | 4.51 | *ugpE* | 16.7 | 1.94 | 0.94 | 0.005879849 | 0.023026342 |
| *folK* | standard | 0.68 | 3.06 | 4.51 | *ymiA* | 23.96 | 1.91 | 0.78 | 0.002399407 | 0.010880791 |
| *hisA* | standard | 0.68 | 3.06 | 4.51 | *yahO* | 74.6 | 1.91 | 0.51 | 3.29E-05 | 2.40E-04 |
| *hisM* | standard | 0.68 | 3.06 | 4.51 | *phoU* | 114.77 | 1.91 | 0.44 | 2.77E-06 | 2.50E-05 |
| *hyaF* | standard | 0.68 | 3.06 | 4.51 | *ykfG* | 11.5 | 1.9 | 1.13 | 0.012368798 | 0.042181183 |
| *insD1* | standard | 0.68 | 3.06 | 4.51 | *pstB* | 120.34 | 1.9 | 0.43 | 2.03E-06 | 1.86E-05 |
| *moaE* | standard | 0.68 | 3.06 | 4.51 | *basS* | 32.19 | 1.89 | 0.68 | 9.49E-04 | 0.004844557 |
| *pdxI* | standard | 3.4 | 15.32 | 4.51 | *slyA* | 260.77 | 1.89 | 0.36 | 3.52E-08 | 4.47E-07 |
| *sapF* | standard | 0.68 | 3.06 | 4.51 | *yhiD* | 15.9 | 1.89 | 0.94 | 0.007083942 | 0.026705609 |
| *waaF* | standard | 1.36 | 6.13 | 4.51 | *kefG* | 73.43 | 1.87 | 0.51 | 4.47E-05 | 3.18E-04 |
| *yafL* | standard | 0.68 | 3.06 | 4.51 | *yobH* | 41.89 | 1.86 | 0.61 | 4.13E-04 | 0.002321485 |
| *ycbV* | standard | 0.68 | 3.06 | 4.51 | *selC* | 48.44 | 1.85 | 0.58 | 2.89E-04 | 0.001710781 |
| *ydaG* | small | 1.36 | 6.13 | 4.51 | *fdx* | 172.13 | 1.85 | 0.44 | 5.09E-06 | 4.40E-05 |
| *yfdX* | standard | 1.36 | 6.13 | 4.51 | *kbp* | 41.95 | 1.84 | 0.61 | 4.87E-04 | 0.002664475 |
| *aat* | standard | 61.83 | 278.82 | 4.51 | *gadF* | 49.84 | 1.84 | 0.63 | 6.72E-04 | 0.003539518 |
| *livJ* | standard | 2.04 | 9.19 | 4.51 | *bglA* | 277.97 | 1.84 | 0.38 | 2.40E-07 | 2.66E-06 |
| *paaK* | standard | 2.04 | 9.19 | 4.51 | *yodD* | 16.48 | 1.83 | 0.92 | 0.007466941 | 0.027947439 |
| *trmD* | standard | 148.11 | 664.89 | 4.49 | *hdeB* | 216.8 | 1.83 | 0.43 | 3.89E-06 | 3.44E-05 |

| | | | | | | | | | | |
|---|---|---|---|---|---|---|---|---|---|---|
| *mgtS* | small | 2234.61 | 9955.35 | 4.46 | *osmC* | 176.67 | 1.83 | 0.41 | 1.61E-06 | 1.52E-05 |
| *bfr* | standard | 13.59 | 60.4 | 4.45 | *yhbE* | 148.23 | 1.81 | 0.43 | 5.00E-06 | 4.33E-05 |
| *osmF* | standard | 4.76 | 21.01 | 4.42 | *mlaD* | 217.43 | 1.8 | 0.37 | 2.49E-07 | 2.73E-06 |
| *tomB* | standard | 27.86 | 122.12 | 4.38 | *cspB* | 69.69 | 1.79 | 0.51 | 9.40E-05 | 6.26E-04 |
| *dkgB* | standard | 11.55 | 50.34 | 4.36 | *serW* | 53.51 | 1.79 | 0.58 | 3.98E-04 | 0.002250482 |
| *bcsG* | standard | 2.72 | 11.82 | 4.35 | *serX* | 53.51 | 1.79 | 0.58 | 3.98E-04 | 0.002250482 |
| *ydeP* | standard | 2.72 | 11.82 | 4.35 | *ortT* | 31.77 | 1.79 | 0.74 | 0.002848726 | 0.012607727 |
| *ycgZ* | standard | 20.38 | 88.42 | 4.34 | *yfeK* | 18.38 | 1.78 | 0.86 | 0.006865127 | 0.025974585 |
| *glk* | standard | 43.48 | 188.22 | 4.33 | *yafX* | 24.7 | 1.78 | 0.76 | 0.00357779 | 0.015231165 |
| *cynR* | standard | 22.42 | 96.73 | 4.31 | *basR* | 41.62 | 1.76 | 0.61 | 7.62E-04 | 0.003938452 |
| *fxsA* | standard | 8.83 | 38.08 | 4.31 | *yabI* | 44.88 | 1.76 | 0.58 | 5.35E-04 | 0.002873773 |
| *yhfG* | standard | 12.91 | 55.15 | 4.27 | *gadE* | 27.23 | 1.76 | 0.76 | 0.004028227 | 0.0168282 |
| *amiB* | standard | 9.51 | 40.27 | 4.23 | *azuC* | 71.86 | 1.76 | 0.62 | 9.66E-04 | 0.004912092 |
| *ldtC* | standard | 16.99 | 71.35 | 4.2 | *mdaB* | 102.97 | 1.75 | 0.45 | 2.21E-05 | 1.67E-04 |
| *rstA* | standard | 64.54 | 270.51 | 4.19 | *ynfS* | 90.26 | 1.75 | 0.46 | 3.43E-05 | 2.50E-04 |
| *ahr* | standard | 9.51 | 39.83 | 4.19 | *ydhR* | 93 | 1.73 | 0.46 | 4.57E-05 | 3.23E-04 |
| *fbaB* | standard | 9.51 | 39.83 | 4.19 | *rcnA* | 13.84 | 1.73 | 0.99 | 0.01356292 | 0.045147211 |
| *bcsF* | standard | 1.36 | 5.69 | 4.19 | *ysgD* | 402.58 | 1.72 | 0.35 | 2.73E-07 | 2.98E-06 |
| *chbG* | standard | 5.44 | 22.76 | 4.19 | *shoB* | 19.74 | 1.72 | 0.83 | 0.007317217 | 0.027419846 |
| *fadE* | standard | 2.72 | 11.38 | 4.19 | *ygdI* | 40.7 | 1.71 | 0.6 | 9.86E-04 | 0.004994682 |
| *ycgB* | standard | 7.47 | 31.08 | 4.16 | *mlaB* | 155.62 | 1.71 | 0.4 | 4.03E-06 | 3.53E-05 |
| *gsiB* | standard | 3.4 | 14.01 | 4.12 | *rem* | 13.58 | 1.7 | 1 | 0.01516317 | 0.049319708 |
| *pxpA* | standard | 3.4 | 14.01 | 4.12 | *ybaP* | 80.94 | 1.7 | 0.47 | 8.16E-05 | 5.53E-04 |
| *wecB* | standard | 2.04 | 8.32 | 4.08 | *mltF* | 22.43 | 1.68 | 0.78 | 0.006371506 | 0.02459144 |
| *ydeM* | standard | 2.04 | 8.32 | 4.08 | *yciX* | 63.21 | 1.67 | 0.51 | 2.67E-04 | 0.001591423 |
| *nimR* | standard | 10.87 | 44.21 | 4.07 | *leuT* | 333.1 | 1.66 | 0.42 | 1.71E-05 | 1.31E-04 |
| *psiF* | standard | 8.83 | 35.89 | 4.06 | *leuV* | 333.1 | 1.66 | 0.42 | 1.71E-05 | 1.31E-04 |
| *ynjB* | standard | 9.51 | 38.08 | 4 | *leuQ* | 333.1 | 1.66 | 0.42 | 1.71E-05 | 1.31E-04 |
| *yiaG* | standard | 10.19 | 40.71 | 3.99 | *trpT* | 53.05 | 1.66 | 0.55 | 6.59E-04 | 0.0034826 |
| *uhpB* | standard | 12.91 | 51.21 | 3.97 | *hdeA* | 666.9 | 1.65 | 0.37 | 2.31E-06 | 2.11E-05 |
| *ecpR* | standard | 5.44 | 21.45 | 3.95 | *elaB* | 154.33 | 1.65 | 0.4 | 1.08E-05 | 8.61E-05 |
| *mntP* | standard | 23.1 | 91.04 | 3.94 | *letA* | 25.84 | 1.64 | 0.73 | 0.005293456 | 0.021180592 |
| *msyB* | standard | 78.13 | 307.71 | 3.94 | *mltD* | 413.19 | 1.64 | 0.34 | 4.54E-07 | 4.79E-06 |
| *dgcQ* | standard | 6.11 | 24.07 | 3.94 | *glmY* | 73.6 | 1.61 | 0.49 | 2.56E-04 | 0.001541773 |
| *ydbJ* | standard | 99.87 | 392.19 | 3.93 | *maeA* | 355.15 | 1.61 | 0.37 | 3.00E-06 | 2.70E-05 |
| *alx* | standard | 7.47 | 29.33 | 3.92 | *ykfF* | 34.95 | 1.6 | 0.64 | 0.002915101 | 0.012813055 |
| *yraQ* | standard | 38.05 | 148.82 | 3.91 | *tatD* | 80.68 | 1.6 | 0.48 | 2.05E-04 | 0.001258503 |
| *ldtA* | standard | 29.89 | 116.87 | 3.91 | *ynaI* | 32.23 | 1.6 | 0.67 | 0.003919051 | 0.016504319 |
| *rhoL* | small | 10.87 | 42.46 | 3.91 | *rseA* | 791.21 | 1.59 | 0.33 | 2.88E-07 | 3.13E-06 |
| *ygiW* | standard | 6.79 | 26.26 | 3.87 | *glgS* | 35.1 | 1.59 | 0.66 | 0.003814277 | 0.016106441 |
| *gudX* | standard | 0.68 | 2.63 | 3.87 | *gcvB* | 3584.49 | 1.59 | 0.32 | 1.68E-07 | 1.91E-06 |
| *ibsB* | small | 2.72 | 10.51 | 3.87 | *msyB* | 63.26 | 1.58 | 0.52 | 6.14E-04 | 0.003265833 |

| | | | | | | | | | | |
|---|---|---|---|---|---|---|---|---|---|---|
| *malX* | standard | 0.68 | 2.63 | 3.87 | *valW* | 46.96 | 1.58 | 0.59 | 0.001741963 | 0.008208737 |
| *mdtD* | standard | 0.68 | 2.63 | 3.87 | *aspU* | 650.02 | 1.58 | 0.34 | 1.23E-06 | 1.18E-05 |
| *moaD* | standard | 1.36 | 5.25 | 3.87 | *aspV* | 650.02 | 1.58 | 0.34 | 1.23E-06 | 1.18E-05 |
| *msrP* | standard | 1.36 | 5.25 | 3.87 | *aspT* | 650.02 | 1.58 | 0.34 | 1.23E-06 | 1.18E-05 |
| *phnN* | standard | 0.68 | 2.63 | 3.87 | *ompX* | 4546.19 | 1.57 | 0.32 | 2.02E-07 | 2.27E-06 |
| *pphA* | standard | 1.36 | 5.25 | 3.87 | *pmrR* | 156.83 | 1.57 | 0.39 | 1.97E-05 | 1.50E-04 |
| *recO* | standard | 1.36 | 5.25 | 3.87 | *tyrV* | 115.05 | 1.56 | 0.44 | 1.12E-04 | 7.33E-04 |
| *rseC* | standard | 0.68 | 2.63 | 3.87 | *tyrT* | 115.05 | 1.56 | 0.44 | 1.12E-04 | 7.33E-04 |
| *sxy* | standard | 1.36 | 5.25 | 3.87 | *mlaC* | 223.38 | 1.56 | 0.37 | 6.04E-06 | 5.08E-05 |
| *trmO* | standard | 2.72 | 10.51 | 3.87 | *emrD* | 40.84 | 1.55 | 0.6 | 0.0025991 | 0.011651268 |
| *ydhP* | standard | 18.34 | 70.91 | 3.87 | *ydhP* | 31.46 | 1.54 | 0.67 | 0.005090086 | 0.020524328 |
| *yfbN* | standard | 0.68 | 2.63 | 3.87 | *dinJ* | 131.95 | 1.54 | 0.41 | 5.98E-05 | 4.14E-04 |
| *yjcO* | standard | 0.68 | 2.63 | 3.87 | *iscR* | 308.39 | 1.54 | 0.51 | 7.04E-04 | 0.003669559 |
| *pyrR* | standard | 2.04 | 7.88 | 3.87 | *sra* | 525.89 | 1.53 | 0.34 | 1.75E-06 | 1.64E-05 |
| *ybjC* | standard | 8.15 | 31.52 | 3.87 | *yoeB* | 53.81 | 1.52 | 0.54 | 0.001361759 | 0.006609666 |
| *paaJ* | standard | 2.04 | 7.88 | 3.87 | *gltS* | 37.19 | 1.5 | 0.62 | 0.004079394 | 0.017019232 |
| *tmcA* | standard | 2.04 | 7.88 | 3.87 | *osmY* | 248.23 | 1.5 | 0.4 | 4.80E-05 | 3.38E-04 |
| *yceM* | standard | 2.04 | 7.88 | 3.87 | *ugpC* | 28.39 | 1.46 | 0.69 | 0.009072358 | 0.032932027 |
| *ydeI* | standard | 2.04 | 7.88 | 3.87 | *soxS* | 136.64 | 1.45 | 0.42 | 1.65E-04 | 0.001041569 |
| *yghB* | standard | 42.8 | 164.58 | 3.85 | *yejG* | 207.82 | 1.45 | 0.4 | 8.98E-05 | 6.04E-04 |
| *ymiA* | small | 138.6 | 530.51 | 3.83 | *ykiD* | 30.44 | 1.44 | 0.66 | 0.008017026 | 0.029651623 |
| *yibF* | standard | 7.47 | 28.45 | 3.81 | *cof* | 36.87 | 1.43 | 0.61 | 0.005648098 | 0.022314267 |
| *yphH* | standard | 11.55 | 43.77 | 3.79 | *rcnR* | 28.58 | 1.43 | 0.68 | 0.00981519 | 0.035219873 |
| *curA* | standard | 22.42 | 84.92 | 3.79 | *rpoS* | 518.95 | 1.41 | 0.33 | 5.85E-06 | 4.95E-05 |
| *npr* | standard | 15.63 | 59.09 | 3.78 | *ryfA* | 56.68 | 1.41 | 0.52 | 0.002227727 | 0.010235766 |
| *ytfF* | standard | 9.51 | 35.89 | 3.77 | *yqhA* | 154.26 | 1.39 | 0.39 | 1.37E-04 | 8.75E-04 |
| *cysE* | standard | 47.56 | 178.59 | 3.76 | *psiE* | 28.88 | 1.39 | 0.68 | 0.011626599 | 0.040374065 |
| *yedA* | standard | 7.47 | 28.01 | 3.75 | *glyU* | 39.24 | 1.38 | 0.6 | 0.006460553 | 0.024823494 |
| *osmY* | standard | 40.09 | 150.14 | 3.75 | *erpA* | 165.91 | 1.35 | 0.47 | 0.001365789 | 0.006615408 |
| *gadW* | standard | 63.19 | 236.37 | 3.74 | *yeaQ* | 65.54 | 1.35 | 0.5 | 0.002133684 | 0.009848486 |
| *dacC* | standard | 55.71 | 208.35 | 3.74 | *dkgB* | 31.73 | 1.35 | 0.65 | 0.011599563 | 0.040332427 |
| *ytiA* | standard | 3.4 | 12.69 | 3.74 | *yceK* | 99.9 | 1.33 | 0.46 | 0.00134666 | 0.006563393 |
| *dnaC* | standard | 9.51 | 35.45 | 3.73 | *adhP* | 30.59 | 1.33 | 0.65 | 0.012832445 | 0.043221442 |
| *phoP* | standard | 233.04 | 864.48 | 3.71 | *cspF* | 36.22 | 1.32 | 0.61 | 0.009769932 | 0.035138064 |
| *hybD* | standard | 2.72 | 10.07 | 3.7 | *cydH* | 77.27 | 1.32 | 0.47 | 0.001728634 | 0.008158215 |
| *tatB* | standard | 2.72 | 10.07 | 3.7 | *yefM* | 123.88 | 1.32 | 0.41 | 5.11E-04 | 0.002764991 |
| *yebE* | standard | 12.91 | 47.27 | 3.66 | *yedR* | 30.32 | 1.31 | 0.65 | 0.014078261 | 0.046418208 |
| *nagA* | standard | 14.95 | 54.71 | 3.66 | *degP* | 308.32 | 1.3 | 0.36 | 9.23E-05 | 6.19E-04 |
| *hemF* | standard | 6.11 | 22.32 | 3.65 | *yqeF* | 37.96 | 1.29 | 0.61 | 0.011566698 | 0.040303115 |
| *dadX* | standard | 2.04 | 7.44 | 3.65 | *yebV* | 154.21 | 1.29 | 0.41 | 5.61E-04 | 0.003003626 |
| *ggt* | standard | 4.08 | 14.88 | 3.65 | *iscS* | 431.78 | 1.29 | 0.45 | 0.001488886 | 0.007167266 |
| *yoeB* | standard | 2.04 | 7.44 | 3.65 | *zapC* | 130.31 | 1.28 | 0.4 | 5.74E-04 | 0.003072022 |

| | | | | | | | | | | |
|---|---|---|---|---|---|---|---|---|---|---|
| *letA* | standard | 52.99 | 193.03 | 3.64 | *yncL* | 120.28 | 1.28 | 0.42 | 9.49E-04 | 0.004844557 |
| *ytjA* | standard | 47.56 | 172.46 | 3.63 | *ohsC* | 109.96 | 1.27 | 0.42 | 0.001015212 | 0.005098873 |
| *uvrY* | standard | 27.18 | 98.05 | 3.61 | *yrbN* | 225.13 | 1.27 | 0.37 | 2.38E-04 | 0.001449485 |
| *yhjD* | standard | 8.15 | 29.33 | 3.6 | *mdtK* | 62.12 | 1.27 | 0.5 | 0.00443095 | 0.018242686 |
| *tehA* | standard | 18.34 | 65.66 | 3.58 | *yghE* | 41.85 | 1.27 | 0.58 | 0.010335855 | 0.036693964 |
| *adhP* | standard | 5.44 | 19.26 | 3.54 | *rsxA* | 53.19 | 1.26 | 0.54 | 0.006530064 | 0.024978693 |
| *cmoB* | standard | 1.36 | 4.81 | 3.54 | *sfsA* | 54.6 | 1.25 | 0.52 | 0.006450973 | 0.024823494 |
| *pncA* | standard | 1.36 | 4.81 | 3.54 | *ytiB* | 51.03 | 1.25 | 0.54 | 0.007595897 | 0.028362246 |
| *uhpC* | standard | 1.36 | 4.81 | 3.54 | *tusA* | 75.69 | 1.25 | 0.47 | 0.003008532 | 0.013056443 |
| *insA4* | standard | 4.08 | 14.44 | 3.54 | *rplS* | 741.32 | 1.24 | 0.34 | 1.17E-04 | 7.62E-04 |
| *pmrD* | standard | 158.3 | 556.33 | 3.51 | *rnlB* | 45.16 | 1.23 | 0.56 | 0.010036429 | 0.035808421 |
| *slp* | standard | 19.02 | 66.53 | 3.5 | *blr* | 68.02 | 1.23 | 0.49 | 0.004412675 | 0.018201483 |
| *yfjD* | standard | 4.76 | 16.63 | 3.5 | *bfr* | 69.08 | 1.23 | 0.49 | 0.004582157 | 0.018766453 |
| *talA* | standard | 13.59 | 47.27 | 3.48 | *ibpA* | 46.01 | 1.2 | 0.55 | 0.011140268 | 0.038903904 |
| *yhbO* | standard | 6.79 | 23.64 | 3.48 | *tatE* | 68.34 | 1.19 | 0.48 | 0.005545779 | 0.022021246 |
| *yidZ* | standard | 29.89 | 103.74 | 3.47 | *iscX* | 499.84 | 1.18 | 0.4 | 0.001193108 | 0.005907016 |
| *yecN* | standard | 42.8 | 147.95 | 3.46 | *obgE* | 194.26 | 1.17 | 0.39 | 9.99E-04 | 0.005046111 |
| *mepM* | standard | 15.63 | 53.84 | 3.45 | *tolC* | 692.49 | 1.17 | 0.33 | 2.01E-04 | 0.001238049 |
| *ecnA* | small | 2.04 | 7 | 3.44 | *iscU* | 305.42 | 1.16 | 0.43 | 0.002823147 | 0.012529967 |
| *fecC* | standard | 2.04 | 7 | 3.44 | *frmR* | 87.67 | 1.15 | 0.45 | 0.004308386 | 0.01787923 |
| *phnD* | standard | 4.08 | 14.01 | 3.44 | *rseC* | 118.42 | 1.15 | 0.41 | 0.002334944 | 0.010619245 |
| *ycgY* | standard | 2.04 | 7 | 3.44 | *eco* | 76.98 | 1.15 | 0.47 | 0.006182743 | 0.024121949 |
| *ychO* | standard | 4.08 | 14.01 | 3.44 | *atpI* | 308.54 | 1.14 | 0.35 | 4.75E-04 | 0.002606775 |
| *ynjD* | standard | 2.04 | 7 | 3.44 | *rpoZ* | 113.46 | 1.14 | 0.44 | 0.004444168 | 0.018273064 |
| *thiL* | standard | 8.83 | 30.2 | 3.42 | *roxA* | 178.9 | 1.14 | 0.38 | 0.001264669 | 0.006212163 |
| *ybiR* | standard | 8.83 | 30.2 | 3.42 | *lpxT* | 53.03 | 1.14 | 0.53 | 0.013268514 | 0.04421425 |
| *ytjB* | standard | 69.3 | 236.8 | 3.42 | *hdeD* | 64.47 | 1.13 | 0.53 | 0.012893055 | 0.043351172 |
| *metI* | standard | 4.76 | 16.2 | 3.41 | *rcnB* | 64.97 | 1.13 | 0.49 | 0.008988767 | 0.032666496 |
| *ybjS* | standard | 93.76 | 318.66 | 3.4 | *yffB* | 84.37 | 1.12 | 0.46 | 0.006420724 | 0.024741928 |
| *dnaK* | standard | 14.95 | 50.77 | 3.4 | *cdsA* | 70.95 | 1.1 | 0.49 | 0.011431427 | 0.03987618 |
| *rcsC* | standard | 12.91 | 43.77 | 3.39 | *iscA* | 310.37 | 1.1 | 0.42 | 0.004388433 | 0.018139242 |
| *phnO* | standard | 10.87 | 36.77 | 3.38 | *osmB* | 100.71 | 1.09 | 0.43 | 0.005613039 | 0.022203793 |
| *pspD* | standard | 40.77 | 137.44 | 3.37 | *lysU* | 87.48 | 1.08 | 0.46 | 0.008192364 | 0.030264355 |
| *hokD* | standard | 38.73 | 130.44 | 3.37 | *ecnB* | 69.09 | 1.08 | 0.48 | 0.010833276 | 0.038044129 |
| *inaA* | standard | 15.63 | 52.53 | 3.36 | *pepB* | 120.64 | 1.08 | 0.42 | 0.004873856 | 0.019754267 |
| *pabB* | standard | 39.41 | 131.75 | 3.34 | *rseB* | 238.27 | 1.07 | 0.36 | 0.001374135 | 0.006645545 |
| *yfdC* | standard | 19.7 | 65.66 | 3.33 | *nadD* | 71.06 | 1.05 | 0.47 | 0.012553295 | 0.042741306 |
| *fumE* | standard | 25.82 | 85.79 | 3.32 | *ivy* | 123.06 | 1.05 | 0.41 | 0.005102016 | 0.020545956 |
| *aroC* | standard | 4.76 | 15.76 | 3.31 | *bax* | 212.78 | 1.04 | 0.36 | 0.002015903 | 0.009331005 |
| *wecF* | standard | 16.99 | 56.03 | 3.3 | *bssS* | 188.72 | 1.03 | 0.37 | 0.002690689 | 0.011976054 |
| *yadX* | small | 23.78 | 78.35 | 3.29 | *bolA* | 157.88 | 1.02 | 0.4 | 0.00569691 | 0.022448028 |
| *degP* | standard | 21.06 | 69.16 | 3.28 | *ydgK* | 78.89 | 1.01 | 0.45 | 0.012656898 | 0.042898198 |

| | | | | |
|---|---|---|---|---|
| *ydhI* | standard | 14.27 | 46.84 | 3.28 |
| *ymdF* | standard | 14.27 | 46.84 | 3.28 |
| *hisQ* | standard | 16.99 | 55.59 | 3.27 |
| *yodC* | standard | 161.7 | 524.82 | 3.25 |
| *abpA* | standard | 24.46 | 79.23 | 3.24 |
| *ybjG* | standard | 303.02 | 980.92 | 3.24 |
| *yeaG* | standard | 29.89 | 96.73 | 3.24 |
| *mrcB* | standard | 48.24 | 155.83 | 3.23 |
| *mrdB* | standard | 1.36 | 4.38 | 3.22 |
| *acpS* | standard | 0.68 | 2.19 | 3.22 |
| *arnF* | standard | 0.68 | 2.19 | 3.22 |
| *essQ* | standard | 0.68 | 2.19 | 3.22 |
| *hcr* | standard | 0.68 | 2.19 | 3.22 |
| *ilvH* | standard | 0.68 | 2.19 | 3.22 |
| *insB2* | standard | 0.68 | 2.19 | 3.22 |
| *insB3* | standard | 0.68 | 2.19 | 3.22 |
| *kduI* | standard | 0.68 | 2.19 | 3.22 |
| *lpxK* | standard | 2.04 | 6.57 | 3.22 |
| *narJ* | standard | 0.68 | 2.19 | 3.22 |
| *sufD* | standard | 0.68 | 2.19 | 3.22 |
| *treA* | standard | 0.68 | 2.19 | 3.22 |
| *yaaI* | standard | 1.36 | 4.38 | 3.22 |
| *ydhT* | standard | 1.36 | 4.38 | 3.22 |
| *ydhU* | standard | 2.04 | 6.57 | 3.22 |
| *ynaK* | standard | 0.68 | 2.19 | 3.22 |
| *ynbA* | standard | 0.68 | 2.19 | 3.22 |
| *ypdC* | standard | 0.68 | 2.19 | 3.22 |
| *yqeC* | standard | 1.36 | 4.38 | 3.22 |
| *yqiA* | standard | 16.99 | 54.28 | 3.2 |
| *ybgA* | standard | 9.51 | 30.2 | 3.18 |
| *ydgJ* | standard | 108.03 | 342.73 | 3.17 |
| *ynfC* | standard | 8.83 | 28.01 | 3.17 |
| *yhbQ* | standard | 74.74 | 236.8 | 3.17 |
| *metL* | standard | 10.87 | 34.14 | 3.14 |
| *eamA* | standard | 14.27 | 44.65 | 3.13 |
| *dusC* | standard | 9.51 | 29.76 | 3.13 |
| *relE* | standard | 4.76 | 14.88 | 3.13 |
| *ygdR* | standard | 307.1 | 952.03 | 3.1 |
| *yfeY* | standard | 57.07 | 176.84 | 3.1 |
| *dnaG* | standard | 17.66 | 54.71 | 3.1 |
| *mukE* | standard | 35.33 | 108.99 | 3.08 |
| *slt* | standard | 15.63 | 48.15 | 3.08 |

| | | | | | |
|---|---|---|---|---|---|
| *lpxB* | 94.1 | 1 | 0.44 | 0.011029168 | 0.038645314 |
| *deaD* | 606.52 | 0.99 | 0.33 | 0.001428271 | 0.006886069 |
| *frmA* | 117.64 | 0.96 | 0.41 | 0.009881474 | 0.03533615 |
| *ybiE* | 142.68 | 0.96 | 0.39 | 0.008000962 | 0.029627231 |
| *yrbL* | 258.5 | 0.94 | 0.35 | 0.004091926 | 0.017048785 |
| *pheM* | 167.34 | 0.93 | 0.38 | 0.008333725 | 0.030642886 |
| *ybhL* | 238.82 | 0.91 | 0.38 | 0.008835762 | 0.032260328 |
| *hspQ* | 188.37 | 0.87 | 0.38 | 0.012704292 | 0.042928435 |
| *ydiH* | 403.56 | 0.86 | 0.33 | 0.005399113 | 0.021548245 |
| *cpxP* | 205.41 | 0.86 | 0.37 | 0.011798686 | 0.040793466 |
| *thrW* | 199.73 | 0.83 | 0.36 | 0.013973818 | 0.046178214 |
| *nlpD* | 735.03 | 0.77 | 0.31 | 0.008684907 | 0.031820928 |
| *csrB* | 2954.91 | 0.68 | 0.29 | 0.014267278 | 0.046991908 |

| | | | | |
|---|---|---|---|---|
| *ybiJ* | standard | 6.11 | 18.82 | 3.08 |
| *moa A* | standard | 26.5 | 81.41 | 3.07 |
| *zraR* | standard | 23.1 | 70.91 | 3.07 |
| *insH 5* | standard | 32.61 | 99.8 | 3.06 |
| *cvpA* | standard | 17.66 | 53.4 | 3.02 |
| *tcdA* | standard | 30.57 | 91.92 | 3.01 |
| *ycjX* | standard | 8.15 | 24.51 | 3.01 |
| *yigL* | standard | 4.08 | 12.26 | 3.01 |
| *ymiC* | small | 282.63 | 839.53 | 3.00 |

**Table S5. Verification of protein expression from the genomic locus for the 17 candidates identified in this study using Ribo-RET.**

| Small Protein | Small protein expression by genomic tagging first reported in | Media used |
|---|---|---|
| MgtS | [16] | LB |
| | [17] | Supplemented N-minimal medium with no added $Mg^{2+}$ |
| MgrB | [16] | LB |
| PmrR | [18] | N-minimal medium, pH 7.7 with 10 μM $Mg^{2+}$ |
| MgtT | [19] | LB |
| YmiC | [20] | LB |
| YmiA | [16] | LB |
| YoaI | [This Study] | Supplemented minimal A medium with 10 mM, 1 mM and no added $Mg^{2+}$ |
| YobF | [16] | LB |
| | [3] | LB + heat shock (45°C) |
| YddY | [20] | LB |
| YriB | [19] | LB |
| YadX | [19] | LB |
| YkgS | [20] | LB |
| YriA | [19] | LB |
| YdgU | [16] | LB |
| YqhI | [20] | LB |
| YadW | [20] | LB |
| DinQ | [21] | LB |

**Table S6. Localization, Tag, and Membrane Topology Prediction of Small Proteins**

| Small Protein | Localization | Epitope tag | Reference | Prediction of transmembrane helix and orientation | | |
|---|---|---|---|---|---|---|
| | | | | TMHMM [22] | TMPred [23] | Phobius [24] |
| MgtS | Membrane | C-terminal/FLAG and C-terminal/GFP | [16,25] | Yes | Predicted helix: 7-25 (19aa); Inside to Outside: N-terminus facing cytoplasm | Cytoplasmic (1-6aa) / Transmembrane (7-25aa) / Non - cytoplasmic (26-31aa) |
| MgrB | Membrane | C-terminal/FLAG and N-terminal/GFP | [1,16] | Yes | Predicted helix: 6-24 (19aa); Inside to Outside: N-terminus facing cytoplasm | Positively charged or n-region (1-5aa) / Hydrophobic α-helical or h-region (6-17aa)/ Non cytoplasmic (22-47) |
| PmrR | Membrane | C-terminal/6XHis | This study | Yes | Predicted helix: 5-27 (23aa); Inside to Outside: N-terminus facing cytoplasm | Cytoplasmic (1-8aa) / transmembrane (9-26 aa) / non cytoplasmic (27-29aa) |
| | | N-terminal/FLAG-6XHis (*S. enterica* PmrR) | [18] | | | |
| MgtT | Cytoplasm | N-terminal/GFP | This study | No | NA | Non cytoplasmic |
| YmiC | Membrane | N-terminal/GFP | This study | Yes | Predicted helix: 8-29 (22aa); Inside to Outside: N-terminus facing cytoplasm | Cytoplasmic (1-8aa) / Transmembrane (9-29aa) / Non - cytoplasmic (30-31aa) |
| YmiA | Membrane | N-terminal/GFP | This study | Yes | Predicted helix: 22-42 (21aa); Inside to Outside: N-terminus facing cytoplasm | Cytoplasmic (1-20aa) / Transmembrane (21-42aa) / Non - cytoplasmic (43-46aa) |

| | | | | | | |
|---|---|---|---|---|---|---|
| YoaI | Membrane | C-terminal/GFP | This study | Yes | Predicted helix: 10-20 (21aa); Outside to Inside: N-terminus facing periplasm | Non - cytoplasmic (1-5aa) / Transmembrane (6-30aa) / Cytoplasmic (31-34aa) |
| YobF | Membrane | C-terminal/6XHis | This study | Yes | Predicted helix: 25-41 (17aa); Outside to Inside: N-terminus facing periplasm | Non cytoplasmic |
| YddY | Cytoplasm | N-terminal/GFP | This study | No | NA | Non cytoplasmic |
| YriB | Cytoplasm | N-terminal/GFP | This study | No | NA | Non cytoplasmic |
| YadX | Cytoplasm | N-terminal/GFP | This study | No | NA | Cytoplasmic |
| YkgS | Cytoplasm | N-terminal/GFP | This study | No | NA | Cytoplasmic |
| YriA | Cytoplasm | N-terminal/GFP | This study | No | NA | Non cytoplasmic |
| YdgU | Membrane | N-terminal/GFP | This study | Yes | Predicted helix: 7-26 (20aa); Inside to Outside: N-terminus facing cytoplasm | Cytoplasmic (1-6aa) / Transmembrane (7-26aa) / Non - cytoplasmic (27aa) |
| YqhI | Cytoplasm | N-terminal/GFP | This study | No | NA | Non cytoplasmic |
| YadW | Cytoplasm | C-terminal/GFP | This study | No | NA | Non cytoplasmic |
| DinQ | Membrane | N-terminal FLAG | [21] | Yes | Predicted helix: 1-22 (22aa); Outside to Inside: N-terminal facing periplasm | Non - cytoplasmic (1-5aa) / Transmembrane (6-23aa) / Cytoplasmic (24-27aa) |

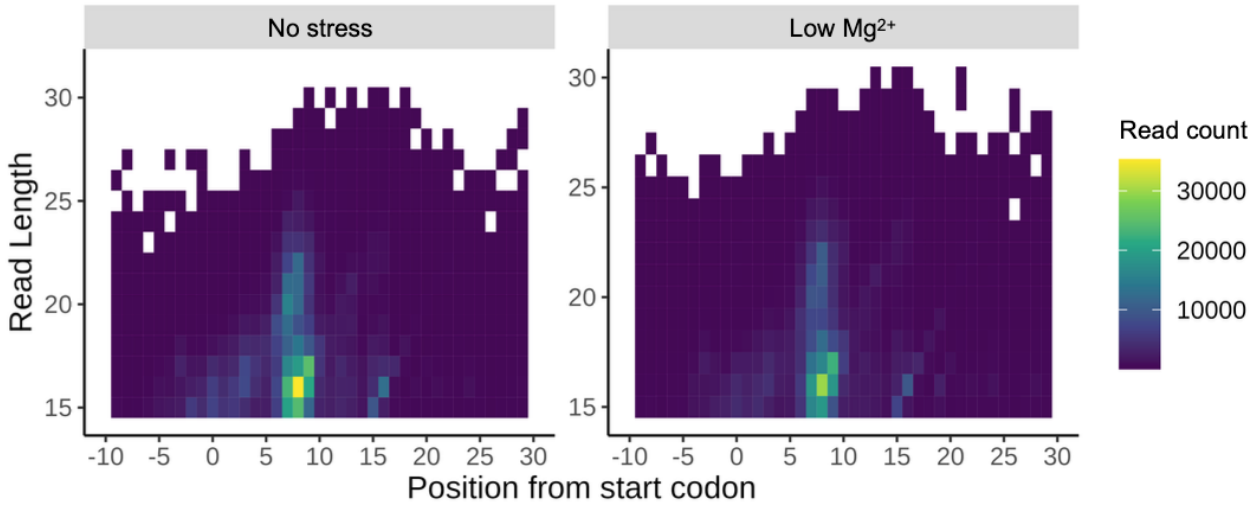


**Figure S1. A Ribogrid analysis representing Ribo-RET reads aligned to the genome.** The rows represent reads of varying lengths, and the columns indicate the position of the 3'-end of a footprint.

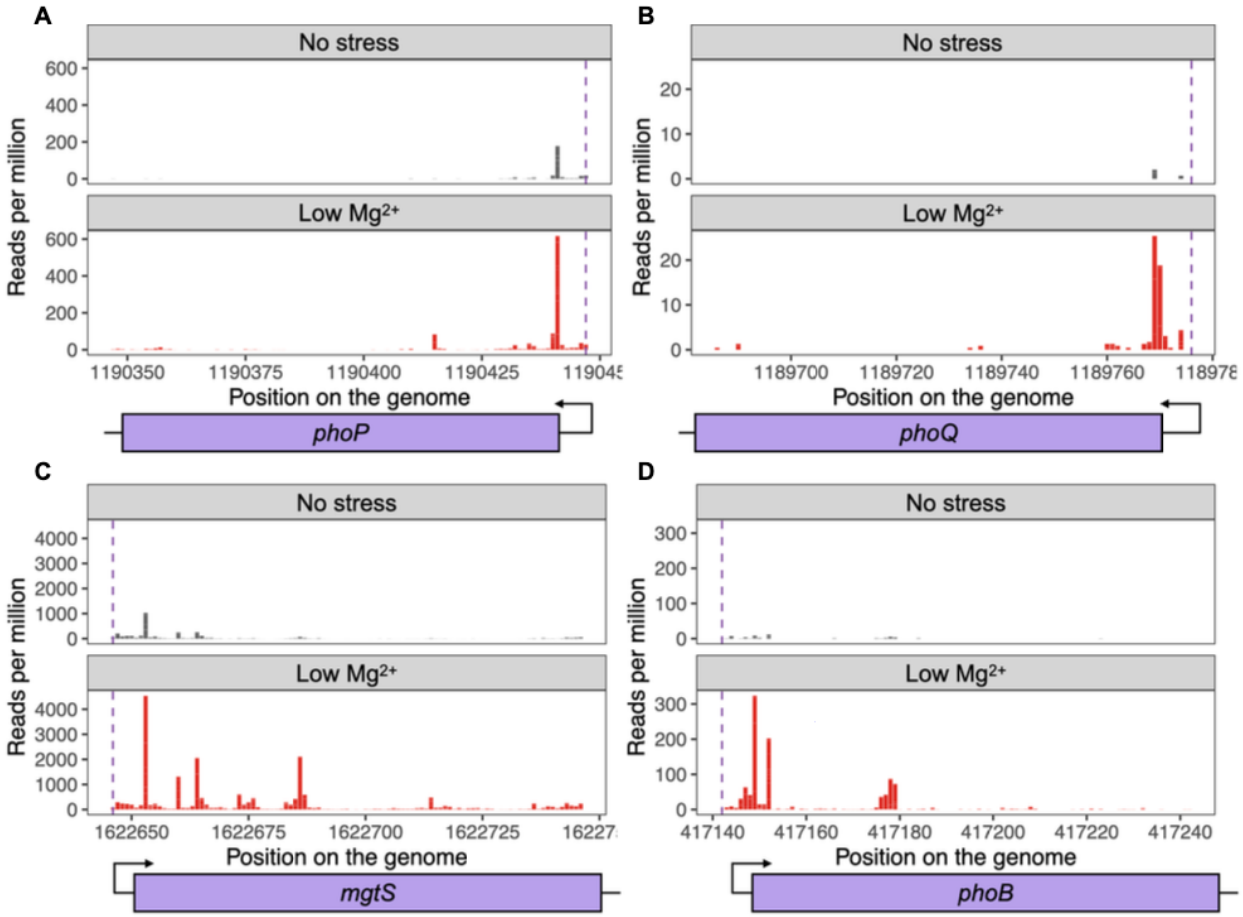


**Figure S2. Validation of Ribo-RET in detecting ribosome occupancy on annotated start site of proteins known to be induced under low $Mg^{2+}$ stress.**
(A-D) Ribo-RET reads mapping to the translation start site of proteins (A) PhoP, (B) PhoQ, (C) MgtS, and (D) PhoB at no stress condition (10 mM $Mg^{2+}$) and low $Mg^{2+}$ stress. A purple dashed line indicates the translation start site.

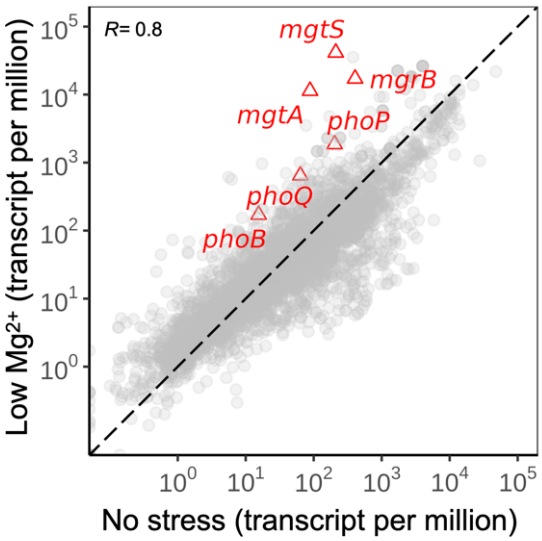


**Figure S3. Validation of RNA-Seq in detecting transcripts known to be induced under low $Mg^{2+}$ stress.** Scatterplot showing the correlation between the normalized RNA-Seq reads mapping to all the annotated genes under low $Mg^{2+}$ stress and no stress. *mgtS, mgrB, phoP, phoQ*, *mgtA,* and *phoB,* known to be induced under magnesium starvation, are highlighted in red triangle, while the rest of the transcripts are highlighted in gray circles. Pearson's coefficient, r= 0.8. The data is derived from the average of two biological replicates.

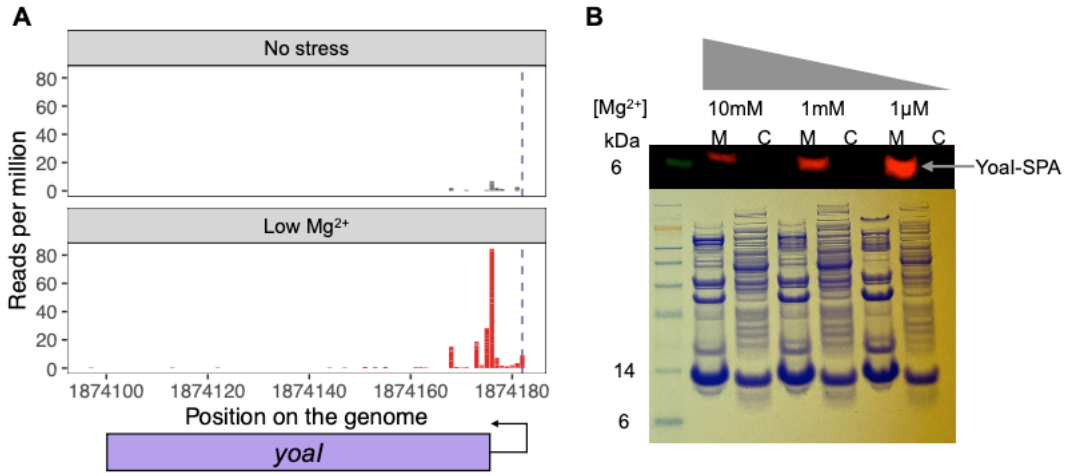


**Figure S4. Validation of low magnesium-dependent expression of a small protein, YoaI in the cell.** (A) Ribo-RET data for small protein YoaI induced under low $Mg^{2+}$ stress. The translation start site is indicated by a purple dashed line. (B) Validation of YoaI expression using a strain containing *yoaI-SPA* genomic fusion (GSO317). Cells were grown in supplemented minimal A medium containing $MgSO_4$ at the indicated concentration. Membrane (M) and cytoplasmic (C) fractions were analyzed by western blotting using M2 anti-FLAG antibodies (top) and by Coomassie Brilliant Blue staining (bottom). The data represents results from two independent replicates.

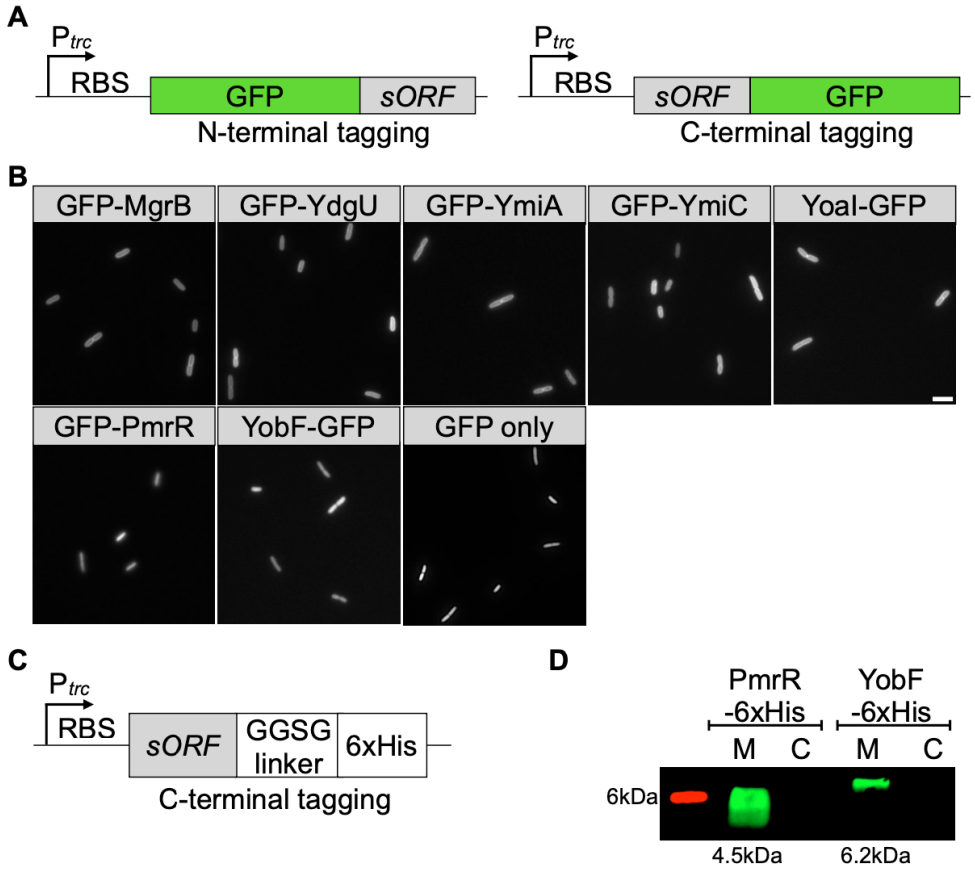


**Figure S5. Membrane localization of small proteins identified by epitope tagging.** (A) Schematic representation of GFP-tagged small protein constructs. (B) Fluorescence micrographs of *E. coli* K-12 MG1655 cells expressing GFP-MgrB (pAL38), GFP-YdgU (pPJ3), GFP-YmiA (pPJ12), GFP-YmiC (pPJ13), YoaI-GFP (pPJ4), GFP-PmrR (pPJ2), YobF-GFP (pPJ6), and GFP only (pAL39). (C) Schematic representation of 6XHis-tagged small protein constructs. (D) Western blot analysis of *E. coli* K-12 MG1655 cells expressing PmrR-6XHis (pSV14) and YobF-6XHis (pSV26), probed with anti-His antibodies. Membrane (M) and cytoplasm (C) fractions are indicated. In Panel B, cells were cultured in supplemented minimal A medium containing 1 mM $Mg^{2+}$ and 50 µg $ml^{-1}$ carbenicillin. In Panel D, the cells were grown in LB containing 100 µg $ml^{-1}$ carbenicillin. After four hours of growth, cells were induced with 500 µM IPTG and harvested two hours post-induction. The data represents results from two independent replicates. Scale bar = 5 µm. (Also see Table S6)

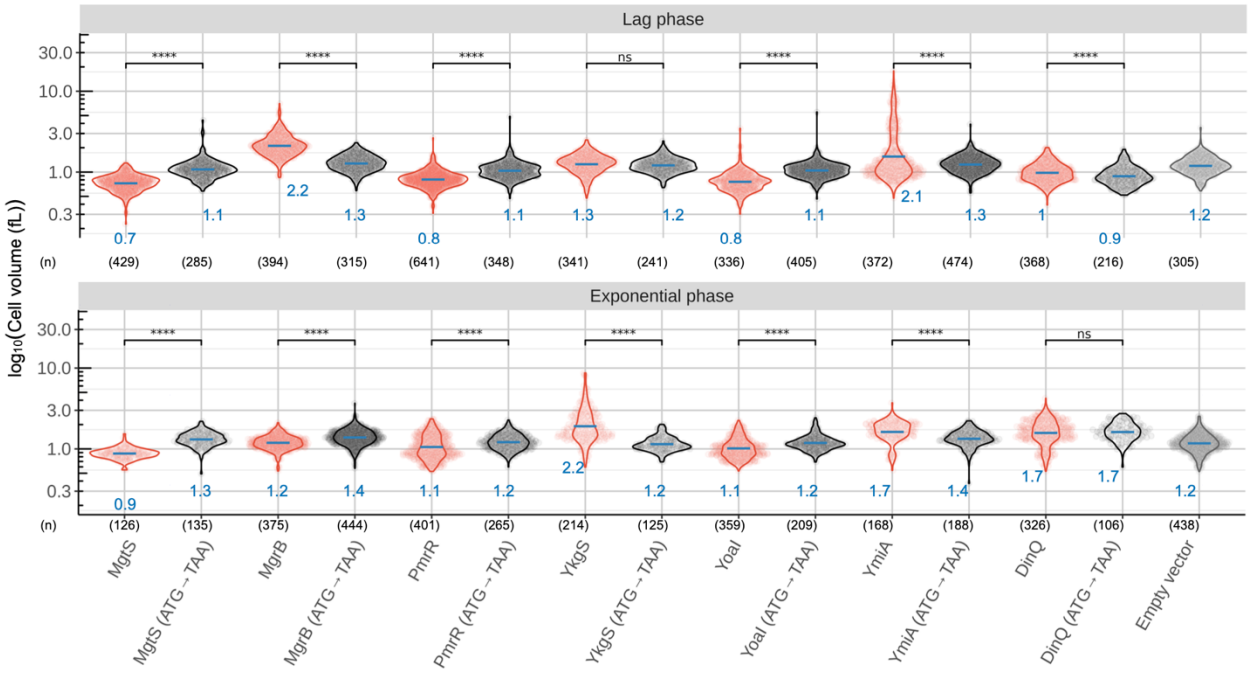


**Figure S6. Quantification of cell size changes associated with overexpression of small proteins, MgtS, MgrB, PmrR, YkgS, YoaI, YmiA and DinQ.** Cell volume quantification (representative micrograph images are shown in Figure 8B) for the cells expressing small proteins during lag (top panel) and exponential phase (bottom panel) after induction are shown. Each circle corresponds to a single cell. Cells expressing small proteins are shown in red, cells expressing the start codon mutants are depicted in black, and the empty vector (pEB52) control is shown in gray. The cultures were grown in supplemented minimal A medium with no added magnesium. For pSV34-36, pSV38-42, pSV60-61, pJS4, and pJS7, the medium contained 50 μg $ml^{-1}$ carbenicillin and 500 μM IPTG, while for pSV54-55, 0.5% arabinose was utilized. Data are derived from two independent replicates and the number of cells analyzed is indicated by (n). Mean cell volumes are shown with blue bars and are noted in blue text. P-values indicate the results of a t-test when the strains expressing small protein were compared to their variant with the translation start codon mutated, ****$P \leq 0.001$, and “ns” = $P > 0.05$.

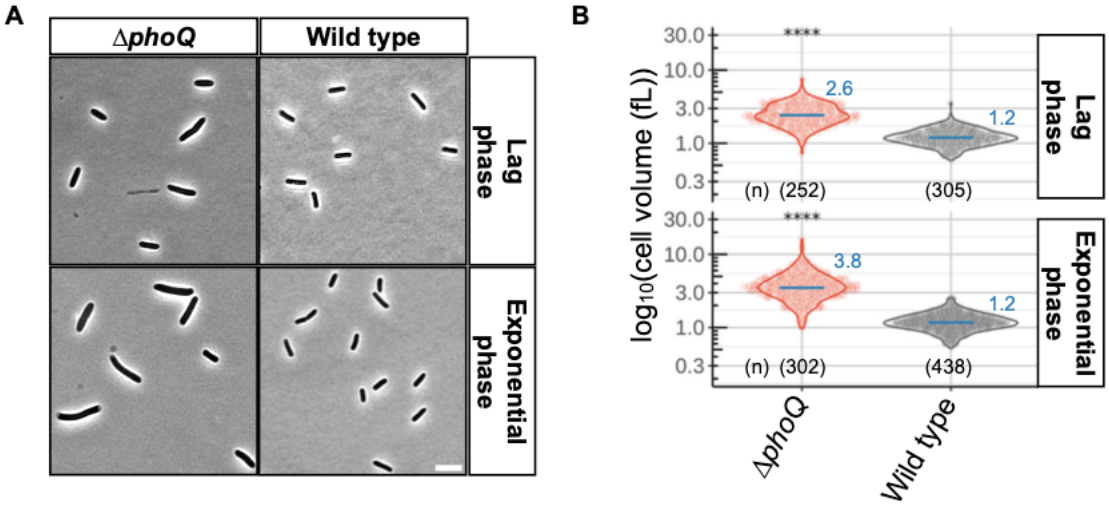


**Figure S7. Cell size changes associated with Δ*phoQ* under magnesium starvation.** (A) Representative phase contrast micrographs of Δ*phoQ* (TIM202), and wild type (MG1655) cells expressing an empty vector control (pEB52) during lag and exponential phase, scale bar = 5 µm. Cells were grown in supplemented minimal A medium with no added magnesium, and 50 µg $ml^{-1}$ carbenicillin. (B) Quantification of cell volume for the cells depicted in panel A. Each circle corresponds to a single cell. Cells expressing Δ*phoQ* are shown in red and wild type cells are shown in gray. Data are derived from three independent replicates and the number of cells analyzed is indicated by (n). Mean cell volumes are shown with blue bars and are noted in blue text. P-values indicate the results of a t-test when Δ*phoQ* cells were compared to the wild-type cells, ****P ≤ 0.0001.

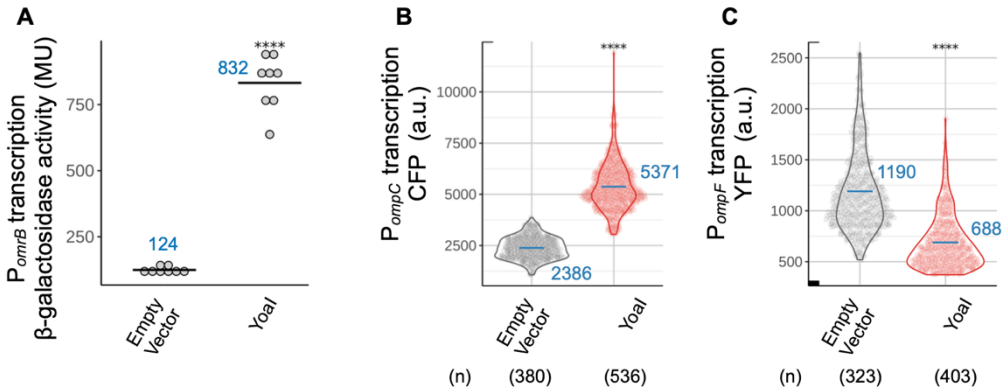


**Figure S8. Effect of YoaI overexpression on the EnvZ-OmpR system.** (A) Transcriptional activity of *omrB* was measured as a function of *lacZ* expression in wild-type (JM2110) strain during the exponential growth phase upon YoaI (pSV34) and empty vector (pEB52) overexpression. Each circle represents a biological replicate, with the mean values from two independent experiments indicated, expressed in Miller units (MU). The cells were grown in LB containing 100 μg $ml^{-1}$ carbenicillin. After three hours of growth, cells were induced with 500 μM IPTG, and β-gal activity was measured two hours post-induction. (B-C) Porin expression was measured using CFP fluorescence (corresponding to *ompC*) and YFP fluorescence (corresponding to *ompF*) in wild-type (MDG147) strain during the exponential growth phase upon YoaI (pSV34) and empty vector (pEB52) overexpression. Each circle corresponds to a single cell. Cells overexpressing YoaI are depicted in red, while those with the empty vector are in gray. The cultures were grown in supplemented minimal A medium containing 10mM $MgSO_4$ (no stress), 50 μg $ml^{-1}$ carbenicillin, and 500 μM IPTG. Data are derived from three independent replicates and the number of cells analyzed is indicated by (n). Mean fluorescence is shown with blue bars and is noted in blue text. P-values indicate the results of a t-test when cells overexpressing YoaI were compared to the empty vector control, ****$P \leq 0.0001$.

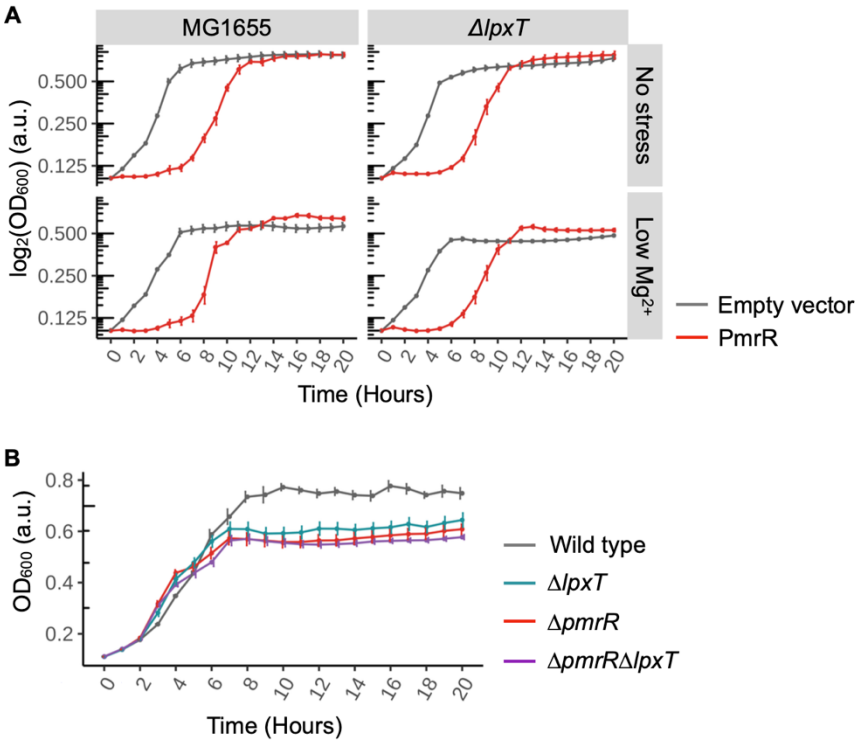


**Figure S9. The phenotypes associated with PmrR are LpxT independent.** (A) Growth comparison of *E. coli* K-12 MG1655 wild-type and Δ*lpxT* strain (SV47) carrying a plasmid encoding the small protein PmrR (pSV35, red line), or an empty vector (pEB52, gray line). The cultures were grown in supplemented minimal A medium containing 50 µg $ml^{-1}$ carbenicillin, 500 µM IPTG, and either 10 mM $MgSO_4$ (no stress) or no added magnesium (low $Mg^{2+}$). (B) The plot represents growth curves of wild-type *E. coli* MG1655 (gray) and mutants corresponding to gene deletions Δ*pmrR* (SV35, red line), Δ*lpxT* (SV47, green line), and Δ*pmrR* Δ*lpxT* (SV54, purple line). Please see Table S1 for details. The cultures were grown in supplemented minimal A medium with no added magnesium. Data represent averages and standard errors of means for four independent cultures.

## References


1. Lippa, A.M., and Goulian, M. (2009). Feedback inhibition in the PhoQ/PhoP signaling system by a membrane peptide. PLoS Genet. *5*, e1000788.

2. Hobbs, E.C., Astarita, J.L., and Storz, G. (2010). Small RNAs and small proteins involved in resistance to cell envelope stress and acid shock in Escherichia coli: analysis of a bar-coded mutant collection. J. Bacteriol. *192*, 59–67.

3. Hemm, M.R., Paul, B.J., Miranda-Ríos, J., Zhang, A., Soltanzad, N., and Storz, G. (2010). Small stress response proteins in Escherichia coli: proteins missed by classical proteomic studies. J. Bacteriol. *192*, 46–58.

4. Baba, T., Ara, T., Hasegawa, M., Takai, Y., Okumura, Y., Baba, M., Datsenko, K.A., Tomita, M., Wanner, B.L., and Mori, H. (2006). Construction of Escherichia coli K-12 in-frame, single-gene knockout mutants: the Keio collection. Mol. Syst. Biol. *2*, 2006.0008.

5. Batchelor, E., Silhavy, T.J., and Goulian, M. (2004). Continuous control in bacterial regulatory circuits. J. Bacteriol. *186*, 7618–7625.

6. Coornaert, A., Chiaruttini, C., Springer, M., and Guillier, M. (2013). Post-transcriptional control of the Escherichia coli PhoQ-PhoP two-component system by multiple sRNAs involves a novel pairing region of GcvB. PLoS Genet. *9*, e1003156.

7. Bastet, L., Korepanov, A.P., Jagodnik, J., Grondin, J.P., Lamontagne, A.-M., Guillier, M., and Lafontaine, D.A. (2024). Riboswitch and small RNAs modulate btuB translation initiation in Escherichia coli and trigger distinct mRNA regulatory mechanisms. Nucleic Acids Res. *52*, 5852–5865.

8. Yadavalli Srujana S., Goh Ted, Carey Jeffrey N., Malengo Gabriele, Vellappan Sangeevan, Nickels Bryce E., Sourjik Victor, Goulian Mark, Yuan Jing, and Silhavy Thomas J. (2020). Functional Determinants of a Small Protein Controlling a Broadly Conserved Bacterial Sensor Kinase. J. Bacteriol. *202*, e00305-20.

9. Miyashiro, T., and Goulian, M. (2007). Stimulus-dependent differential regulation in the Escherichia coli PhoQ PhoP system. Proc. Natl. Acad. Sci. U. S. A. *104*, 16305–16310.

10. Goldberg, S.D., Clinthorne, G.D., Goulian, M., and DeGrado, W.F. (2010). Transmembrane polar interactions are required for signaling in the *Escherichia coli* sensor kinase PhoQ. Proc. Natl. Acad. Sci. U. S. A. *107*, 8141–8146.

11. Bullock, W.O. (1987). XL1-blue : a high efficiency plasmid transforming recA Escherichia coli strain with beta-ga-lactosidase selection. Biotechniques *5*, 376.

12. Guzman, L.M., Belin, D., Carson, M.J., and Beckwith, J. (1995). Tight regulation, modulation, and high-level expression by vectors containing the arabinose PBAD promoter. J. Bacteriol. *177*, 4121–4130.

13. Cherepanov, P.P., and Wackernagel, W. (1995). Gene disruption in Escherichia coli: TcR and KmR cassettes with the option of Flp-catalyzed excision of the antibiotic-resistance determinant. Gene *158*, 9–14.

14. Datsenko, K.A., and Wanner, B.L. (2000). One-step inactivation of chromosomal genes in Escherichia coli K-12 using PCR products. Proc. Natl. Acad. Sci. U. S. A. *97*, 6640–6645.

15. Amann, E., Ochs, B., and Abel, K.J. (1988). Tightly regulated tac promoter vectors useful for the expression of unfused and fused proteins in Escherichia coli. Gene *69*, 301–315.

16. Hemm, M.R., Paul, B.J., Schneider, T.D., Storz, G., and Rudd, K.E. (2008). Small membrane proteins found by comparative genomics and ribosome binding site models. Mol. Microbiol. *70*, 1487–1501.

17. Wang, H., Yin, X., Wu Orr, M., Dambach, M., Curtis, R., and Storz, G. (2017). Increasing intracellular magnesium levels with the 31-amino acid MgtS protein. Proc. Natl. Acad. Sci. U. S. A. *114*, 5689–5694.

18. Kato, A., Chen, H.D., Latifi, T., and Groisman, E.A. (2012). Reciprocal control between a bacterium's regulatory system and the modification status of its lipopolysaccharide. Mol. Cell *47*, 897–908.

19. Weaver, J., Mohammad, F., Buskirk, A.R., and Storz, G. (2019). Identifying Small Proteins by Ribosome Profiling with Stalled Initiation Complexes. MBio *10*. https://doi.org/10.1128/mBio.02819-18.

20. VanOrsdel, C.E., Kelly, J.P., Burke, B.N., Lein, C.D., Oufiero, C.E., Sanchez, J.F., Wimmers, L.E., Hearn, D.J., Abuikhdair, F.J., Barnhart, K.R., et al. (2018). Identifying New Small Proteins in Escherichia coli. Proteomics *18*, e1700064.

21. Weel-Sneve, R., Kristiansen, K.I., Odsbu, I., Dalhus, B., Booth, J., Rognes, T., Skarstad, K., and Bjørås, M. (2013). Single transmembrane peptide DinQ modulates membrane-dependent activities. PLoS Genet. *9*, e1003260.

22. Möller, S., Croning, M.D., and Apweiler, R. (2001). Evaluation of methods for the prediction of membrane spanning regions. Bioinformatics *17*, 646–653.

23. Ikeda, M., Arai, M., Okuno, T., and Shimizu, T. (2003). TMPDB: a database of experimentally-characterized transmembrane topologies. Nucleic Acids Res. *31*, 406–409.

24. Käll, L., Krogh, A., and Sonnhammer, E.L.L. (2004). A combined transmembrane topology and signal peptide prediction method. J. Mol. Biol. *338*, 1027–1036.

25. Fontaine, F., Fuchs, R.T., and Storz, G. (2011). Membrane localization of small proteins in Escherichia coli. J. Biol. Chem. *286*, 32464–32474.